UNIVERSITY OF BOLOGNA

Electric Vehicle Engineering

Exam of **ELECTRIC MACHINE DESIGN M:**

DESIGN OF

Induction motor (IM)

and

Surface mounted permanent magnet sync motor (SPM)

Professor:

Prof. Giacomo Sala

Students:

Franceco Gambelli

ACCADEMIC YEAR 2023/2024

Contents

Chapter 1

Abstract

1.1 Motors

The industrial and automotive filed share many topologies of electric motor that can be involved in tens of different application. First of all is fair to said that even if the architecture are pretty similar, their application and their supply can have a huge difference, also by many order of magnitude in some performances data.

1.1.1 Induction motor

The first motor topology is the Induction motor (IM). It is composed by a winded stator and a squirrel cage rotor, the rotor can also allow a winding solution for high power application such as wind generation, but this is not our case of study. Basically this motor is supplied from the stator by an inverter for the automotive application or as in this case study directly from the grid so it is not take into consideration the control part that should take into consideration some values like that will change in flux weakening conditions. Moreover the principle of working of this machine is the magnetic field of the stator that is produced by the supply current, that induce a magnetic filed in the rotor that ad that time generate a short circuit current between the bars and the rings of the rotor that is opposed to the variation of the Magneto motive force. These fluxes interact each other in the airgap, where is located the main contribute that will produce the torque at the shaft, and they also will be linked by a formula that emphasize the differences of the speed of the equivalent rotating magnetic fluxes through the slip factor. This study will be carried on through a constrained design, so by looking at commercial catalogues and solution in order to be able to full finish the desired design taking into consideration the main limitation given from the market (lamination, materials, commercial obj)

Figure 1.1: IM

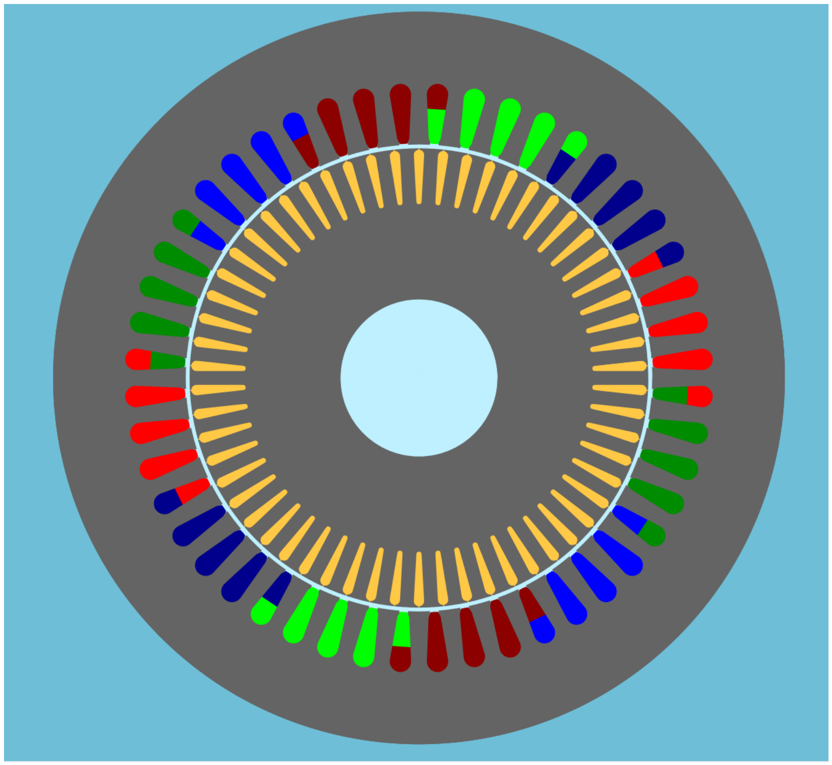

Figure 1.2: IM

1.1.2 Surface Mounted Permanent Magnet

The surface mounted permanent magnet motor is a synchronous motor that is made of an outer stator and an in and the rotor in which the stator has a three phase winding system and for this project it was chosen the tooth wind design while the rotor is a circular crown mounted on a shaft in which are present permanent magnet on the surface of the external diameter of the rotor. The space between the two geometry is called air gap and in this region there flux density of the magnet and the one from the stator interact each other in order to create a magnetic loading that provide to the motor an output torque. This motor is fed by an inverter, so it is important to take into consideration the control limits due to the non ideality of the harmonic spectrum. The design of this motor is an unconstrained design that allow to be free from geometrical and industrial constrain, by the way during the whole design are taken into consideration realistic value that can be feasible for a classic manufacturing process or a possible mass production, in fact also the material are chosen between the commercial one in order to limit the total cost of the entire machine.

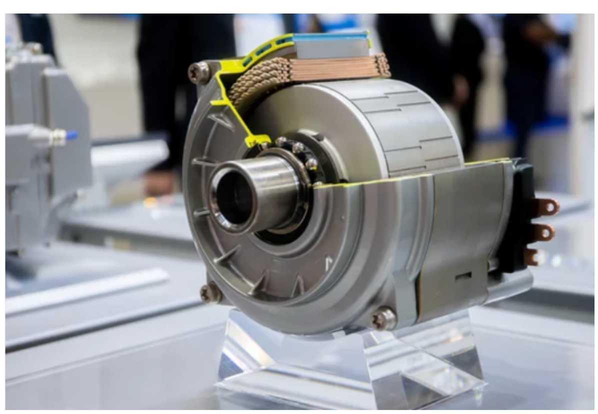

Figure 1.3: SPM

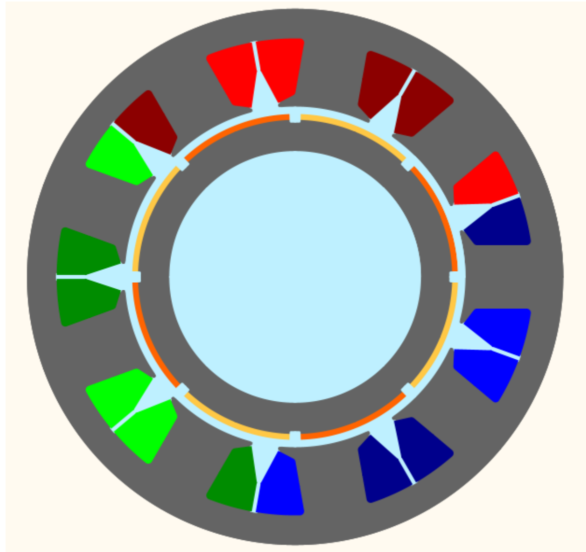

Figure 1.4: SPM

Chapter 2

Induction motor

2.1 Requirements

IM REQUIREMENTS The aim of this project is to follow a constrained design of an induction machine by having a some Design requirements: performances, efficiency and others. The first assumption is

Design requirements for

TEFC THREE-PHASE INDUCTION MOTOR

self-ventilated motor with cage rotor

Efficiency class IE2

Power (S1)	33.5 [kW]
Voltage (line to line, rms)	470 [V]
Frequency	50 [Hz]
Rated speed	1477 [rpm]
Full load efficiency	0.92
Power factor (at full load)	0.87

Figure 2.1: Design requirements

to estimate the number of pole pair, since the induction motor is an asynchronous motor where the, the difference of the speed of the magnetic fluxes generated by the stator and the mechanical speed of the rotor at rated operating conditions, r should be regulated by the speed the motor is work at nominal condition with a slip factor of few percentages, so it is proper to say that this motor must have 2 pole pairs so 4 poles. Then is possible to obtain the analytical proof of what's it was just said and in addition obtain other value:

- Phase voltage $V_{ph} = \frac{V_l l}{\sqrt{3}} = 271.354(V)$
- Phase current $I_{ph} = \frac{Power}{3 * V_{ph} * \eta * cos\phi} = 51.413(A)$
- Electrical angular frequency $w = frequency * 2 * \pi = 314.159(rad/s)$
- Mechanical angular frequency (of the flux in the airgap) $w_p = \frac{w}{p} = 157.079(rad/s)$

- Slip at rated condition $s = \frac{w_p - w_{mec}}{wp} = 0.0153$
- Frequency of the current induced in the bars of the rotor $fr = s * frequency = 0.766(Hz)$

To move on with the initialization of the main parameters, the magnetic loading is the value of the flux density at the air gap considering it sinusoidal (later is shown the real value that take into consideration other interference that will lead to a saturation).
Later on, this value it also will be called Magnetic Loading of the motor, and it will be the characterizing parameter of the flux density that is present in the teeth and yokes. This value can vary in a limited way for motor with similar size (LD^2) and given rating values, materials and cooling system; so the industry experience suggest us to use

$$B_M = 0.7 \div 0.9 = 0.9T \tag{2.1}$$

This value is used also to introduce the flux per pole, $\phi_{M\tau} = \frac{2*B_m*L*\tau}{\pi} = 0.0171$ where τ is the pole pitch. $\tau = \frac{2*\pi*R}{w*p} = \frac{\pi*D}{2*p} = 0.1649m$

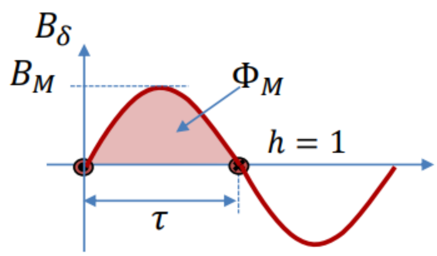

Figure 2.2: Tau

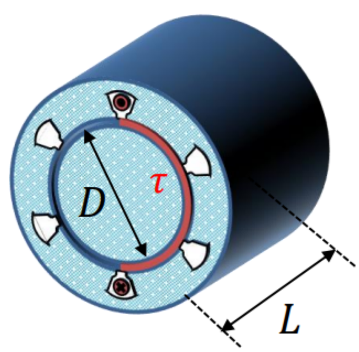

Figure 2.3: Dimensions

Thanks to these values it is possible to estimate also the value of the Electro Motive Force (EMF), it is induced by the main harmonic (the fundamental electrical harmonic p-th) $EMF = E = \frac{w*N*K_w*\phi_{Mt}}{\sqrt{2}*2}$ and it depends on the Number of series conductor per phase N and from the winding factor K_w
This value is also approximated in an initial stage as the value of phase voltage but multiplied by a factor lower than 1, usually it is raged between $0.95 \div 0.99$, this coefficient is there to take into consideration the voltage drop across the stator parameters (resistance and inductance) that is done later on

$$E = 0.95 \div 0.99V_{ph} = 260.5004(V) \tag{2.2}$$

Moreover, as it shows after this motor use a star (or Y) connection for its terminals since it is not needed to increase the value of the phase voltage by a factor $\sqrt{3} \div 1.73$ to obtain for example higher number of equivalent conductor per slot but with the star connection the gain is in the elimination of the harmonics of order 3 and them multiples

The electric loading instead[1], give us the quantitative estimation of the current needed in the stator, like a linear distribution of the rms current. $\Delta = \frac{3NI}{D\pi} = \frac{N_s S_{slot} F_f J}{D\pi}$ It is necessary to emphasize that if the diameter increase also the linear current density will increase because with a bigger diameter the S_{slot} increase followed by an increase of the F_f, having more space the degree of freedom increasing for the winding insertion, and also it is possible to experience an increase of the current density J; the following plot is made up many data extracted from commercial lamination catalogue that verify this consideration Moreover, the electric loading strongly depends on the type of cooling system proposed,

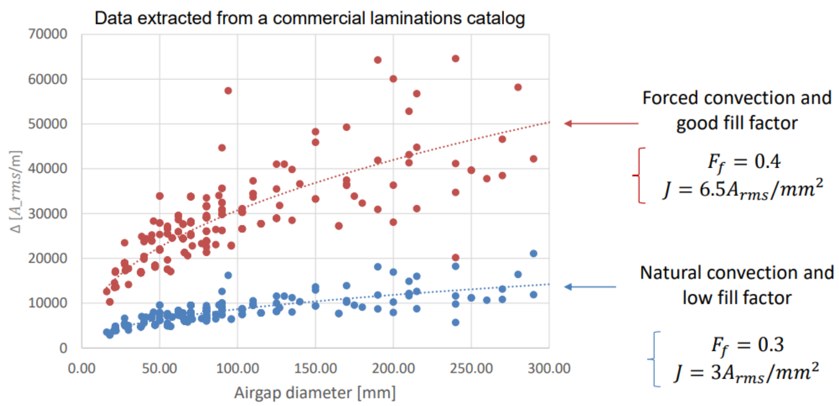

Figure 2.4: Electric loading

since this value can vary the maximum value of current density accepted (by considering the suggested value taken from industrial experience). By following the requirement, this motor is a self-ventilated also called Totally Enclosed Fan-Cooled (TEFC), that means:

- Enclosed machine
- smooth or finned casing
- External shaft-mounted fan
- CODE: IC 411 which means that it is present in a surface cooled frame with self circulation in both primary and secondary circuits *[2]

By proceeding with another fundamental value that need to be estimated at the beginning, that is the aspect ratio. I depend on the ratio between the active length and the pole pitch, but it can also be seen in relation to the number of pole that lead to different range of m by changing them, as is shown in the following table The previous plot is obtained by following this general $m = (0.25 \div 0.5)\sqrt{4p}$ obtained by evaluating from industrial data.

To have a comment on the m factor:

- high value of m result in long motors that present more difficulties for the extraction of the generated heat
- low m values lead to longer end windings, higher peripheral speed and higher costs

During the years many researchers and companies expertise studied this factor behaviour, and it

[1]This value can vary in a limited way for motor with similar size (LD^2) and given rating values, materials and cooling system; so the industry experience suggest us to use $\Delta = 15000 \div 60000(\frac{A_{rms}}{m}) = 35040(\frac{A_{rms}}{m})$

[2]CEI EN IEC 60034-6

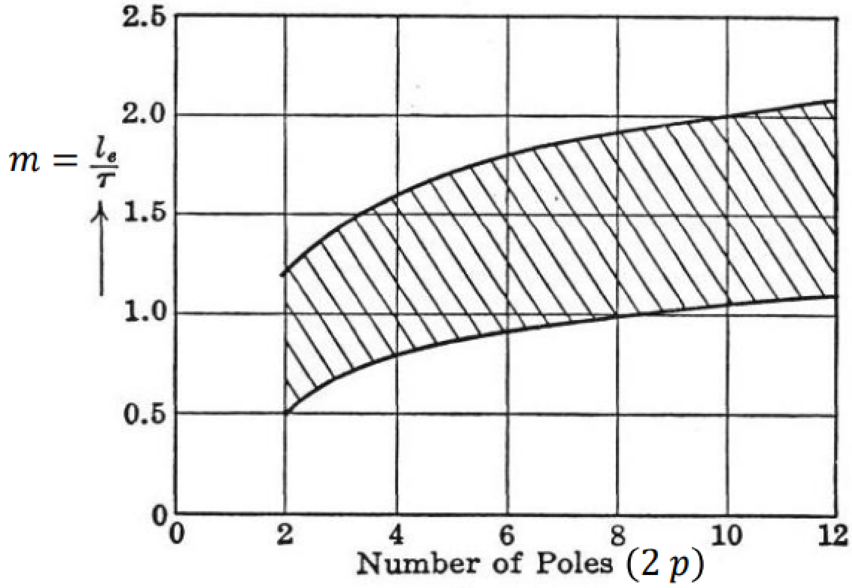

Figure 2.5: Aspect ratio

comes out the following general assumption that can be done for a first guess:

- $m = 0.5 \div 0.25$ typlical range for IM
- $m = 1 \div 1.5$ good fower factor
- $m = 1.5$ good efficiency
- $m = 1.5 \div 2$ good price and lower costs

The final vlaue of m is $m = 1.1455$

2.2 Stator

2.2.1 Initial sizing and catalogue

The very first step that is mandatory for the initial sizing is the one that concern the stator parameters, in peculiar looking at the airgap diameter[3] and number of equivalent conductor in a slot. This workflow if mainly guided by the strong dependency between these two parameters but also is Alway take into consideration that our design is related to maximizing the torque value that is deepened forward, but just to have a clue the main actor for the Torque equation are $T = B_m m\Delta$. The equation to evaluate the airgap diameter is the result of the Power equation(equation) [4] by introducing $L = \frac{m\pi D}{2p}$ and the result is the following

$$D \simeq (\frac{P2\sqrt{2}2p^2}{\eta cos\phi f\pi^3 K_w m B_M \Delta})^{\frac{1}{3}} = 0.2072(m) \tag{2.3}$$

Before starting to look at some catalogues, it is needed to calculate the total active length (L) because it is a parameter that not only allow to choose a proper chase for that motor but also during the choice of the laminations it must be considered that the thickness of the lamination should be an integer multiple of the total active length.

$$L = \frac{P2p\sqrt{2}}{wK_w\pi D^2 B_M \Delta cos\phi\eta} = 0.186(m) \tag{2.4}$$

$$L = \frac{m\pi D}{2p} = 0.186(m) \tag{2.5}$$

Now it is possible to move on by looking at some industrial catalogue in order to choose a lamination that is compatible with our value of parameters. I looked in the catalogue of Eurotranciatura S.p.A., and the best choice become the EU 5700A A with the following values[5].

EU 5700A									
Stator					**Rotor**				
D ext	**D int**	**Slot area**	**h yoke**	**Ns**	**D ex**	**D int**	**Bar area**	**h yoke**	**Nb**
330	210	202.7	32.11	48	210	70	112.25	42.9	58

2.2.2 Validations

Once having collect all the value from the catalogue, the following steps are aimed to validate this chosen lamination, from a geometrical point of view but also by considering losses and performances. By focusing on the height of the stator yoke and the airgap diameter, it can be used an equation that give the estimation of how much the ferromagnetic material is used. This formula give in output the number of pole pairs, the result could be:

- lower than the number of pole pair chose, that means that it was not taken advantage of the lamination enough, in other words, there is too much iron for this application that bring an overweight and an additional cost without needed

- higher value instead means that there are for sure points in which this lamination experience high values of saturation that are not convenient due to the fact that a huge drop of MMF need higher current

[3] Airgap diameter = inner stator diameter = outer rotor diameter before manufacture the airgap from that

[4] $P \simeq \frac{wK_w\pi mDD^2 B_m\Delta\eta cos\phi}{\sqrt{2}2p2p}$

[5] all values are in $mm^2 or mm^2$

$$p = \frac{0.25 \div 0.5D}{hys^6} = 1.96 \tag{2.6}$$

In this simulation this the number of pole pairs that it is obtained from this formula, using 0.3 as coefficient, is 1.96 so it is a good result since it is very near to the estimated value

It is necessary to say that by slightly change the Diameter in order to find an integer value that correspond to the diameter of a catalogue lamination, also the length is affected by this variation. The best way to proceed is to adjust the value of L by considering the industrial diameter in order to preserve the relation $LD^2 = constant$ that appear in the Torque equation[7].

D (m)	D new (m)	L (m)	L new(m)
0.207	0.210	0.186	0.182

2.2.3 Winding

To be able to have a good estimation of the values that take part in this design process, it is important to move forward to another main actor, the winding. Before going in deep, it is mandatory to introduce the winding factor K_w. This is the coefficient that carry with it the information about the distribution of the winding K_d and the shortening K_{sh}.

$$K_w = K_d K_{sh} = 0.9494 \tag{2.7}$$

The motor should be designed with p pairs of Poles and the winding has to be designed to maximize the main component $(p - th)$ of the flux produced or linked by each phase, this lead to maximize the winding factor. Since the magnetic axes produced by a group of coils is placed in the range covered by the winding of that phase, it is needed to proper wind the stator by considering the number of poles and also the multiplicity of the geometry:

$$M = GCD(\frac{N_s}{3}, 2p) = 4 \tag{2.8}$$

For distributed winding layout the smallest multiplicity corresponds to one pole (M=2p) covering the $\frac{2\pi}{2p}$ mechanical radians ($\pi electrical$); referring to one full periodicity ($\frac{2\pi}{p}$) the electrical angle θ is often used referred to the mechanical angle θ_m as $\theta = p\theta_m$ A

$0° \, el \leq p\,\psi_{slot} < 60° \, el$ → phase 1 (positive conductor orientation)
$60° \, el \leq p\,\psi_{slot} < 120° \, el$ → phase 3 (negative conductor orientation)
$120° \, el \leq p\,\psi_{slot} < 180° \, el$ → phase 2 (positive conductor orientation)
$180° \, el \leq p\,\psi_{slot} < 240° \, el$ → phase 1 (negative conductor orientation)
$240° \, el \leq p\,\psi_{slot} < 300° \, el$ → phase 3 (positive conductor orientation)
$300° \, el \leq p\,\psi_{slot} < 360° \, el$ → phase 2 (negative conductor orientation)

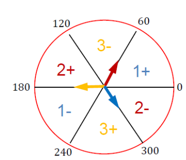

Figure 2.6: Winding layout

(The coils can be physically different and connected in series or in parallel in order to obtain the same MMF and avoiding recirculating current) so the important is to obtain a proper distribution of conductors in the slots

[7]also the values of B_M is affected by this change, but it is calculated at the end, by considering also the simulated value that comes out of the FEA; the value of Δ is invariant since once it was calculated by its own formula, also the first assumption was changed in order to be equal to the real value, and it ended up to be the same

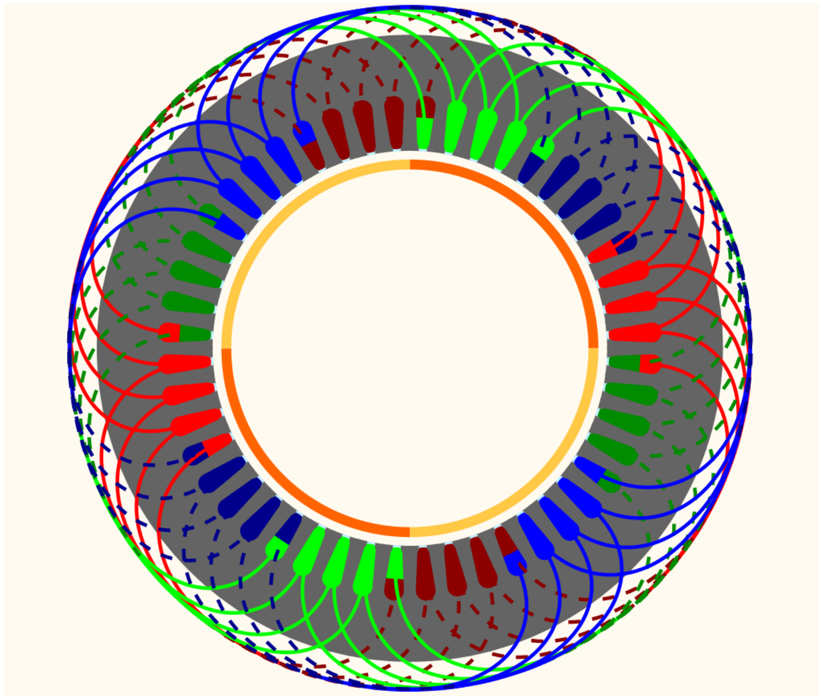

Figure 2.7: Total winding layout

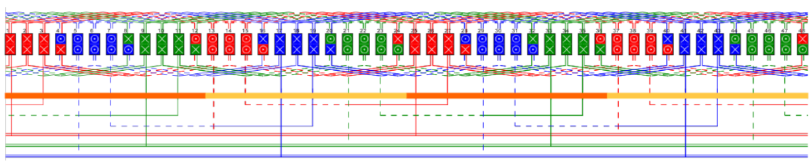

Figure 2.8: Total winding layout

So the distribution effect take into consideration how the wind our coils depend on the constraint of number of pole pairs, while the shortening introduce the double layer layout which means that the end winding will be lowered that each slot is physically separated in half (top/bottom) in order to allow the presence of different phase conductor in the same slot, this also implies that the end-winding will be lowered due to the fact that the return's conductor is no more placed at a distance of a pole pitch $\tau = \frac{2\pi R}{2p}$ [8] but in a value lower than that equal to stator pole pitch τs (formula TAUS). So the overall performances of a winding layout are quantified by this factor, low value help to limit the effect of the h-th harmonic on the performances (torque and losses) but at the same time it must not reduce too much the contribution of the fundamental harmonic (1-st or p-th in terms of mechanical degrees).

$$K_w = K_{sh} K_{dh} = 0.949 \tag{2.9}$$

$$K_{dh} = \frac{sin(hq\frac{\alpha}{2})}{qsin(\frac{h\alpha}{2})} = 0.957 \qquad \alpha = \frac{p2\pi}{N_s} = 0.261 \tag{2.10}$$

[8]distance between two active sides os a coil

Figure 2.9: Distribution

$$K_{sh} = cos(\frac{h\beta}{2}) = 0.9914 \qquad\qquad \beta = q_{sh}\alpha = 0.261 \tag{2.11}$$

Figure 2.10: Shortening

The values that come out from this analytical calculation is very accurate with the ones proposed in the following table:

$h=1$	$q_{sh}=0$	$q_{sh}=1$	$q_{sh}=2$	$q_{sh}=3$	$q_{sh}=4$
$q=1$	1.000	0.866			
$q=2$	0.966	0.933	0.837		
$q=3$	0.960	0.945	0.902	0.831	
$q=4$	0.958	0.949	0.925	0.885	0.829
$q=5$	0.957	0.951	0.936	0.910	0.874

$h=3$	$q_{sh}=0$	$q_{sh}=1$	$q_{sh}=2$	$q_{sh}=3$	$q_{sh}=4$
$q=1$	1.000	0.000			
$q=2$	0.707	0.500	0.000		
$q=3$	0.667	0.577	0.333	0.000	
$q=4$	0.653	0.604	0.462	0.250	0.000
$q=5$	0.647	0.616	0.524	0.380	0.200

$h=5$	$q_{sh}=0$	$q_{sh}=1$	$q_{sh}=2$	$q_{sh}=3$	$q_{sh}=4$
$q=1$	1.000	0.866			
$q=2$	0.259	0.067	0.224		
$q=3$	0.218	0.140	0.038	0.188	
$q=4$	0.205	0.163	0.053	0.079	0.178
$q=5$	0.200	0.173	0.100	0.000	0.100

$h=7$	$q_{sh}=0$	$q_{sh}=1$	$q_{sh}=2$	$q_{sh}=3$	$q_{sh}=4$
$q=1$	1.000	0.866			
$q=2$	0.259	0.067	0.224		
$q=3$	0.177	0.061	0.136	0.154	
$q=4$	0.158	0.096	0.041	0.146	0.136
$q=5$	0.149	0.111	0.016	0.088	0.146

$h=9$	$q_{sh}=0$	$q_{sh}=1$	$q_{sh}=2$	$q_{sh}=3$	$q_{sh}=4$
$q=1$	1.000	0.000			
$q=2$	0.707	0.500	0.000		
$q=3$	0.333	0.000	0.333	0.000	
$q=4$	0.271	0.104	0.191	0.250	0.000
$q=5$	0.247	0.145	0.076	0.235	0.200

$h=11$	$q_{sh}=0$	$q_{sh}=1$	$q_{sh}=2$	$q_{sh}=3$	$q_{sh}=4$
$q=1$	1.000	0.866			
$q=2$	0.966	0.933	0.837		
$q=3$	0.177	0.061	0.136	0.154	
$q=4$	0.126	0.016	0.122	0.048	0.109
$q=5$	0.109	0.045	0.073	0.104	0.011

$h=13$	$q_{sh}=0$	$q_{sh}=1$	$q_{sh}=2$	$q_{sh}=3$	$q_{sh}=4$
$q=1$	1.000	0.866			
$q=2$	0.966	0.933	0.837		
$q=3$	0.218	0.140	0.038	0.188	
$q=4$	0.126	0.016	0.122	0.048	0.109
$q=5$	0.102	0.021	0.093	0.060	0.068

Note: the harmonics multiple of 3 (3, 9, 15, …) are not generated by distributed winding layouts with star connection of the phases (and in delta connected windings if there are no respective rotor induced emf harmonics) because the common mode current is null ($i_0 = \frac{2}{3}(i_1 + i_2 + i_3) = 0$). In this case, the phase currents are function of the current space vector $\bar{\imath}$ ($\bar{\imath} = \frac{2}{3}(i_1 + i_2\bar{\alpha} + i_3\bar{\alpha}^2)$). In general: $i_1 = \frac{i_0}{2} + \Re e\{\bar{\imath}\}$; $i_2 = \frac{i_0}{2} + \Re e\{\bar{\imath}\bar{\alpha}^2\}$; $i_3(t) = \frac{i_0}{2} + \Re e\{\bar{\imath}\bar{\alpha}\}$, and the harmonic fields multiple of 3 (still considering electrical ones) are:
$\bar{H}_h = \frac{n2}{\text{hp}\pi\delta} K_{wh} \frac{3}{2} i_0$ → the field components produced by the common mode current are stationary and pulsating at the frequency of the common mode current (generate losses and torque ripple).

45

Figure 2.11: Design requirements

This table has two values as input, q_{sh} is the value that indicate of how many slot of distance is shifted the phase of our original slot; and the q is the number of slot under each pole for each phase; in my case $q = 4$ and $q_{sh} = 1$ The aim to try to reduce the low order harmonic disturbances and at the same time is preserved the amplitude of the fundamental one (as it shown in the following figure) Moreover the initial estimation of $K_w = 0.95$ was good enough but to be more precise this value was used to evaluate all the content that present this coefficient in their formulas.

Now what is necessary to introduce if the physical aspect of the coil present in our motor, firstly the wire are made by copper. The choice was between the aluminium and the copper but even if the aluminium leads to a lower mass density on the other hand it is less incline to let the current pass (higher resistivity, ÷1.5 times grater) and also it is more expensive.

The geometrical definitions for the winding are the following :

- $2n$ are the active seres conductors of a coil, each conductor is placed in a different slot

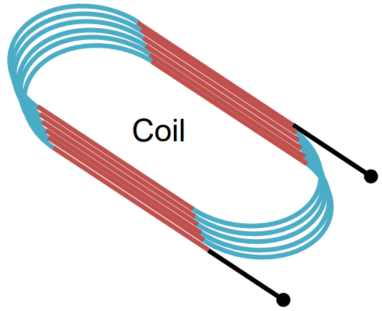

Figure 2.12: Coil

- $N = qpqn = 144$ is the number for series conductor per phase
- $n = 9$ is the number of equivalent conductors in each slot (more slots means more chance to split the winding in more coils)
- $n_b = 6$ number of parallel wire that create a bundle (this value also affect the diameter of the single wire that is chosen among the following catalogue A)

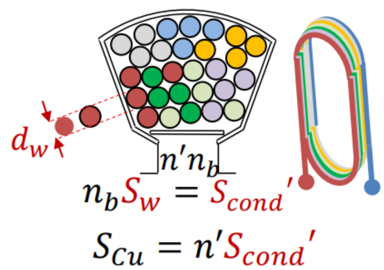

Figure 2.13: Slot and wire

In particular, there is the interest in the series equivalent conductor in each slot.

$$n = \frac{E\sqrt{2}}{2\pi f K_w q B_M L D} = 8.97 \simeq 9 \tag{2.12}$$

This value need to be round to the closest integer (or half if a parallel configuration is expected) number, in this case the result is $8.97 \div 9$ that is easily approximate with the following integer so it is possible to take this value has the number of equivalent conductor in series in each slot. Since for this design is continent to have a shortening of the stator winding, value of the physical conductor in series in each slot should be an even number.To reach this goal, it is a good idea to have two parallel paths; $z = 2$ number of parallel.

$$n' = zn = 2 * 9 = 18 \tag{2.13}$$

Thanks to this parallel configuration, some additional consequence is evaluated:

- The parallel configuration can introduce a different voltage drop along each branch, due to the un ideality of the conductor, this may lead to a circulating current (DROP MMF)
- In this specific case with the parallel that increase the number of the physical conductor in

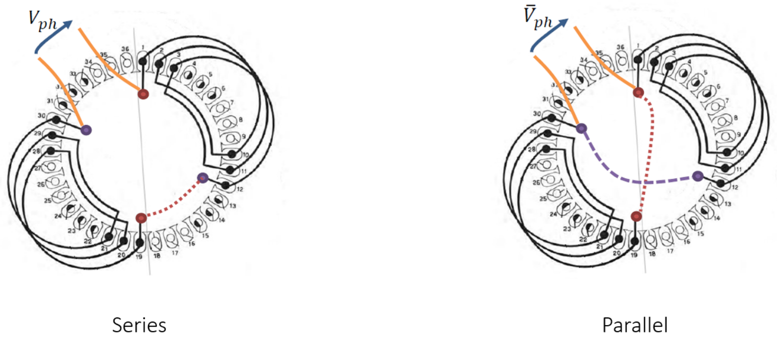

Figure 2.14: From series to parallel (qualitative)

seres in each slot, come out as advantage since a number of conductors lower than 10 is usually considered not so easy to manage the winding

The numbers of series conductor per phase $N = 2pqn$, is a fundamental parameter that is used often during the whole design, but especially is useful to the evaluation of the real value of the magnetic loading.

2.2.4 Slot parameters

From the catalogue (A) is possible to obtain also the geometrical values referred to the slots

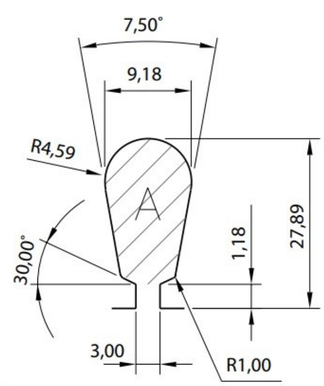

Figure 2.15: Stator slot (qualitative)

It was previously shown the value of the total area of a slot but is needed to introduce also the area of the total conductors in each slot (also called Copper Area)

$$S_{cu} = n_b n' S_w = 77.026mm^2 \tag{2.14}$$

$$S_w = \pi(\frac{dw}{2})^2 = 0.713mm^2 \tag{2.15}$$

The difference between the Slot Area and the Copper Area are evaluated thought a factor called Fill Factor. This value can range between, $0.38 \div 0.42$ depending on many reasons :

- The conductors must be insulated from the components that do not have a galvanic contact with them like the iron lamination and the mechanical components and from conductors of other phases

- if the shortening is present it is more likely to be from $0.38 \div 0.40 = 0.38$ since there is and additional

- if there are many conductors and many bundles, the implies also additional coating, so it might happen to have a lower value

This huge difference is motivated by the fact that it is needed to have a coating around each wire in order to electrically insulate the wire (according to the rated voltage, the transient overvoltages and the voltage wave shape) and is also difficult to have a high fill factor also because of the particular shape of the slots and most of the time an automated winding procedure lead to even lower fill factor, since the distribution may be random inside the slot.

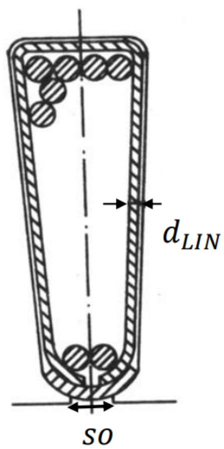

Figure 2.16: Insulation from iron

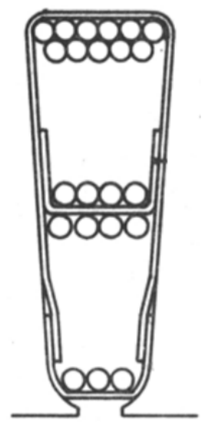

Figure 2.17: Insulation between different phase

On the winding, it is possible to add other interesting consideration

- changing n varies the airgap flux density B_M [9]

- L can be updated to obtain and integer n without affecting B_M

- the winding connection $(Y to \Delta)$ can be exploited to increase n by 3

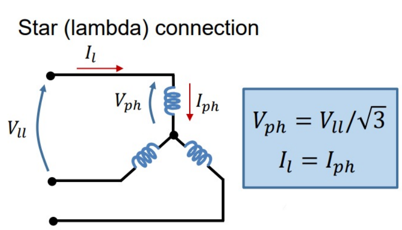

Figure 2.18: Star/Y connectionl (qualitative)

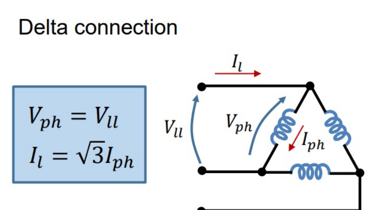

Figure 2.19: Delata connectione

- groups of coils can be connected in parallel to allow having n' = nz conductors per slot. In this way, it is n' that has to be an integer.

[9] this check is done at the end of the FEA analysis, since it is convenient to evaluate the values by also considering saturation and simulation results

2.2.5 Limitation

The previous design flow should respect some constrains:

- The current density is strongly affected by two main parameters: the first one is the type of cooling that is used for this motor in this case the self ventilated motor (or TEFC) introduce the limit of the $J \leq 6.5\frac{A_{rms}}{mm}$ for the current density

$$J = \frac{I_ph}{S_{cond}} = 6.007mm^2 \qquad S_{cond} = \frac{S_{Cu}}{n} = 8.558mm^2 \tag{2.16}$$

- The actual conductors in the slot must have an industrial diameter d_w that must not be limited (to max 1-1.2 mm) to allow easily insert it in the slot.

- The slot filling factor Ff should consider the use of commercial wires d_w that must be easily to insert in the slot opening, so $d_w \leq$ slot opening)

$$d_w = 2\sqrt{\frac{S_w}{\pi}} = 0.95mm \qquad s_o = 3.0mm \tag{2.17}$$

  Is usually suggest tho chose the wind dimension at leat $d_w = s_o - 1.6mm$ so in this case this suggestion is respected

- A particular attention is in the distribution in the conductors in order to avoid at maximum parasitic effect like the skin effect or the circulating current(that can be avoided thanks to their layout by using litz wires, but become inconvenient for at low frequency operation, that way in this project are avoided)

2.2.6 Insulating materialss

To provide a electrical thermal and mechanic isolation in this machine are needed the some insulating material. Mainly in the slots we can find them around the wire and inside this lot in order to reduce at minimum the vacuum between the wire, but it is also important too ground D internal surfaces of the slot and separate two different phases if the shortening is present. The choice of this material are evaluated after a proper thermal analysis of the machine at working condition, by using commercial material. A deeper analysis for law in the appendix A.

2.3 Airgap

The airgap is the region of the motor in which the fluxes produced by the stator induced a current in the rotor bar that are contributing also to the airgap fluxes, this flux and the rotor is asynchronous with respect to the magnetic field at airgap.

It is possible to look for an airgap thickness by considering some relation between the magnetic loading Δ and other numbers as the number of conductor in series per pole per phase N, the phase current I_{ph} and the diameter D. By comparing this value in the table.

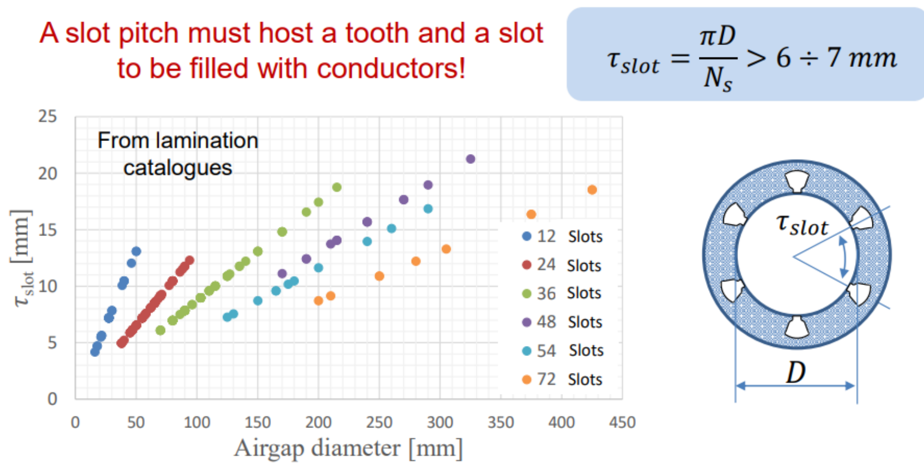

Figure 2.20: Airgap

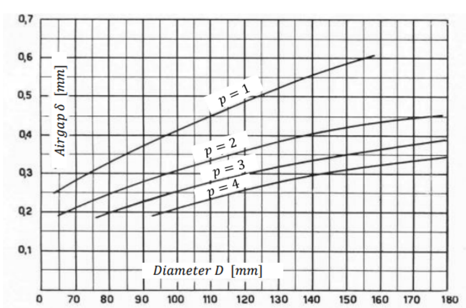

Figure 2.21: Airgap

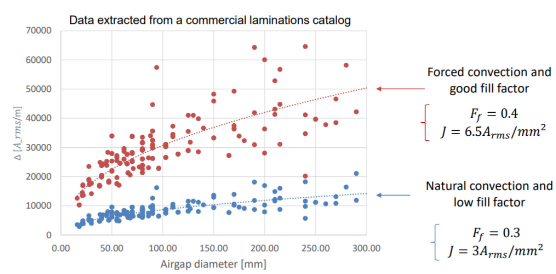

Figure 2.22: Airgap

It is good to underline that all these four way to reach the effective value of the airgap thickness converge in a range of acceptability that will depend on the single cases. This result is important to be able to validate the result of this design with the design already exploited by the industrial world after years of experience. The general formula to evaluate the airgap thickness is the following:

$$\delta \simeq 5.5 \frac{D}{\sqrt{2p}} = 0.577mm \tag{2.18}$$

By look at the plot that involve power for high efficiency motor, it is possible to stress this value until 1 mm, so in order to reach also more reliable value of power factor (since here not all the real contribution are taken into consideration so it is possible to obtain a too high value of Power Factor), it is possible to increase the airgap until 0.8 mm[10].

[10]with $\delta = 0.98$ mm is possible to obtain the same Power Factor needed from the requirement but since this motor is more likely devolve to application that not stress a lot of efficiency above the value expected from the norms, it is convenient to remain slightly below the threshold that is shown in the plot with the power, and it is accepted a higher value of power factor that is detailed that in the following chapters

In reality, what really is must be taken as a forced constraint is the lower limit of the airgap that is set by the mechanical tolerances that are needed to properly work.

$$\delta_{min} = 3.06 - \frac{6560}{D(mm) + 2280} = 0.425(mm) \tag{2.19}$$

The tolerances, in particular in this region are crucial since the airgap is obtained by mechanically shaping the rotor geometry until reaching the desired the thickness of the gap, that will be the space between the two physical geometry (stator and rotor) and also it will be the core region in which the flux is going to act in order to produce torque.

2.4 Rotor

ROTOR (parlare del die cas 8The deign of the rotor starts from the choice of the conductors. Winding layout similar to the one of the stator is possible, but for the values of current that are involving this region is better to introduce the squirrel cage configuration

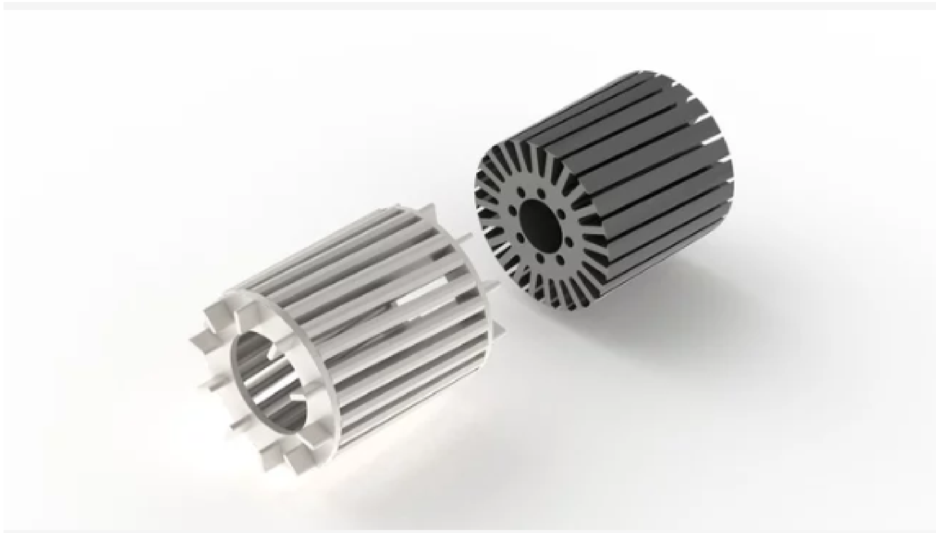

Figure 2.23: Squirrel cage and rotor lamination

For this conducting part, the material to adopt is usually one between the aluminium or copper as for the winding by using the aluminium it increases the resistivity of the conducting material but at the same time it reduce costs and mass density (A). One chose the aluminium, the manufacturing process suggest using the die cast process because of the low melting temperature point in order to obtain a Fill factor for the rotors bar that can be approximated to 1 and moreover this process is fast and easy to adapt to different laminations.

The rotor that is made of two parts, the lamination made in silicon carbon has the stator [11]. The second element of the rotor is the squirrel cage that is the result of a die cast process of aluminium, from that it is possible to obtain the rotor bars and the two end rings that short circuit the bars.

Some geometrical parameters are directly provided by the catalogue: the number of rotor slot (that are also compatible with the general guideline provide to us for the unconstrained design) that means the manufacturer follow a common guideline without trying to find a new configuration, that will need lots of additional validation on the software but also during their working life.

Poel pairs p	Stator slots N_s	Rotor slots N_{sR}
p=1	18 24 36	10-16-22 10-16-18-22-28 10-16-22-28-30-40-46
p=2	24 36 48	14-18-22-(26)-30 10-14-22-26-28-30-42-46 10-14-18-20-30-32-34-38-40-42-54-58
p=3	36 54 72	26-27-28-30-32-34-38-40-44-45-46 34-38-39-40-44-45-46-50-52-56-58-62-63-64-68-69 50-51-52-56-57-58-62-63-64-68-70-74-76-80-81-82-86-87-88-92-93

Figure 2.24: Slots relation

[11] usually to optimize the costs of the final product it can be used the same lamination sheet to extract both the stator and rotor geometry and only in a second moment obtain also the air gap thickness by shaping there rotor

Now looking also at the geometries introduce for the rotor, they are given in the catalogue, but they are not scaled, so they are just quantitative values,

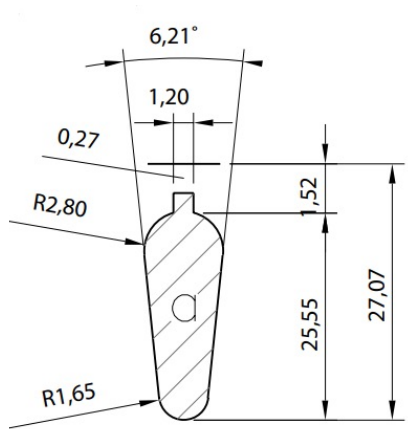

Figure 2.25: Rotor slot

As it was done for the stator, also with the rotor is it possible to reduce some harmonic content by introducing another means, the skewing. The skewing is the procedure that implies a constant rotation of each sheet around their common axle, that pass through the centre of the geometry, until it is obtained a misalignment between the bottom and the upper sheet of an integer number of rotor bars or stator slots, these two way are characterized by the coefficient α_r or α_s.

Figure 2.26: rotor skewing

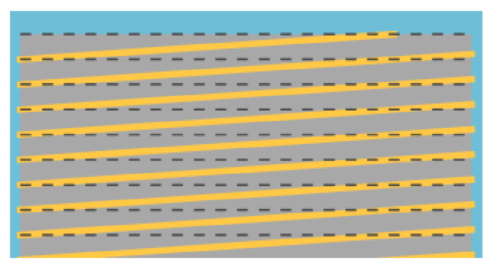

Figure 2.27: Rotor skewing

This new degree of freedom is express through the formula of K_{skew}:

$$K_{skew} = \frac{2sin(\frac{h\alpha_{skew}}{2})}{h\alpha_{skew}} = 0.9971 \tag{2.20}$$

$\alpha_{skew} \simeq K\alpha_{slot}$	
α_{slot} **Stator**	α_{slot} **Rotor**
$\alpha_{slotS} = \frac{p2\pi}{N_s}$	$\alpha_{slotR} = \frac{p2\pi}{N_r}$

From the previous table it was possible to look at the analytic workflow that is needed to reach a value, hence the result on the harmonic behaviour is given by the next picture that take into consideration a lamination different from that one (with different numbers of slots and bars) but is interesting to underlined how the harmonic content can vary by changing these parameters (q_{sh} and a_{skew}) ;

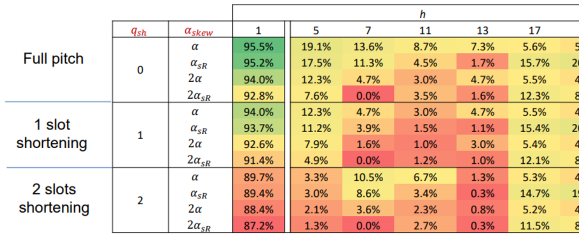

	q_{sh}	α_{skew}	h: 1	5	7	11	13	17	
Full pitch	0	α	95.5%	19.1%	13.6%	8.7%	7.3%	5.6%	5
		α_{sR}	95.2%	17.5%	11.3%	4.5%	1.7%	15.7%	20
		2α	94.0%	12.3%	4.7%	3.0%	4.7%	5.5%	4
		$2\alpha_{sR}$	92.8%	7.6%	0.0%	3.5%	1.6%	12.3%	8
1 slot shortening	1	α	94.0%	12.3%	4.7%	3.0%	4.7%	5.5%	4
		α_{sR}	93.7%	11.2%	3.9%	1.5%	1.1%	15.4%	20
		2α	92.6%	7.9%	1.6%	1.0%	3.0%	5.4%	4
		$2\alpha_{sR}$	91.4%	4.9%	0.0%	1.2%	1.0%	12.1%	8
2 slots shortening	2	α	89.7%	3.3%	10.5%	6.7%	1.3%	5.3%	4
		α_{sR}	89.4%	3.0%	8.6%	3.4%	0.3%	14.7%	19
		2α	88.4%	2.1%	3.6%	2.3%	0.8%	5.2%	4
		$2\alpha_{sR}$	87.2%	1.3%	0.0%	2.7%	0.3%	11.5%	8

Figure 2.28: rotor skewing

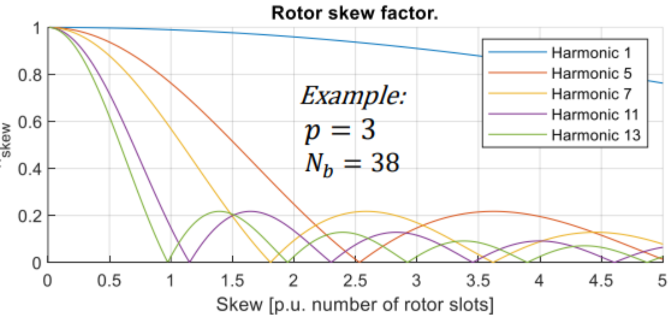

Figure 2.29: Rotor skewing

Bar skew has a similar effect to that of the distribution factor seen for three-phase windings. This aim of this manufacturing technique is to prevent the stator and rotor teeth from being perfectly facing each other and aligned for the entire axial length of the motor, in particularly this improves the performance by reducing three main components :

- reduce the torque pulsations due also to the force of attraction between the stator and rotor teeth can determine a sticking torque (electromagnet effect) higher than the driving torque. Even at full speed, unacceptable torque pulsations may remain so in order to reduce as much as possible, it is chosen a skew angle close to an integer number of stator or rotor slot pitches, then the slotting torque is minimized.

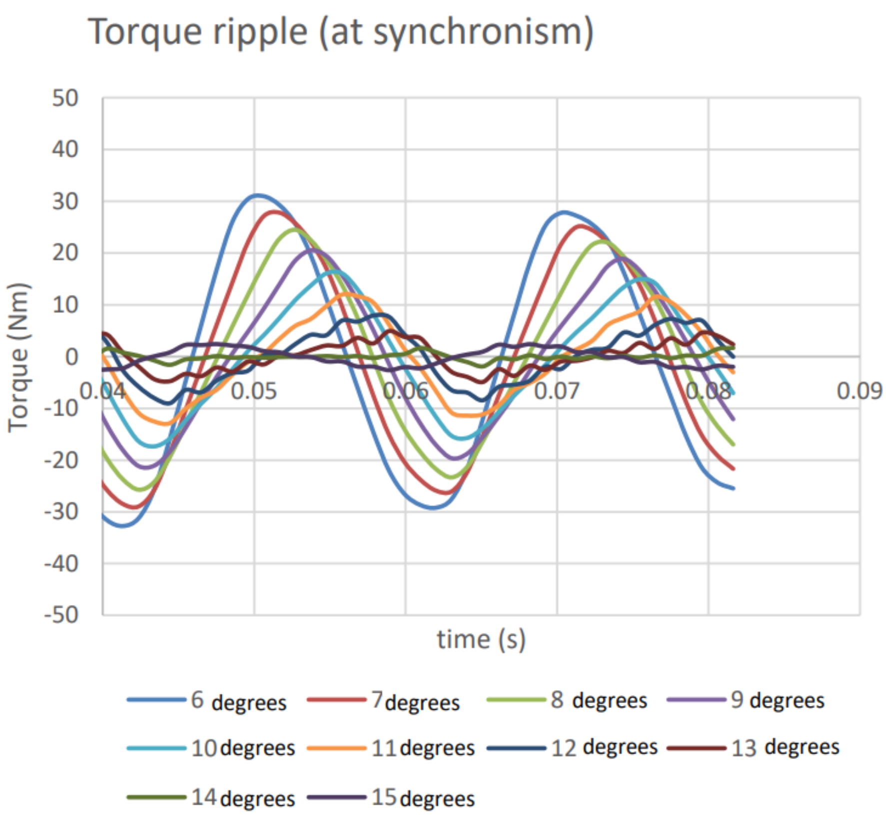

Figure 2.30: Torque ripple

- reduce the field harmonic and trying to keep high the one that produce torque, but at the same time is suggested to reduce the $7-th$. The squirrel cage rotor ideally reacts to all field harmonics at the air gap generating asynchronous torque and/or torque ripples. The torque characteristic due to the seventh harmonic has a synchronism value at low positive speeds. In particular cases, the rotor may jam at speed ω_{c7} during machine start-up.

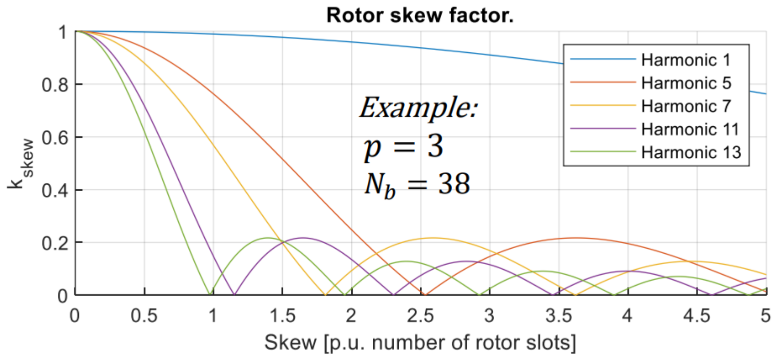

Figure 2.31: Skew

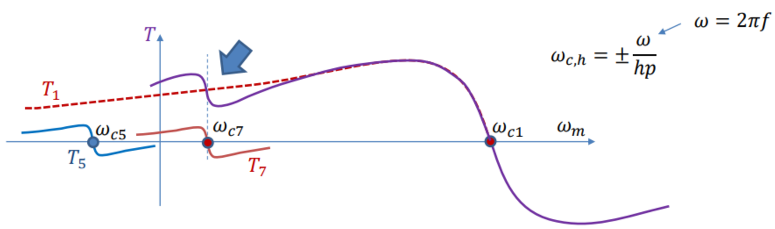

Figure 2.32: Charatteristic

- reduce the emf induced in the rotor

$$E_R = j\frac{w_R K_{skew}\phi_{M\tau}}{2\sqrt{2}} \tag{2.21}$$

Once arrive at that point, it is possible to evaluate the current that flow in the rotor. The currents in the arches of each ring, between neighbouring rotor slots (bars), can be evaluated in terms of phasors, and then they can be evaluated as their equivalent values:

$$I_{bar} = \frac{I_{ph}cos\phi 3}{N_b}(\frac{NK_w}{K_{skew}}) = 317.231(A) \tag{2.22}$$

$$I_{ring} = \frac{I_b}{2sin\frac{p\pi}{N_b}} = 1467.0470(A) \tag{2.23}$$

2.4.1 Limitation

With this value of current as in the stator It is possible to evaluate a current density parameter J_x that is lower in magnitude in respect to the stator one, and also it is possible to distinguish between bar current density J_b and ring current density J_r.

$$J_b = \frac{I_b}{S_{slotR}} = 2.832 \qquad J_r = \frac{I_r}{S_ring} = 2.832 \tag{2.24}$$

IT was assumed that the two current density should be the same since the ratio between the currents and the slot area is very similar; moreover, this density is limited to be lower than $4.5\frac{A_rms}{mm^2}$ depending on :

- the ratio between the resistivity of copper in respect to the aluminium is 1 : 1.6 on the average condition, so the aluminium have a higher resistivity (A) but it is counterbalanced by the fact that it is possible to exploit at its maximum the bar area since it present a fill factor near to 1

- Cooling system always have a major impact on that value since it can vary a lot depending on the different solution

2.5 Sizing

The following parameter evaluation it was done by following the approximation of having a sinusoidal contribution of the flux at airgap [12]

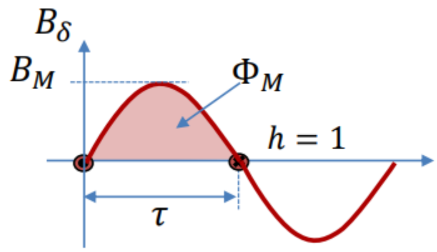

Figure 2.33: Sinusoidal flux at airgap

2.5.1 Teeth

The teeth are designed for a peak flux density BMT star, limited by the material B(H) characteristic and by the iron losses.

To limit the iron saturation and AC losses, a reasonable range for conventional IMs is:

$$(1.3) \leq B_{Mt} \leq (1.8 \div 1.8)T \tag{2.25}$$

The lower limit is where the operating condition at high ow speed (or high frequency) while the upper limit is indicated for low speed application.
Higher values can be tolerated in the rotor teeth because the rotor iron losses are negligible, unless MMF drop becomes too high.

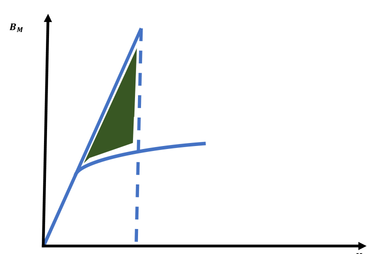

Figure 2.34: B-H curve (qualitative)

So it is suggested to work around the knee of saturation in order to stress at maximum the flux density without loosing in efficiency

[12]It will be evaluated later the real value of the flux at airgap, now it is just taken into consideration the peak value corresponding to a pure siusoid

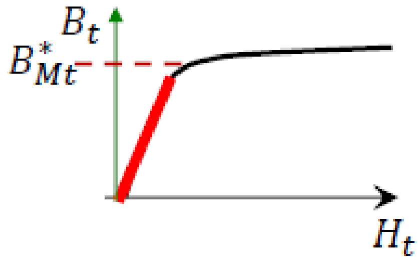

Figure 2.35: BH curve

The path of the teeth is smaller than the one in the yoke. The drop of MMF have to be compensated by an increasing of the current, so more there is saturation more MMF drop it is present and more current is needed to magnetize the iron core listed of producing torque. $B_{M_y} < B_{M_t}$ [13]

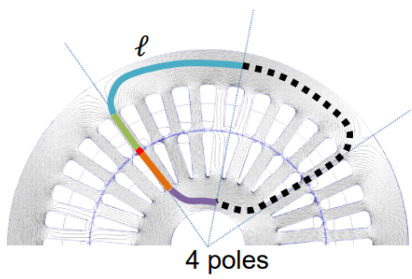

Figure 2.36: Flux path

By following the constraint design that fix the tooth width is possible to evaluate both the flux that cross the tooth and the one who cross the slot pitch (that for a first moment are considered equal):

$$\phi_{Mt} \simeq \tau_s L B_M \qquad \phi_{Mt} = w_t L B_{Mt} = 0.01719 \tag{2.26}$$

$$B_{Mt} = \frac{\tau_s}{w_t} B_M = 1.627 \tag{2.27}$$

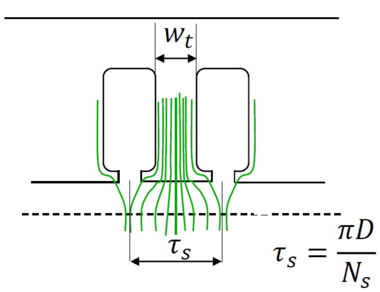

Figure 2.37: Geomery

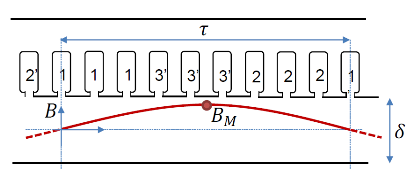

Figure 2.38: Tau

[13] B_{M_y} is the value of magnetic flux density of the yoke while $< B_{M_t}$ is the teeth one and these values are strongly affected by geometrical parameters, since a thin tooth means an higher limitation in terms of flux density

2.5.2 Yoke

Same consideration can be done for the yokes but with different thresholds since here it is experience an higher MMF drop for the same saturation level due to the longer path available for the flux[14];

$$(1.1) \leq B_{My} \leq (1.5)T \tag{2.28}$$

Similar to what it was done in the stator, the half of the flux per pole $\phi_{M\tau}$ that crosses the yoke by considering sinusoidal the distribution of the aigap flux is the following:

$$\Phi_{M\tau} = \frac{2}{\pi} B_M L \tau = B_M L \frac{D}{p} \tag{2.29}$$

By considering the flux density evenly distributed in the yoke so:

$$\phi_{My} = \frac{\Phi_{M\tau}}{2} \simeq 0.5 B_M L \frac{D}{p} \qquad \phi_{My} = h_y L B_{My} \tag{2.30}$$

And the flux density in the yoke can be calculated as:

$$B_{My} = \frac{D B_M}{2 p h_y} = 1.471 \tag{2.31}$$

It is needed to underline that the rotor yoke is limited by the rotor shaft diameter. Also, ferromagnetic shafts can help to obtain a lower flux density in the yoke (lack of lamination in the shaft is not a problem because the rotor frequency is lower). Then it lowers the losses and MMF drops make often $h_{yR} h_y$.

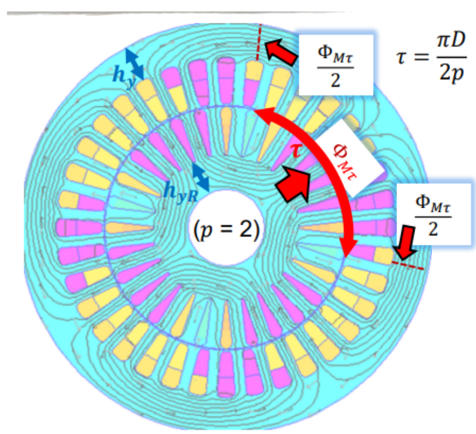

Figure 2.39: Yoke

2.5.3 Geometry

The geometry of the stator and rotor slots, end winding, and end ring were previously introduced by looking at the catalogue but now is better to underline some geometrical detail that are useful for the next design steps

Slots

This motor has a single cage configuration, so the geometry of the rotor is similar to the one of the stator. Both geometries should be divided in subsection in order to be able to replicate the real geometry also in the FE software and in addition add some comment.

[14]In induction motor is common to have yokes volumes higher than teeth volumes, this lead to higher losses

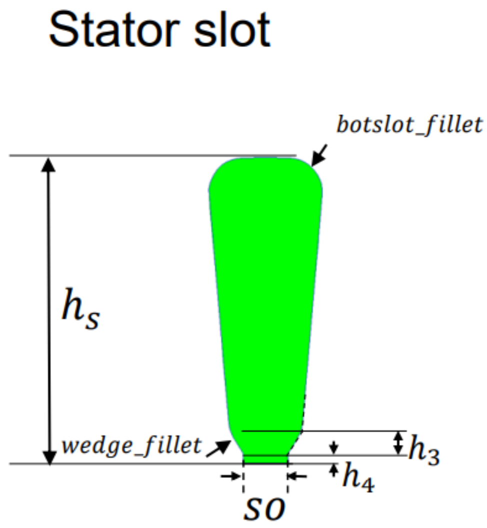

Figure 2.40: Stator slot

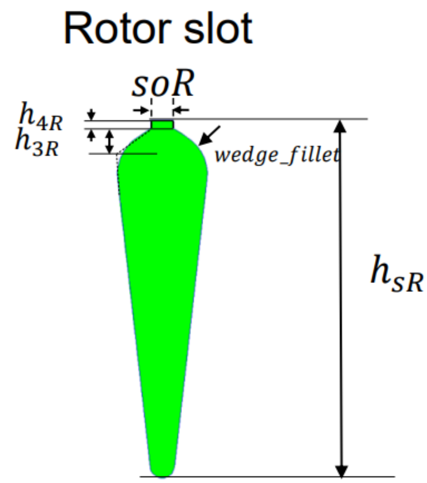

Figure 2.41: Rotor slot

This value are useful for build the geometry in the software, but by looking at the following picture is interesting to look also at how the winding are shared in the geometry of the stator [15], it is possible to have some region in which is no present any conductor as $h2$ or is easier to appreciate how the phases share the same slot

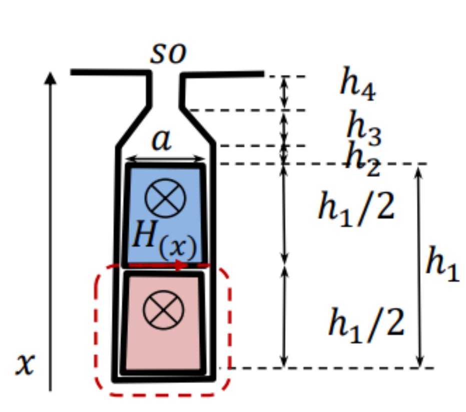

Figure 2.42: Geometry of slot (qualitative)

The next picture is an example of how the slot of this project might look like :

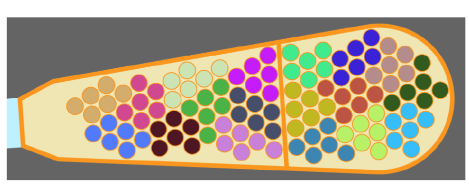

Figure 2.43: Geometry of slot (quantitative)

[15]Rotor bar have a fill factor ÷1 so it is not needed a detailed description as it is done for the stator

End winding

And now it is possible to evaluate the length of the end winding that is the non active region of the coil, this length depends on the winding manufacturing and also the winding choice like the shortening.

$$L_{ew} = k_{ew}\tau_{ew} = k_{ew}\frac{2\pi(D+h_s)y_q}{N_s 2} \div 2.3\tau \qquad y_q = 3q - q_{sh} \tag{2.32}$$

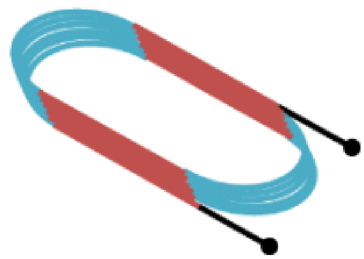

Figure 2.44: End winding (blue)

2.6 Volume and Weight

Most of the geometry seen since now, was evaluated for a 2 D geometry and only few parameters were useful to describe the third space orientation like the end winding or end rings. Now what is important to underline is that this motor in the real life is represented in a 3D way.(A)

2.6.1 Volumes and Weights

2.6.2 Stator teeth

$$V_t = N_s w_t h_s L \qquad G_t = \psi_{lam} V_t \tag{2.33}$$

2.6.3 Stator yoke

$$V_y = \frac{\pi}{4}(D_{ext}^2 - (D_{ext} - 2h_y)^2) \qquad G_y = \psi_{lam} V_y \tag{2.34}$$

2.6.4 Rotor teeth

$$V_{tR} = N_r w_{tR} h_{sR} L \qquad G_{yR} = \psi_{lam} V_{yR} \tag{2.35}$$

2.6.5 Rotor yoke

$$V_y = \frac{\pi}{4}((D_{int}^2 - 2h_y)^2 - D_{int}^2) \qquad G_y = \psi_{lam} V_y \tag{2.36}$$

2.6.6 Stator Copper

$$V_{Cu} = 6qpnS_{cond}(L + L_{ew}) = N_s S_{Cu}(L + L_{ew}) \qquad G_{Cu} = \psi_{lam} V_{Cu} \tag{2.37}$$

2.6.7 Rotors Bars

$$V_b = N_{sR} S_{slotR} L \qquad G_b = \psi_b V_b \tag{2.38}$$

2.6.8 Rotors Rings

$$V_r = 2S_{ring}(D - h_{sR}L \qquad G_r = \psi_r V_r \tag{2.39}$$

2.6.9 Case choice

Each motor (rotor + stator) should be able to be inserted a proper cage in order to increase the strength against external interference (dust, liquid of mechanical interference). Moreover, there case allow the cooling system to let the liquid (in this case air) to flow above the stator, in the fins region) where it will extract thermal power and so reduce the temperature). So to do that it is mandatory to choose a proper case that is not over estimated in order to not increase the weight and the occupied volume. By looking at some main parameter (active length, fins thickness, frame number [16], end winding length) it is possible to choose a proper case[17], the following tables are referred to a TEFC motor IC41 :

[16] that is related to the lamination chosed

[17] CEI EN IEC 60072 1 Dimensions and output (power) series.

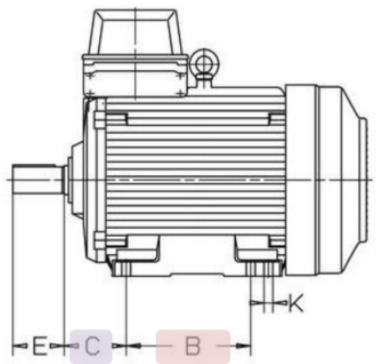

Figure 2.45: Case

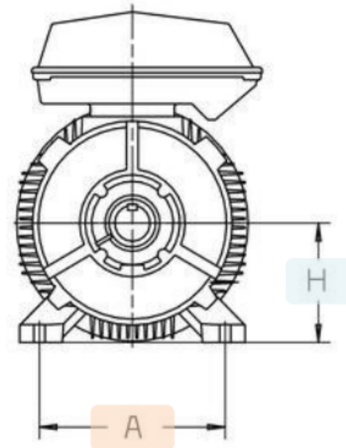

Figure 2.46: Case

Shaft height H [mm]

Frame number [a]	H Nominal mm	H Maximum deviation mm	A[d] mm	B[d] mm	C[d] mm
56M	56	−0,5	90	71	36
63M	63	−0,5	100	80	40
71M	71	−0,5	112	90	45
80M	80	−0,5	125	100	50
90S	90	−0,5	140	100	56
90L	90	−0,5	140	125	56
100L	100	−0,5	160	140	63
(112S)	112	−0,5	190	114	70
112M	112	−0,5	190	140	70
(112L)	112	−0,5	190	159	70
132S	132	−0,5	216	140	89
132M	132	−0,5	216	178	89
(132L)	132	−0,5	216	203	89
(160S)	160	−0,5	254	178	108
160M	160	−0,5	254	210	108
160L	160	−0,5	254	254	108
(180S)	180	−0,5	279	203	121
180M	180	−0,5	279	241	121
180L	180	−0,5	279	279	121
(200S)	200	−0,5	318	228	133
200M	200	−0,5	318	267	133
200L	200	−0,5	318	305	133

Figure 2.47: Standards

Frame size	Shaft extension diameter 2 poles mm	Shaft extension diameter 4, 6, 8 poles mm	Rated output 2 poles kW	Rated output 4 poles kW	Rated output 6 poles kW	Rated output 8 poles kW
56M	9	9	0,09 or 0,12	0,06 or 0,09		
63M	11	11	0,18 or 0,25	0,12 or 0,18		
71M	14	14	0,37 or 0,55	0,25 or 0,37		
80M	19	19	0,75 or 1,1	0,55 or 0,75	0,37 or 0,55	
90S	24	24	1,5	1,1	0,75	0,37
90L			2,2	1,5	1,1	0,55
100L	28	28	3	2,2 or 3	1,5	0,75 or 1,1
112M	28	28	4	4	2,2	1,5
132S	38	38	5,5 or 7,5	5,5	3	2,2
132M		38	-	7,5	4 or 5,5	3
160M	42	42	11 or 15	11	7,5	4 or 5,5
160L		42	18,5	15	11	7,5
180M	48	48	22	18,5	-	-
180L		48	-	22	15	11
200L	55	55	30 or 37	30	18,5 or 22	15
225S	55	60	-	37	30	18,5
225M		60	45	45		22
250M	60	65	55	55	37	30
280S	65	75	75	75	45	37
280M		75	90	90	55	45
315S	65	80	110	110	75	55
315M		80	132	132	90	75
315L		90	160 or 200	160 or 200	110, 132, 160	90, 110, 132

Figure 2.48: Standards

In the value that are more suitable with this parameter are the following:

(180S)	180	−0,5	279	203	121	14,5	M12
180M	180	−0,5	279	241	121	14,5	M12
180L	180	−0,5	279	279	121	14,5	M12
(200S)	200	−0,5	318	228	133	18,5	M16
200M	200	−0,5	318	267	133	18,5	M16
200L	200	−0,5	318	305	133	18,5	M16
225S	225	−0,5	356	286	149	18,5	M16
225M	225	−0,5	356	311	149	18,5	M16
(225L)	225	−0,5	356	356	149	18,5	M16
250S	250	−0,5	406	311	168	24	M20
250M	250	−0,5	406	349	168	24	M20
(250L)	250	−0,5	406	406	168	24	M20

Figure 2.49: Standards

In this case the suitable case goes from the 225S and over due to the limitation of the external diameter and also the need of inset fins

2.6.10 Raw material cost

The evaluation of the cost of this motor can be done by roughly considering the price of the raw material. It is important to consider that it is completely neglecting the human or the machinery effort that is needed in order to provide a finial result as the motor finished, but just to have a clue of where is the lower limit of the money that need a motor like this to be built.

MAterial	Weight	Eur/kg	Eur	Total
Iron	108.64	1.6	173.82	
Copper	15	8	120	
Insulating materials	x	x	x	
Total				293.82

2.7 Perfomances

The standards determine efficiency classes for mains-powered asynchronous machines. The efficiency levels for each class depend on the number of poles of the machine (considering the 4-pole motors have the most restrictive limits) [18] (A).

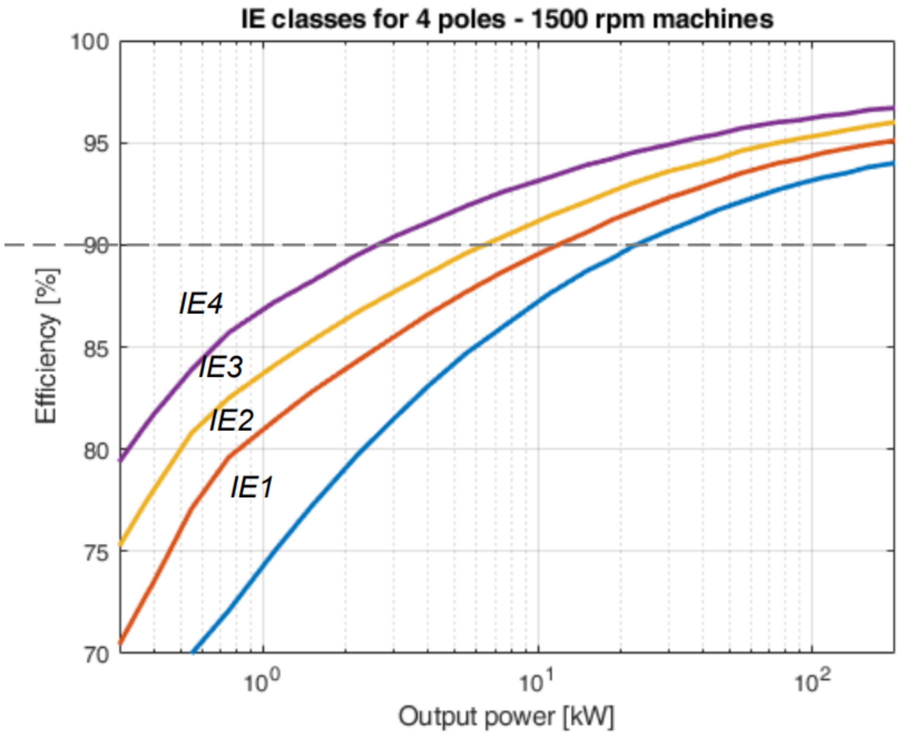

Figure 2.50: Efficiency classes

The expected value for this design is to have a motor of IEC class 2 that at rated power condition $33.5kW$ work with an efficiency of 92%

In order to check this value is convenient to start looking to some value that are affecting the efficiency of this motor, that are differentiated in different type of losses

2.7.1 Losses

iron non related to bh curve, are related to the current that change flux in time so at hysteresis loop. hyst loop, hysteresis little change with B value,

Iron losses

The iron losses are the ones that affect all the region made of iron, so the lamination region. As it is deepened explained in the appendix (A), it is possible to obtain some coefficient that allow to evaluate the specific losses in different operating condition depending on the peak value of H and B that are used in that specific region.

$$\frac{P_{loss}}{G_{fe}} = K_i f B^2 \alpha + K_c f^2 B^2 (\frac{W}{kg}) \tag{2.40}$$

[18] CEIENIEC60034-30-1 – International Energy Efficiency classes of line operated AC motors(IE code)

$K_c = \frac{s^2}{\rho}$ is the contribution that take care of the iron loses due to the eddy current, and it depends on the lamination thickness ($0.35 \div 0.5$ mm usually) and on the ρ resistivity.

$$P_{fe,total} = P_{fe,teethS} + P_{fe,teethR} + P_{fe,yokeS} + P_{fe,yokeR} = 68.842 + 166.718 + 0.997 + 0.60 = 237.166(W) \quad (2.41)$$

$$P_{fe,x} = k_l G_x P_{loss} \quad (2.42)$$

Here the lamination factor $1 < k_l < 2$ take into consideration the manufacturing process needed to realize the desired lamination geometries and also the post process like the post aneling that is needed to restore a part of the magnetic properties of the material

In reality, the iron losses directly depend on the magnetizing current that are induced by the change of the flux during the time and that is reflected on the hysteresis loop (A) that is partially affected by the variation of the magnetic density. But looking at the behaviours of the MMF it is possible to say that at the very first if a certain iron region is experience the saturation, due to the non ideality of iron (with permeability << than infinite), to reach the saturated value of B, it is needed a high current to be magnetized and the iron at high saturation have all the magnetic domain (Weiss) already oriented so a very huge current is needed to increase the magnetic density of few values

Stator Joule losses

The Joule losses in the stator of induction motors can be calculated from the copper volume, the resistivity of the conductors at the operating temperature, and the current density as:

$$P_{jS} = P_{Cu} = \rho_{cu} V_{Cu} J^2 = 1265.438(W) \quad (2.43)$$

Note: in case of uneven current distribution, additional losses must be considered. This can be due to high frequency currents (e.g., above 400 Hz for high-speed applications) or, more often, current distortion (harmonics and/or inverter supply). For this project, the assumption is to consider the current equally distributed in the conductor

Rotor Joule losses

The currents in the rotor bars and rings at rated operation can be assumed to be almost sinusoidal and evenly distributed due to cage skewing and low rated rotor frequency, f_r few Hz).

$$P_{jR} = P_b + P_r = \rho_{cu} V_{Cu} J^2 = 558.713(W) \quad (2.44)$$

It is fair to underline that the ring and bars' currents are evaluated at rated condition when the reference point of view is in the stator that see how the rotor change in the time. Note: the resistance of the rotor conductors must be considered at the expected temperature, plus a slight increase (8-10%) due to die-casting process of Aluminium.

Mechanical losses

Ventilation, windage, and friction losses depend on the speed, machine geometry, and mechanical design (ventilation system, aerodynamic, and bearings).

Figure 2.51: Ventilation system

This contribution can be evaluated by considering that these mechanical losses are typically correlated by an exponential relation between these losses and the mechanical speed, in a qualitative way the following plot represent this relation[19]:

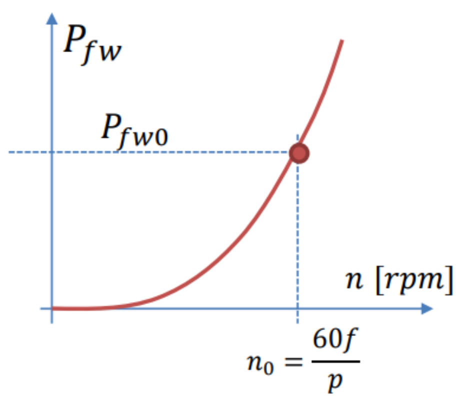

Figure 2.52: Friction losses

The equation that provide a good estimation of the total mechanical power

$$P_{fw} = P_{fw0}(\frac{n}{n_0})^3(W) = 222.853(W) \tag{2.45}$$

$$P_{fw0} = k_w D(L + 0.6\tau)(\frac{\omega_m D}{2})^2(W) = 233.427(W) \tag{2.46}$$

where $k_w = 15(\frac{Ws^2}{m^4})$ this is a small and medium-sized TEFC motor

Additional losses

Induction motors present additional losses in the active parts caused by field harmonics and supply voltage distortion (not perfectly sinusoidal). These losses are mainly caused by eddy currents in the

[19] TEFC induction motor

magnetic circuit, frame, and rotor bars. According to IEC 60034-2, these additional losses can be evaluated as a percentage of the input power (electrical power P_{mains}). For rated power 1kW < P < 10 MW they can be evaluated as:

$$P_{add} = P_{mains}(0.025 - 0.005log_{10}(\frac{P(Watt)}{1000}) = 632.668(W) \tag{2.47}$$

$$P_{mains} = 3VIcos\phi 36413(W) \tag{2.48}$$

There is also some at standards that allow to use $P_{add} \simeq 0.005P_{mains}$

2.7.2 Efficiency

Motor efficiency

The efficiency of the motor is defined as

$$\eta = \frac{P}{P + P_{fe} + P_j + P_{jR} + P_{fw} + P_{add}} = 0.9199 \simeq 0.92 \tag{2.49}$$

The efficiency is important to reduce costs (fuel consumption). International Electrotechnical Commission(IEC) standards identify the minimum efficiency for industrial motors according to their power rating and application (grid connected at fixed speed, inverter fed at variable speed). The higher the power rating, the higher the efficiency requirements. Even in applications where high efficiency has not strict requirements, the losses P_fe, P_Cu, P_fw) must be kept low to limit the temperatures of the components and avoid damaging the motor materials:

- Insulating system then accelerated ageing then machine electrical failure

High efficiency is important in high power-density motors to avoid unaffordable cooling systems

Figure 2.53: IM

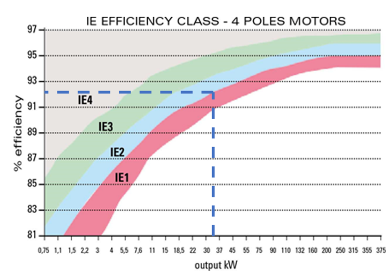

Figure 2.54: Efficiency class

Rotor efficiency

$$\eta_R = \frac{P + P_{fw}}{P + P_j + P_{jR} + P_{fw}} = 1 - s = 0.9659 \tag{2.50}$$

$$s = \frac{P_{jR}}{P + P_{jR} + P_{fw}} \tag{2.51}$$

The slip at rated operation should be in a reasonable range (e.g., motors of similar size). Higher rated slip value could lead to a motor with low efficiency (high losses and over temperatures), whereas a lower slip may result in an oversized motor (volumes/costs).

Slightly different result can be obtained if the induction motor needs to operate at very high efficiency, then the rotor bars should be made of copper instead of aluminium in order to reduce the specific losses and let the motor operate at low rated slip and maintaining a high rotor efficiency

Figure 2.55: IM

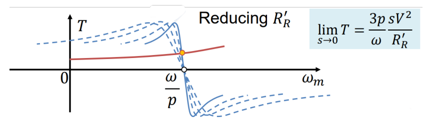

Figure 2.56: Charatteristic

2.7.3 Power factor

The power factor is the ratio between the electrical active power provided to the motor by the supply (grid or converter) and the apparent power:

$$cos\phi = \frac{P_{el,in}}{A} = \frac{\frac{P}{\eta}}{\sqrt{(\frac{P}{\eta}^2 + Q_t^2}} = 0.8709 \tag{2.52}$$

The overall reactive power of the electric motor Q_t can be evaluated with different levels of approximation. A first evaluation can be done using a corrective factor that multiplies the reactive power associated to the magnetic energy in the airgap only :

$$Q_{t,approx} = \omega \frac{B_M^2}{2\mu_0} \pi D L \delta K_{Q_t} \tag{2.53}$$

Where KQt $\simeq 1.8 \div 2$ is an empirical corrective factor that adds the reactive contributions of:

- Stator and rotor leakage inductances
- Stator and rotor Carter's factors (airgap flux distortion caused by the slots openings)
- MMF drops in the laminations (silicon in steel) (especially in case of significative saturation). If we are saturating the lamination, since the permeability of iron is not infinite so we can calculate the drop of MMF, so the extra magnetic energy needed to magnetize the lamination , this value become important if the flux density (in teeth or yoke) is next or above the knee of the BH curve because if it works in linear region H is very little for any value of B, but if the saturation start for a little variation of B it happens a huge increase of H, and having the value of MMF equal to the value of H multiply the length of the considered path.

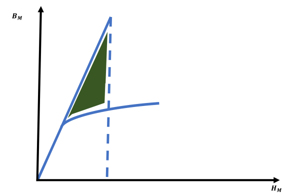

Figure 2.57: B-H curve (qualitative)

If it works in the saturation region of the BH curve, to have an increase of few percent of magnetic flux, it is needed a larger increase of H. having higher H, mean have a larger current to magnetize the circuit.

2.7.4 Standards

CEI EN IEC 60034-12 - Starting performance of single-speed three-phase cage induction motors.

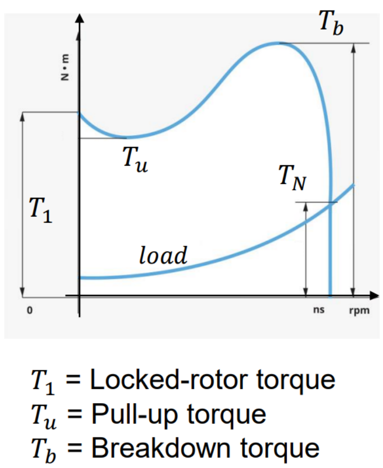

Figure 2.58: Standards points

Gamma di potenza *Power range* (kW)	Numero di poli *Number of poles* 2			4			6			8		
	T_1	T_u	T_b	T_1	T_u	T_b	T_1	T_u	T_b	T_1	T_u	T_b
> 0,4 ≤ 0,63	1,9	1,3	2,0	2,0	1,4	2,0	1,7	1,2	1,7	1,5	1,1	1,6
> 0,63 ≤ 1,0	1,8	1,2	2,0	1,9	1,3	2,0	1,7	1,2	1,8	1,5	1,1	1,7
> 1,0 ≤ 1,6	1,8	1,2	2,0	1,9	1,3	2,0	1,6	1,1	1,9	1,4	1,0	1,8
> 1,6 ≤ 2,5	1,7	1,1	2,0	1,8	1,2	2,0	1,6	1,1	1,9	1,4	1,0	1,8
> 2,5 ≤ 4,0	1,6	1,1	2,0	1,7	1,2	2,0	1,5	1,1	1,9	1,3	1,0	1,8
> 4,0 ≤ 6,3	1,5	1,0	2,0	1,6	1,1	2,0	1,5	1,1	1,9	1,3	1,0	1,8
> 6,3 ≤ 10	1,5	1,0	2,0	1,6	1,1	2,0	1,5	1,1	1,8	1,3	1,0	1,7
> 10 ≤ 16	1,4	1,0	2,0	1,5	1,1	2,0	1,4	1,0	1,8	1,2	0,9	1,7
> 16 ≤ 25	1,3	0,9	1,9	1,4	1,0	1,9	1,4	1,0	1,8	1,2	0,9	1,7
> 25 ≤ 40	1,2	0,9	1,9	1,3	1,0	1,9	1,3	1,0	1,8	1,2	0,9	1,7
> 40 ≤ 63	1,1	0,8	1,8	1,2	0,9	1,8	1,2	0,9	1,7	1,1	0,8	1,7
> 63 ≤ 100	1,0	0,7	1,8	1,1	0,8	1,8	1,1	0,8	1,7	1,0	0,7	1,6
> 100 ≤ 160	0,9	0,7	1,7	1,0	0,8	1,7	1,0	0,8	1,7	0,9	0,7	1,6
> 160 ≤ 250	0,8	0,6	1,7	0,9	0,7	1,7	0,9	0,7	1,6	0,9	0,7	1,6
> 250 ≤ 400	0,75	0,6	1,6	0,75	0,6	1,6	0,75	0,6	1,6	0,75	0,6	1,6
> 400 ≤ 630	0,65	0,5	1,6	0,65	0,5	1,6	0,65	0,5	1,6	0,65	0,5	1,6

Figure 2.59: Standards table

2.8 Equivalent circuits

The equivalent electric circuits are the schematic way to represent the electrical (and mechanical) parameters that simulate the behaviour of the induction motor. The result obtained from this model are pretty accurate, and they can be checked by compare them with the output value of finite element analysis.

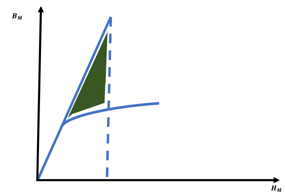

Figure 2.60: B-H curve (qualitative)

At priori it must be known the connection on the winding terminal in order to have in input the actual values of voltages and current, since this motor has a star connection :

$$V_{ph} = \frac{V_{ll}}{\sqrt{3}} \qquad I_{ph} = I_l \tag{2.54}$$

2.8.1 resistances

The circuit is made of 3 main resistances, that stands for the losses in the conductors for both the stator and rotor and a resistance that take into account the iron losses. In addition, there is also another additional resistance in the rotor branch that is there to take into consideration the effect of the slip on the overall effect on the performances

Stator Resistance

$$R_s = \frac{P_{Cu}}{3 * I_{ph}^2} = 0.1596(\Omega) \tag{2.55}$$

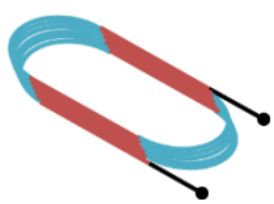

Figure 2.61: Coil

Rotor Resistance

$$R_{Rot} = (\frac{P_b + P_r}{N_b * I_b^2})(\frac{NK_w}{K_{skew}})^2 \frac{3}{N_b} \qquad R(s) = R_{Rot}(\frac{1-s}{s}) = 0.0931(\Omega) \tag{2.56}$$

Where:

$$R_{Rot} = R_{bar} + R_{ring} \tag{2.57}$$

$$R_{bar} = (\frac{P_r}{N_b * I_b^2})(\frac{NK_w}{K_{skew}})^2 \frac{3}{N_b} * KR(f) = 0.0619(\Omega) \quad R_{bar} = (\frac{P_r}{N_b * I_b^2})(\frac{NK_w}{K_{skew}})^2 \frac{3}{N_b} = 0.0312(\Omega) \tag{2.58}$$

The $KR(fr) = \frac{R_{ac}(fr)}{R_{dc}}$ is the contribution of the rotor resistance that change with the rotor frequency during operation at variable slip. This contribution is deeply explained in the FEA chapter

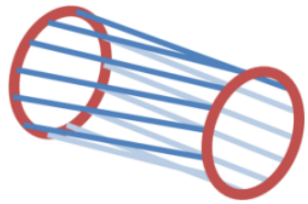

Figure 2.62: Squirrel cage

Iron Resistance

$$R_{fe} = \frac{3E_{ph}^2}{P_{fe}} = 858.3911(\Omega) \tag{2.59}$$

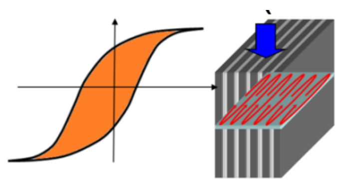

Figure 2.63: AC losses

2.8.2 Leakage inductances

Stator leakage inductances

Under specific hypotheses, some analytical models and semi-empirical formulae are used for a preliminary design.

The stator leakage flux in IM is the sum of four main contributes :

- Slot leakage $L_{l,slot} = 2pqn^2L\lambda_{slot} = 5.247e-04(H)$
- end-winding leakage $L_{l,ew} = 2pq^2n^2\tau_{ew}\lambda_{ew} = 2.90e-04(H)$
- Airgap harmonic contribution $L_{l,\delta} = 2pqn^2L\lambda_{\delta} = 7.793e-05(H)$
- Zig Zag $L_{l,zz} = \frac{5}{6}L_{\mu}(\frac{2p}{N_s})^2 = 2.353e-04(H)$

The previous equation presents all a contribution that is also called permeance, and it is represented by the values $L\lambda$. Each lambda is a permeance per unit length, and it is fair to distinguish them for the different contribution that they carry.

Slot leakage permeance per unit length λ_{slot} con be evaluated by assuming the slot rectangular (instead of the real geometry that is trapezoidal in order to maintain the teeth width constant)

$$\lambda_{slot} = \frac{\mu_0}{q}((\frac{h_1}{3a} + \frac{h_2}{a} + \frac{h_3}{a-s_o}ln(\frac{a}{s_o}) + \frac{h_4}{s_o})q) - \frac{1}{4}(\frac{h_1}{4a} + \frac{h_2}{a} + \frac{h_3}{a-s_o}ln(\frac{a}{s_o}) + \frac{h_4}{s_o})q_{sh}) \tag{2.60}$$

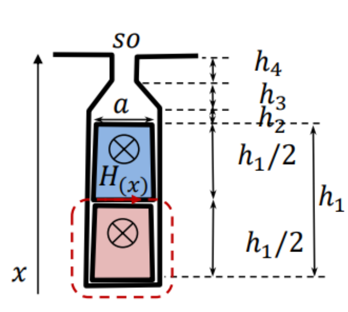

Figure 2.64: Slot geometry (qualitative)

The end winding leakage permeance per unit length (λ_{ew}) is a complex contribution to take into consideration, and it strongly depends on the end winding layout (how are manufactured) so for a three phase windings it can be approximated with the following equations:

$$\lambda_{ew} = mu_0(0.18 \div 0.30) = \mu_0 0.26 \tag{2.61}$$

For what concern the airgap harmonics leakage permeance per unit length λ_δ [20], All the analytical model of the electric motor refers to the fundamental harmonic only ($p - th$). All the other field harmonics at the airgap generate losses and secondary torque contributions (like ripple). All these harmonics are produced by the stator winding, and they do not significantly interact with the rotor, so it can be considered as leakage components. This contribution can be represented as :

$$\lambda_\delta = mu_0 \frac{\tau 3}{\delta \pi^2} \sum_{h=1}^{\sim 17..} (\frac{K_w}{h})^2 \tag{2.62}$$

The Zig Zag leakage inductance is due to the fact that in motors with a thick airgap, some contribution of the flux can close tangentially, thanks to the high reluctance of this part this contribution is almost negligible

In the other hand can happen for motor with thin airgap, that the flux can be involved in a closing path in which it does not link the rotor conductor

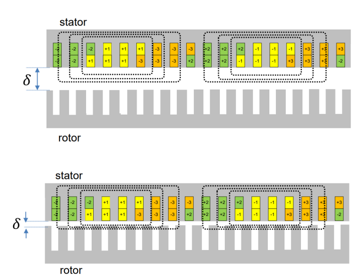

Figure 2.65: Alternative flux paths

Moreover, the flux line can follow different path during the motor operation:

[20]this contribution take also into consideration the belt leakage inductance is harmonic of order grater than one are considered

- At very high slip values, the rotor is mainly inductive, and it reacts by limiting the penetration on the flux core that became with high reluctance

- At high current values like in locked rotor operation ($s = 0$) the flux density increase inducing a high saturation of the lamination and as a consequence it increases the reluctance (becoming very inductive) of the conventional path

and the value of zig zag leakage inductance is related to the percentage of the airgap flux produced by the stator that do not cross the rotor conductor[21].

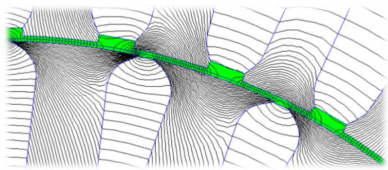

Figure 2.66: Leakage

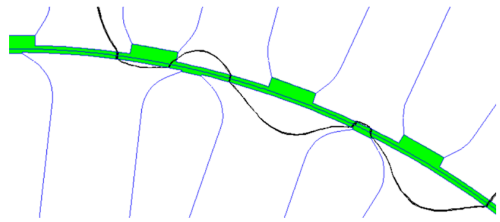

Figure 2.67: Zig zag

From this simulation:

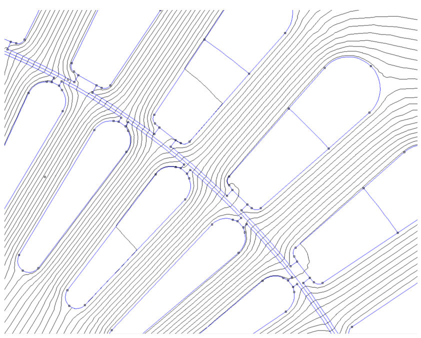

Figure 2.68: Carter factor effect

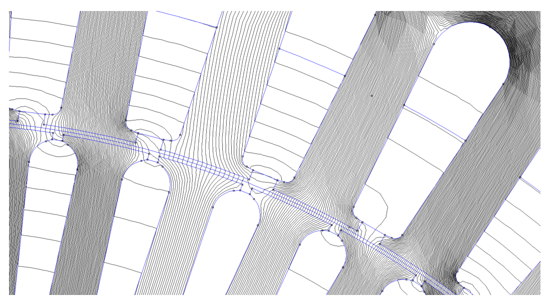

Figure 2.69: Zig zag

Rotor leakage inductances

All the consideration done for the stator can be done for the rotor, but here the total leakage inductance is given by the contribution of three values : The stator leakage flux in IM is the sum of four main contributes :

- Bar leakage $L_{l,slotR} = 2L\lambda_{slotR}\frac{3}{N_b}K_L(f) = 6.40720e-04(H)$

- end ring leakage $L_{l,ring} = \frac{2\pi D3}{N_b^2}\lambda_{ring}(\frac{NK_w}{K_skew})^2\frac{1}{(2sin(\frac{p\pi}{N_b}}))^2 = 1.545e-04(H)$

- Zig Zag $L_{l,zz} = \frac{5}{6}L_\mu(\frac{2p}{N_b})^2 = 1.611e-04(H)$

All these contributions have the same properties of the stator but referred to the rotor, in particular also the two specific permeances can be calculated as it follow:

[21]This contribution become more relevant, up to 15% of the total leakage inductance when there are high current or at the start up

$$_{slot}= \frac{\mu_0}{q}((\frac{h_1}{3a} + \frac{h_2}{a} + \frac{h_3}{a - s_o} ln(\frac{a}{s_o}) + \frac{h_4}{s_o}) \tag{2.63}$$

$$\lambda_{ring} = mu_0(0.18 \div 0.30) = mu_0 0.26 \tag{2.64}$$

Magnetizing inductance

The last inductance present in the equivalent circuit is the L_μ also known as mutual or magnetizing inductance, and it is the main actor in the evaluation of arigap flux because it depends on the flux lines that cross the airgap and goes from stator to rotor and vice versa and moreover it induce the EMF that generate the currents in the rotor. In fact, is also used to evaluate how much power is converted to mechanical output power, thought the $cos\phi$. These therms can be evaluated at first thought a simplified empirical equation:

$$\omega L_\mu = X_\mu \simeq \frac{3V_{ph}^2}{Q_{\mu,approx}} \tag{2.65}$$

where the value of the reactive power here is estimated :

$$Q_{\mu,approx} = \omega(\frac{B_M^2}{2\mu_0})(\pi DL\delta)K_{Q_\mu} = 15935.9567(VAR) \tag{2.66}$$

In the previous equation the values $K_{Q_\mu} \simeq 1.6 \div 1.8$ that should take into consideration the carter factor that is the coefficient for the distortion of the airgap flux generate by the slots, and also the MMF drops in the lamination in presence of saturation. So it is better to obtain this value in a more precise way, by passing though specific analytical evaluation and at the end, verify this value with a FE analysis.

Analytical L_μ

To reach a good estimation of the magnetizing inductance, it is fair to introduce properly the effect that this value represent in the equivalent circuit. Since the magnetizing current is the current needed to the L_μ, produced by the stator, to magnetize the all the part that are crossed by the flux lines, and along that lines is possible to evaluate the MMF drop. With the Ampere's law, the MMF produced by the three phase winding should compensate also the MMF drop that appear in a non-ideal situation in which the soft magnetic materials do not have permeability equal to infinite.

So if the condition is ideal (MMF[22] drop only in the airgap) the formula of this MMF is the following;

$$MMF_\mu = 2MMF_\delta = 2H\delta = \frac{2N4K_w I_{\mu.ph}\sqrt{2}}{22p\pi} \tag{2.67}$$

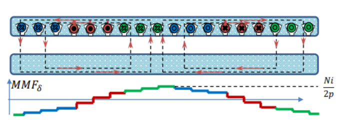

Figure 2.70: Stator MMF

This MMF_μ is the source of the airgap flux, and to be produced it is needed to have the following magnetizing phase current that is also helpful to obtain the value of inductance.

$$I_{\mu.ph} = MMF_\mu p\pi \qquad L_\mu = \frac{E}{\omega I_{\mu,ph}} \tag{2.68}$$

[22] H=H$_1 + H_2 + H_3 = \frac{3NK_w i}{2p\pi\delta}$

Now these two formulas are always valid, but it is more interesting to look at a more realistic situation with non idealities, so the total magneto motive force drop is no more limited to the airgap region but now also the lamination can be included in these phenomena. It is continent to divide the lamination in area of interest in which the material behave in an almost constant way, so for both the rotor and the stator it is considered the yoke and teeth region:

$$MMF_{\mu}p = 2MMF_{\delta} + 2MMF_{t} + 2MMF_{tR} + 2MMF_{y} + 2MMF_{yR} \tag{2.69}$$

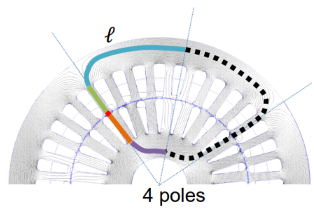

Figure 2.71: MMF regions

Airgap MMF drop MMF_{δ}

The MMF drop in the case of uniform airgap is $MMF_{\delta} = \frac{B_M \delta}{\mu_0} = 717.191(A)$, in order to consider also the over length of the airgap flux lines due to the presence of the stator and rotor slot, is introduced a coefficient K_c called Carter's factor. $MMF_{\delta} = \frac{B_M \delta}{\mu_0} K_c$

$$K_{CarterS} = \frac{1}{1 - \frac{\frac{so}{\tau_s}}{1+5\frac{\delta}{so}}} \qquad K_C = K_{CarterS}K_{CarterR} \tag{2.70}$$

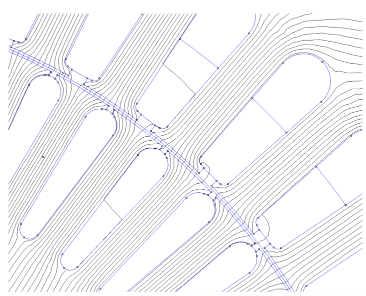

Figure 2.72: Carter factor effect

For the same flux per pole $\Phi_{M\tau}$ the peak of the airgap flux is reduced from B_M to B_{Msat} and since $B_{Msat} = \frac{\Phi_{M\tau}}{\alpha_{sat} L\tau}$ in the formula for the MMF is suggested to use the saturated value in order to obtain a more realistic result since the airgap flux density have no more a near to a sinusoid but more near to a trapezoidal shape.

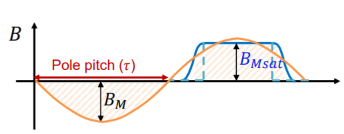

Figure 2.73: Saturation of BM

Teeth MMF drop MMF_t and MMF_t

From the flux density at the airgap $B_{M,sat}$ the flux densities in the stator (and rotor) teeth are evaluated as:

$$B_{Mt,sat} = \frac{\tau_s}{w_t} B_{M,sat} = 1.493(T) \tag{2.71}$$

The B-H curve characteristic (A) of the lamination identifies a working point of the ferromagnetic material associated to a value of field strength $H_{Mt,sat}$ (according to the level of saturation that is reached by analytic evaluation of α_{sat} because $B_{M,sat} = \frac{\Phi_{M\tau}}{\alpha_{sat} L\tau}$ so it is needed an iterative process that converge in a point (A).

$$MMF_t = H_{Mt,sat} h_s = 24.167(A) \tag{2.72}$$

h_s is the slot height, equal to the tooth height.

The same approach is used to determine the MMF drop in the rotor teeth:

$$MMF_{tR} = H_{MtR,sat} h_{sR} = 174.885(A) \tag{2.73}$$

For all the previous MMF in teeth, there is the possibility of being in a high saturation levels, usually when $B_{M,sat}$ $1.8T$. This condition leads the flux to flow in two parallel paths with high reluctance: through teeth and slot areas (in which the flux behave as in the air). In this case study does not appear these phenomena but since it is suggested to work near the saturation knee it is interesting to take into consideration also this possibility.

2.8.3 Yoke MMF drop MMF_y, MMF_{yR}

The flux per pole is not supposed to change, since it is fixed by the EMF. In the BH curve, it is possible to identify an average working point for the yoke that is associated to the value of the field strength $H_{My,sat}$ that is $B_{y,ave} = 0.85 B_{My} = 1.250$

$$B_{My} = \frac{DB_M}{2ph_y} \qquad B_M = \frac{\Phi_{M\tau}}{\frac{2L\tau}{\pi}} \tag{2.74}$$

$$MMF_y = H_{My,sat} \frac{\tau_y}{2} = 23.94(A) \tag{2.75}$$

$$MMF_{yR} = H_{MyR,sat} \frac{\tau_y}{2} = 1.09(A) \tag{2.76}$$

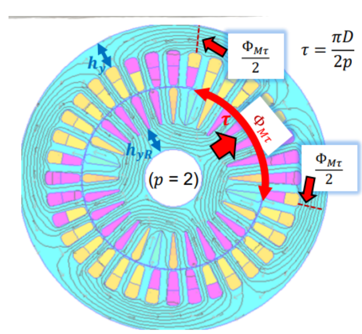

Figure 2.74: Motor slice

Since a high saturation in the yoke is not as common as the saturation in the teeth, the parallel path is not analysed

At the end of the previous steps (and required iterations), the overall MMF drop is known, and the required magnetizing current can be calculated by using the same formulas obtained before. This current is necessary to generate the desired flux per pole of the motor.

$$I_{\mu.ph} = \frac{MMF_{\mu} p\pi}{NK_w\sqrt{2}} \simeq 20(analytical) \simeq 16(FEA)(A) \qquad L_{\mu} = \frac{E}{\omega I_{\mu,ph}} \tag{2.77}$$

2.8.4 Power factor

The power factor $cos(\phi)$ is the parameter that estimate the relation between the reactive power absorbed by the machine to magnetize the circuit in comparison with the total power that can be converted in mechanical power. The reactive power can be seen has the sum of three main contribution :

$$Q_t = Q_{\mu} + Q_{ls} + Q_{lR} = 20549.915(VAR) \tag{2.78}$$

where :

- $Q_{\mu} = 3\frac{E^2}{\omega L_{\mu}}$
- $Q_{ls} = 3\omega L_{ls} I^2$
- $Q_{lR} = 3\omega L_{lR} I_R^2$

And the power factor :

$$cos(\phi) = \frac{\frac{P}{\eta}}{\sqrt{(\frac{P}{\eta})^2 + Q_t^2}} = 0.8707 \tag{2.79}$$

2.9 Finite Element Analysis

The Finite element software used for the validation of this motor is FEMM[23]. All the following result are obtained by trying to be more precise as possible by having an high number of mash point.

Full simulation vs slip

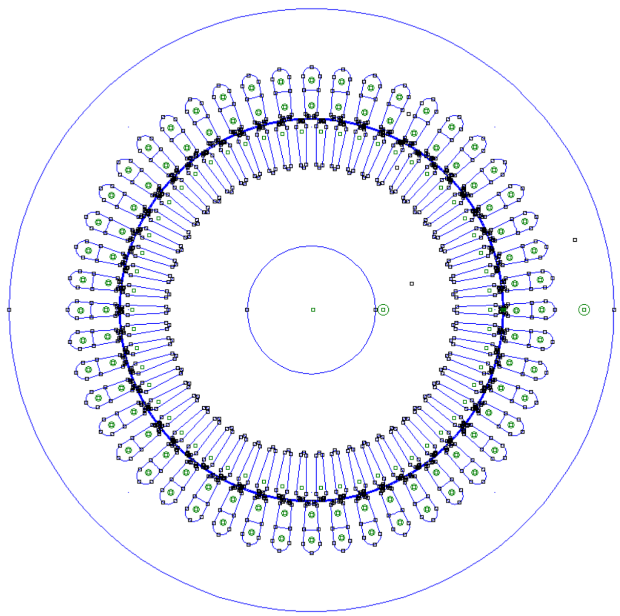

Figure 2.75: SIM 1

This is the simulation that take into consideration both the stator and the rotor and provide the simulation at different slip value of the equivalent circuit parameters by adopting a linear BH curve instead of the real one that saturate. It is possible to evaluate parameters like torque currents and flux density at different slip values

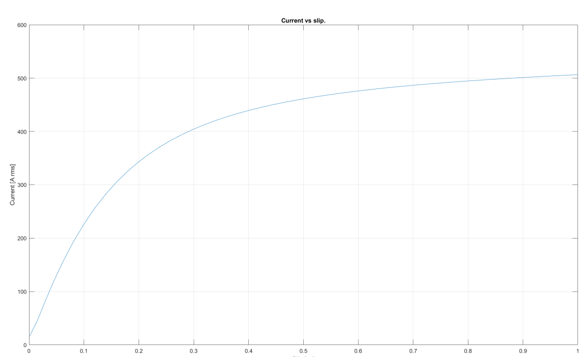

Figure 2.76: Current vs slip

[23]coupled with Matlab script

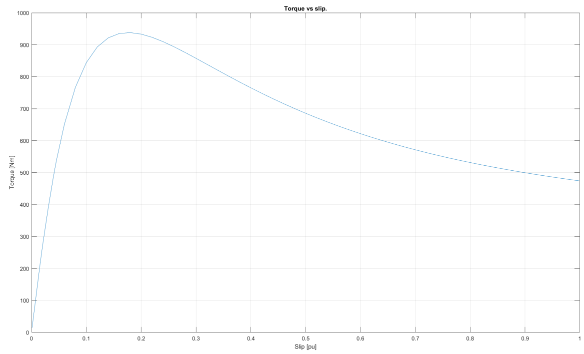

Figure 2.77: Torque vs slip

Stator leakage

This simulation provide the value of the stator slot leakage inductance by using the only stator geometry and it is possible to see the present line are the one related to the slot leakage and they do not cross the airgap since it was imposed a boundary condition[24] that ensure that the flux lines do not cross the inner stator diameter. It is an interesting parameter because give the estimation of how precise is the analytical workflow in respect to the finite element. In this case it is very precise since the error between the two values is so small that ca be neglected

$$L_{l,slotS,A} = 5.24715e - 04 \qquad L_{l,slotS,FEA} = 5.24406e - 04 \tag{2.80}$$

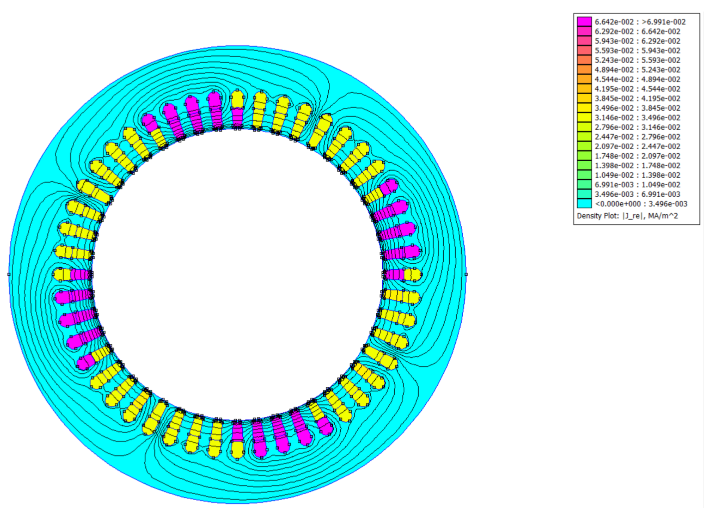

Figure 2.78: Stator slot leakage

Rotor bar

In this simulation, it is possible to have a look at the rotor bar behaviour[25] when the rotor's frequency change from zero is maximum value (by changing the slip). So being able to understand the behaviour of this component allow to be more precise also in the analytical calculation, since to reach an high level of precision in the design workflow it was needed to include also this result that comes from FEA.

[24]Dirichlet

[25]also there is present the Dirichlet boundary condition

For the rated condition it was considered these two contribute equal to 1 (no affected by FEA) but all the other working point use this results.

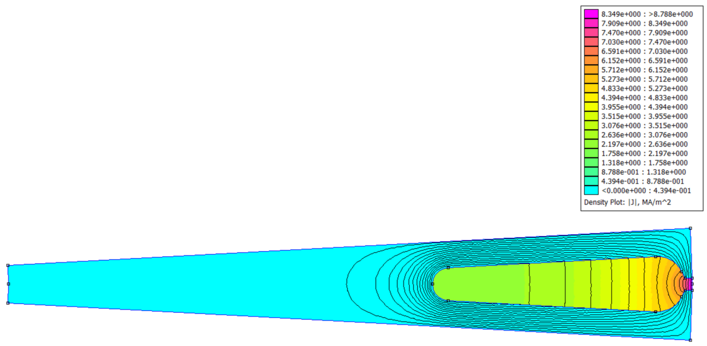

Figure 2.79: Rotor bar

In output is also provided the polynomial function that characterize these two curves.

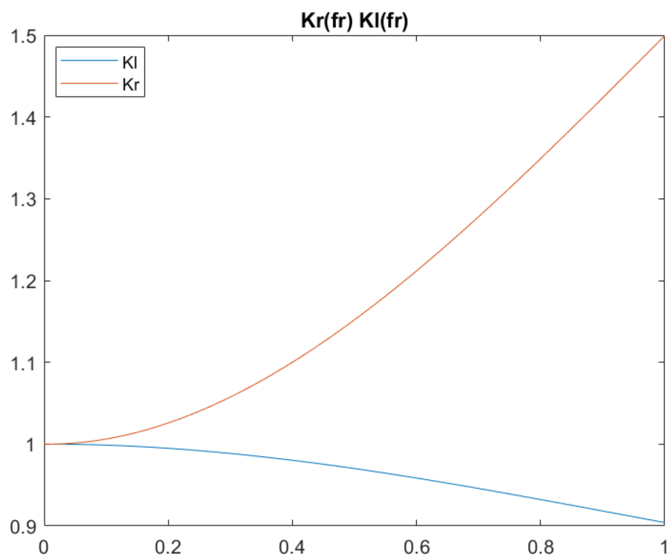

Figure 2.80: AC rotor contribution

Stator inductance with saturation

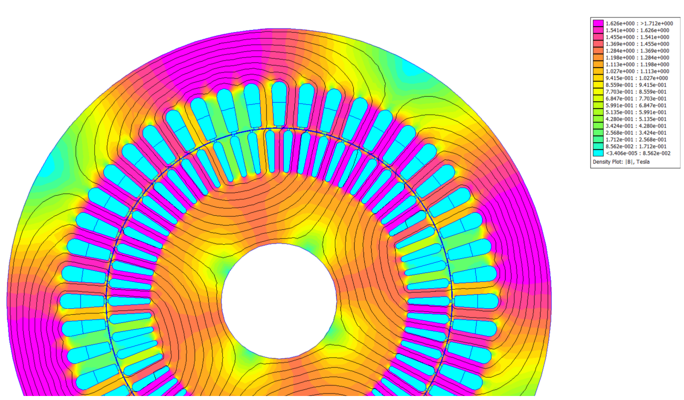

Figure 2.81: SIM saturation

The last simulation of the induction motor is mainly concerned to provide the effects of the saturation on the magnetizing inductance and on the EMF. To achieve a comparison between analytical and finite element result, it is considered the non ideal curve of the material chosen for the lamination and the software provide an output at synchronism condition. The output are:

- A plot in which is possible to see the comparison between the electromotive force over the magnetizing current, this is a good estimation for the analytical workflow. Since the magnetizing current is asked as an input value, the simulation just provides the graphical the difference in terms of electromotive force betewwn the FEA values and the one that it was estimated at the beginning $E \simeq 0.96V_{ph}$ with the is almost negligible.

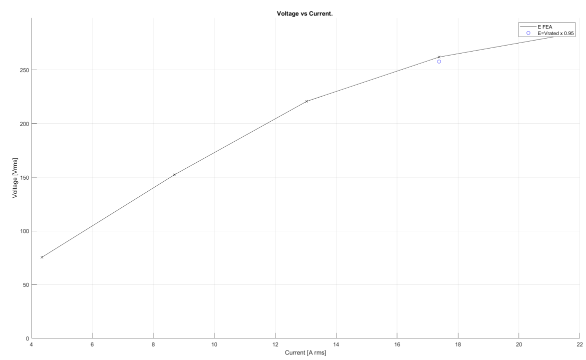

Figure 2.82: E vs magnetizing current

- Another output is the sum of the stator inductance and the magnetizing inductance. Since the stator slot leakage inductance was practical identical to the one of the FEA, to evaluate the error between the two L_μ it was assumed that the analytical $L_{l,stator}$ is the same for both the FEA and the design. so it ended up that the error between the two magnetizing inductances is about 12% and using the FEA as the more realistic, the magnetizing current it was updated, giving a good results in the whole simulation.

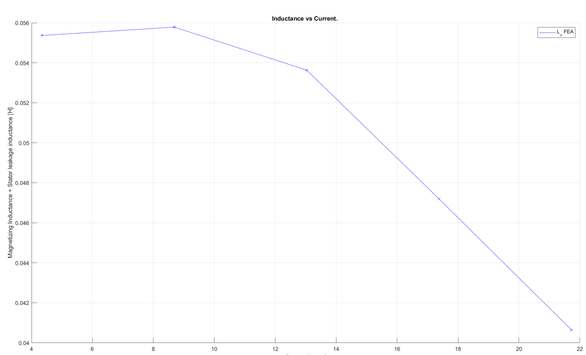

Figure 2.83: Stator and magnetizing inductances

- Another information that we can find is there flux density at the air gap, that is interesting to parasitic effect to the sinusoidal shape and so the slotting effect can be pointed out through the harmonic content. Moreover, the FFT show the third harmonic since the machine goes a little in saturation and this fact is reflected in the presence of that harmonic. It can underline also the slotting effect that act on the hamoric of order $\frac{N_s}{}2 \pm 1$ and $\frac{N_b}{2} \pm 1$

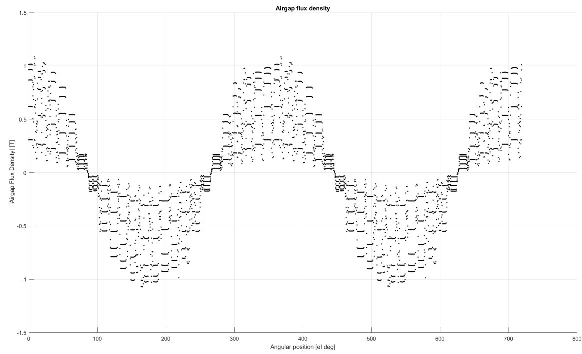

Figure 2.84: Airgap flux denisty

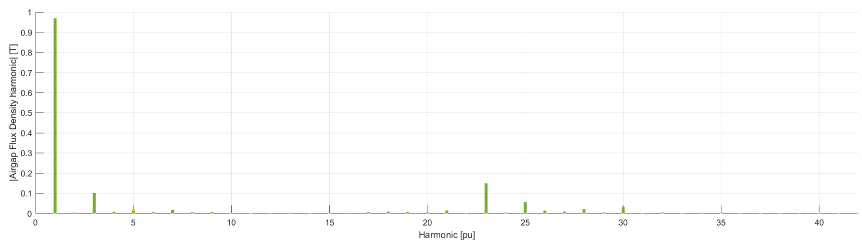

Figure 2.85: Airgap flux density fft

2.10 Motor charatteristics

The solution of the electric circuit allows drawing all the motor characteristics. All the circuit parameters must be evaluated with enough accuracy. For a better evaluation, the rotor resistance and leakage inductance should be considered as function of the rotor frequency ($f_r = sf$) by means of the functions $k_R(f_R)$ and $k_L(f_R)$, that are predicted by analytical models or, better, via FEA.

2.10.1 Output power vs speed

The power is the main requirement to be satisfied as much is possible, thanks to this plot is at rated condition of 1477 rpm is possible to reach 33200 W that is almost the output power 33500 requested W

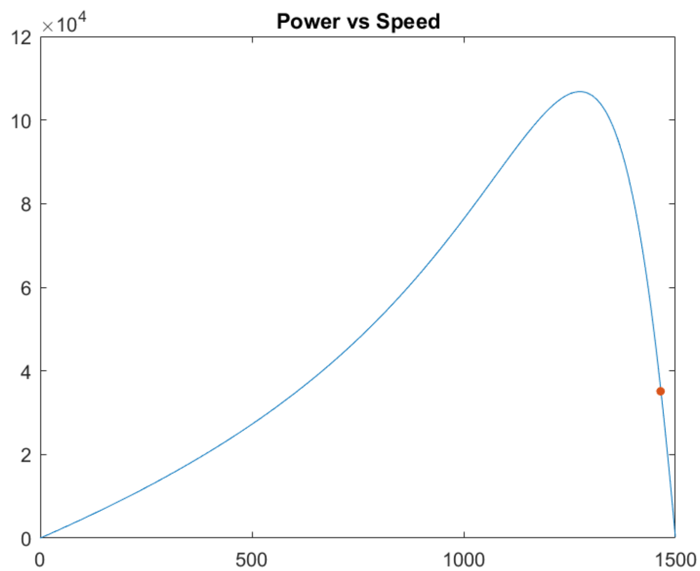

Figure 2.86: P vs speed

2.10.2 Torque vs speed

The torque at rated condition is 228.7 Nm are reached few rpm lower than the rated condition, while as it was anticipated before, due to the standards also the start up torque 422 Nm and the maximum torque 1215Nm are needed

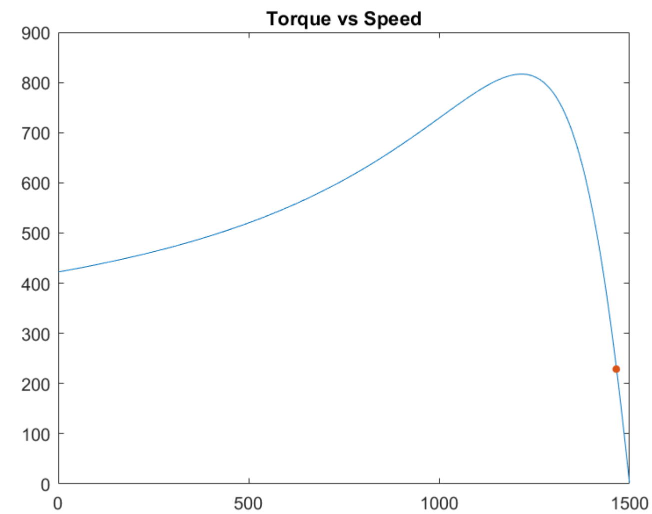

Figure 2.87: T vs speed

2.10.3 Stator current vs speed

From this plot is possible to look at the different behaviour of the analytical stator current and the one from the FEA, the difference in the two plot can be present due to some non ideality that are taken into consideration in the FEA but not in the analytical process, moreover the FEA has two order of magnitude less that the sampling point used for the analytical evaluation

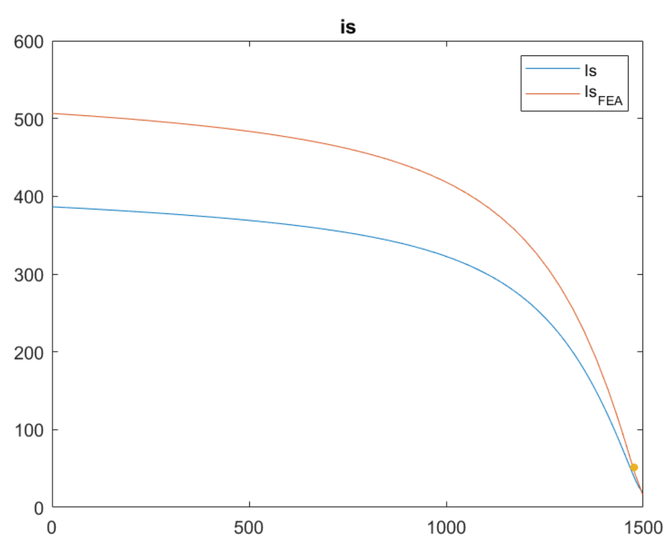

Figure 2.88: Stator current vs speed

2.10.4 Stator current and Torque vs speed

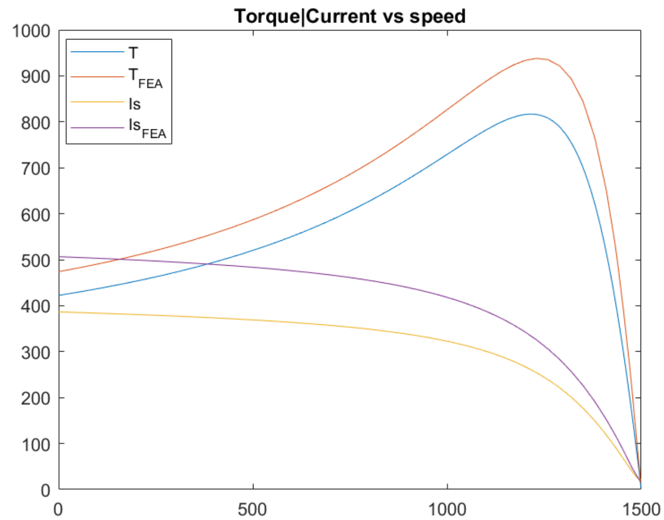

Figure 2.89: Torque and stator current vs speed

2.10.5 Rotor current vs speed

The rotor current presents a very high magnitude especially at low speed because it depends on from a value that is inversion proportional to this leap that decrease when the mechanical speed increase so the rotor current experienced the worst condition at startup.

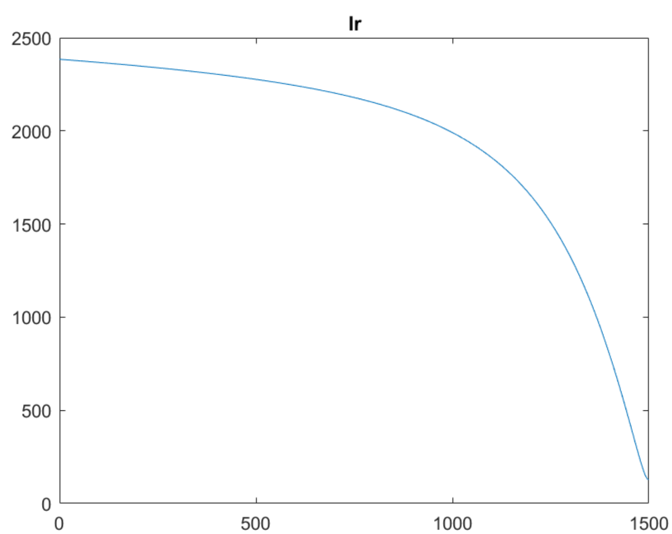

Figure 2.90: Rotor current vs speed

2.10.6 Magnetizing current vs speed

For the magnetizing current is interesting to see that at 0 speed it doesn't reach the zero because at synchronism Still flow

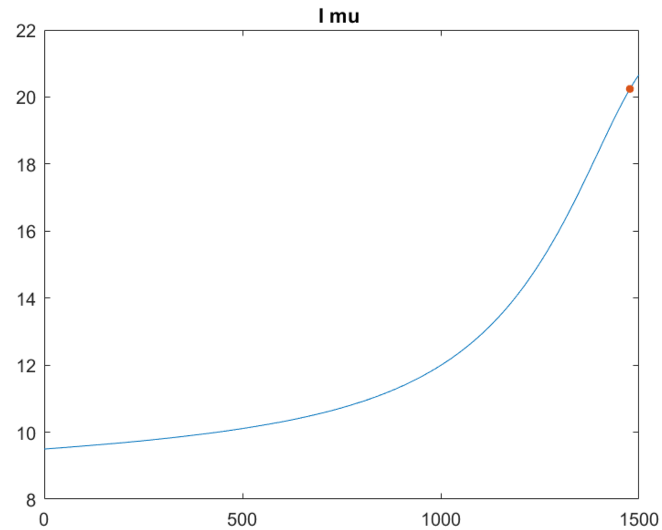

Figure 2.91: Magnetizing current vs speed

2.10.7 Efficiency vs Output Power

The efficiency has two working point for the same input power (one stable and one unstable), but the real working point is the higher one since the motor perform better in the stable condition

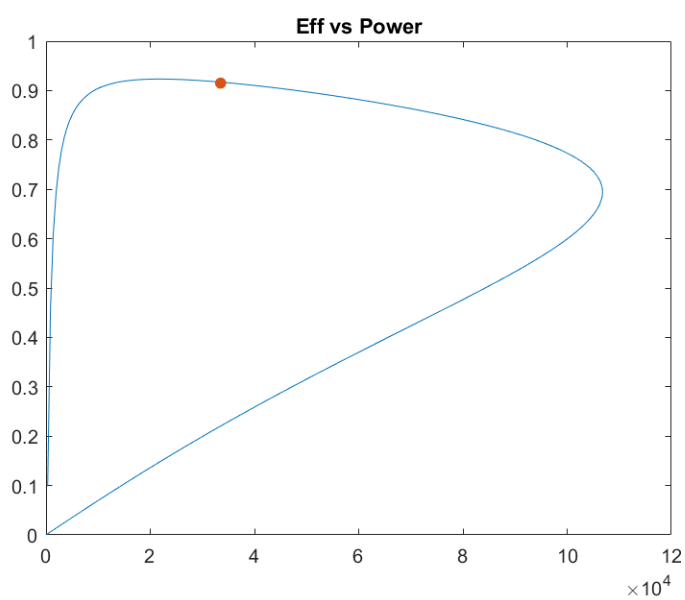

Figure 2.92: Efficiency vs power

2.10.8 Power factor vs Output Power

The Power factor has two working point for the same input power (one stable and one unstable), but the real working point is the higher one since the motor perform better in the stable condition

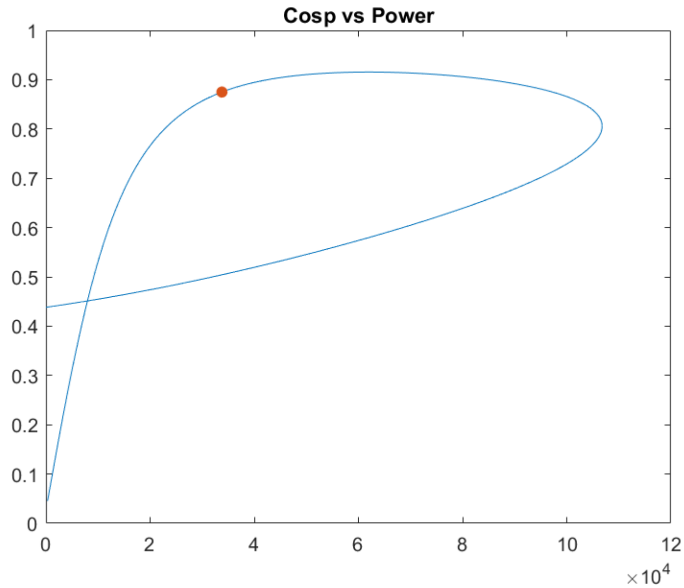

Figure 2.93: PF vs power

2.11 Thermal model

It is possible to evaluate the average temperature inside the different part of the motor by using uh terminal model debt to reproduce the internal thermal power flow and thanks to the equivalent resistances it is possible to obtain the difference of temperature across different paths. This model adopts the analogy between the thermal and the electrical circuit, where the current is represented by the thermal power, and the voltage is represented by the temperature.

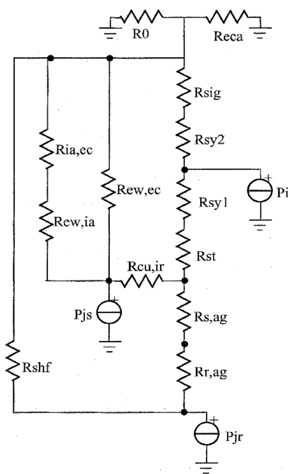

Name	Description
R_{eca}	Forced convection thermal resistance between external case and ambient
R_0	Natural convection thermal resistance between external case and ambient
$R_{ia,ec}$	Convection thermal resistance between internal air and endcaps
R_{sy1}	Radial conduction thermal resistance of the stator yoke lower half part
R_{sy2}	Radial conduction thermal resistance of the stator yoke upper half part
R_{st}	Radial conduction thermal resistance of the stator teeth
$R_{cu,ir}$	Conduction thermal resistance between stator copper and stator slot
$R_{ew,ec}$	Convection thermal resistance between stator winding external connections and external case
$R_{ew,ia}$	Convection thermal resistance between stator winding external connections and inner air
$R_{s,ag}$	Convection thermal resistance between stator teeth and airgap air
$R_{r,ag}$	Convection thermal resistance between rotor and airgap air
R_{sig}	Conduction resistance of the interface gap between the stator core and the external case
R_{shf}	Axial conduction thermal resistance of the shaft

Figure 2.94: Thermal model

The first step to take is to design properly the resistances that are the main actor in this scheme. By using the results obtained by analytical and finite element analysis it is possible to ever some initial condition that take into consideration the efficiency, the losses of the iron and the copper, but also all the geometrical aspect that are needed in order to build a proper thermal path.

In addition to the previous calculus, here is taken into consideration also the case design, since this motor has a case of 200 L. From decades it's possible to obtain the fins height and the external surface thickness. These are the two values that can be adopted as a degree of freedom at the end of the procedure in order to estimate how the temperature are affected by geometrical quantities that increase their surface in which the thermal exchange happen.

	ThermalResistancesNames	ThermalResistancesValues
1	'Reca'	0.023029058681111
2	'R0'	0.319908147287640
3	'Ria_ec'	0.055970816760894
4	'Rsy1'	0.002216419952831
5	'Rsy2'	0.001989307824878
6	'Rst'	0.009378028049180
7	'Rcu_ir'	0.010142668882724
8	'Rew_ec'	4.238582013234636
9	'Rew_ia'	0.199346609931362

Figure 2.95: Resistances

The simplified model is build as it follow:

- In the sizing flow of this thermal circuit, all start with the resistance from the external case to the ambient, these consider also the presence of a self ventilated motor. R1

- Another parameter is the resistance between the stator core and the external case, and it is represented by two series resistance R2

- Another important resistance is R3, that consider the path from the inner surface of the stator through the teeth to the yoke.

- R4 Is the value that represents the resistance between the winding and the stator lamination so in this resistance are taken into consideration there insulating materials and the resin inside the slots

- R5 this resistance consider the two path of the hand winding through the external case, since there is no potting the hand winding directly face the case passing through the inner hair that is present in that region.

- R6 is the resistance of the air gap between the rotor and the stator, it mainly represents the convection through the hair in this region

- R7 this resistance consider the axial direction of the thermal path from their author to the case considering the conduction in the shaft, the radial conduction through the rotor yoke, the axial conduction of the shaft to the rotor lamination and finally the axial conduction from the external shaft to the rotor

	ThermalResistancesNames	ThermalResistancesValues
1	'R1'	0.021482601969773
2	'R2'	0.016041979921005
3	'R3'	0.011594448002010
4	'R4'	0.010142668882724
5	'R5'	0.240811764239378
6	'R6'	0.181064117592389
7	'R7'	0.607106826773640

Figure 2.96: Simplified resistances

	Var1	Var2
1	'Q1'	2.061318587046503e+03
2	'Q2'	1.655856258401303e+03
3	'Q3'	1.418689947579871e+03
4	'Q4'	1.042900072561201e+03
5	'Q5'	2.225386702371390e+02
6	'Q6'	3.757898750186706e+02
7	'Q7'	1.829236584080616e+02

Figure 2.97: Thermal power

It is possible to appreciate the different results when their heights of fins change, this solution can lead to a higher surface for the thermal exchange but in the other hand did they mention if the fins should be compatible with the external case dimension, so there are always constrains in the choices. In order to appreciate the difference, the following picture represents the temperature value by increasing their fins' height. It is fair to underline that by changing this value is not sufficient to decrease the temperature class depth in all the cases is there F glass that allow an over temperature of an 145 Celsius degree with an output temperature of 155 Celsius degree, since this value is pretty high a deeper evaluation of the thermal path can be done in order to adjust some parameter that can lead to a reduction of thermal class since the working temperature here are pretty near to the upper limit of the lower level class

	TemperatureNames	TemperatureValues
1	'T case (external surface)'	97.750617991654678
2	'T stator yoke'	1.243138308409990e+02
3	'T stator teeth (inner surface)'	1.407627576691887e+02
4	'T copper (stator)'	1.513405477829453e+02
5	'T rotor'	2.088048197895982e+02
6	'T ambient (Air)'	40
7	'T thermal class'	155

Figure 2.98: Temp, low fins

	TemperatureNames	TemperatureValues
1	'T case (external surface)'	84.282486738414462
2	'T stator yoke'	1.108456995877588e+02
3	'T stator teeth (inner surface)'	1.272946264159485e+02
4	'T copper (stator)'	1.378724165297051e+02
5	'T rotor'	1.953366885363581e+02
6	'T ambient (Air)'	40
7	'T thermal class'	155

Figure 2.99: Temp, medium fins

	TemperatureNames	TemperatureValues
1	'T case (external surface)'	75.908254532201042
2	'T stator yoke'	1.024714673815453e+02
3	'T stator teeth (inner surface)'	1.189203942097350e+02
4	'T copper (stator)'	1.294981843234916e+02
5	'T rotor'	1.869624563301446e+02
6	'T ambient (Air)'	40
7	'T thermal class'	155

Figure 2.100: Temp, high fins

Thermal class **IEC 60085**	Y	A	E	B	F	H	C(N)	C(R)	C(S)
Maximum hotspot temperature	***90°***	***105°***	***120°***	***130°***	***155°***	***180°***	***200°***	***220°***	***240°***
Maximum overtemperature	***50°***	***65°***	***80°***	***90°***	***115°***	***140°***	***160°***	***180°***	***200°***

Figure 2.101: Temperature classes

Chapter 3

SPM

3.1 Requirements

The aim of this project is to follow an unconstrained design of a surface mounted permanent magnet machine (SPM) by having a some Design constrain: performances, aspect ratio and others. The goal

Surface Mounted Permanent Magnet Motor
natural convection

Torque (S1)	140 [Nm]
Poles (2p)	8
Rated speed	3350 [rpm]
DC link voltage	500 [Vdc]
Torque overload (p.u.)	2
Maximum external diameter (Dext lamination)	300 [mm]
Maximum active length (L lamination)	160 [mm]

Figure 3.1: Design requirements

of the design is to obtain the requested torque by respecting the limit imposed for the design. Mainly the torque average can be managed by adjusting the following parameter for an initial sizing:

$$T = \frac{\pi}{2\sqrt{2}} K_{skew} K_{wind} L D^2 B_{MR} \Delta \propto L D^2 B_M \Delta \tag{3.1}$$

That can also be seen as $T\omega_m = P = 3VI\eta cos(\phi)$ but more in specific for this machine Torque at the MTPA (max torque per Ampere) con be seen as the sum of three main contribution : average torque, the cogging toque that is present also at no load and torque ripple at on load.

$$T = (\frac{3E_R I}{\omega_m}) + (\frac{MMF_R^2 dP_m}{2dm}) \sum_{\rho=5,7,11}^{..} (\mp \frac{E_{Rh} I cos((h+1))}{\omega_m}) \tag{3.2}$$

This introduction about the torque is needed because with this machine it is possible to take into consideration different topologies of stator, and each of them introduce benefit and disadvantages that also are related to the torque.

So it is convenient to introduce some useful parameter in order to be able to set a precise workflow;

3.1.1 Voltage

At the input of this machine is present a DC bus that provide 500V, from that it is possible to obtain the line to line voltage and phase voltage.

- Voltage peak line to line: $V_{pk,ll} = 0.95V_{DC} = 475(V)$ where 0.95 is the control margin needed for the inverter
- Voltage line to line rms $V_{rms,ll} = \frac{V_{pk,ll}}{\sqrt{2}} = 335.875(V)$
- Phase voltage $V_{rms,ph} = \frac{V_{rms,ll}}{\sqrt{3}} = 193.917(V)$

3.1.2 Delta

higher slot deep, increase delta (high volume and high leakage flux)

Another parameter to taking consideration in a first design step is the electrical loading, scenes it is strongly affected by the cooling system in this motor a suitable range for this value goes from 30,000 to 60,000. It is also strongly dependent on the geometry and current density. An high slot depth lead to high volumes and high leakage flux, while an high current density increase the losses.

$$\Delta = \frac{3NI}{\pi D} = 33000(\frac{A_{rms}}{m}) \tag{3.3}$$

3.1.3 BMR

The value of the magnetic loading B_{MR} due to the only contribution of the magnet of the rotor. The working point to analyse is in MTPA (maximum torque per Ampere) and in this condition B_{MR} has the dominant compared to the total flux density B_M generated by the stator and rotor (this indirectly lead to a lower loss from the point of view of the conductor and also allow to reduce their soft magnetic material in the stator)

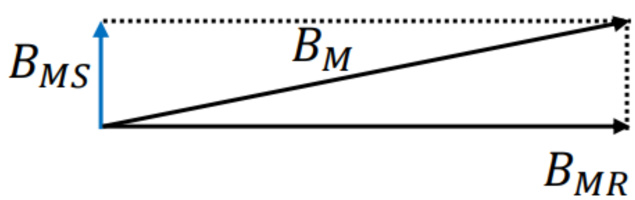

Figure 3.2: Flux density distribution

3.1.4 Frequency

The rated speed is fixed $n = 3350$ rpm, as a consequence of working in a synchronous motor, it is already possible to evaluate the mechanical frequency ad the electrical one.

$$f_{mec} = \frac{3350rpm}{60} = 55.83(Hz) \qquad f = pf_{mecc} = 233.33(Hz) \tag{3.4}$$

3.2 Stator

The previous introduction about the torque, pole pairs and other parameter is needed because with this machine it is possible to take into consideration different topologies of stator, and each of them introduce benefit and disadvantages that also are related to the torque.

3.2.1 Stator topology

In this motor with eight pole $2p = 8$ it is possible to choose between many configurations: distributed with 24,48 or 72 slots or a fractional with 6,12,9,18 slots. Distributed winding Whit lot of slots it is easy to have deep and thin slots that lead to an high leakage inductance and the winding factor decrease leading to a lower toque but a lower distorted harmonic.On the other hand, a distributed winding with low number of slots produce torque and Bemf ripples. While the fractional layout have a lower value of the cogging torque.The coil pitch is lower than the pole pitch also a shortening contribution appear automatically, but for a multiplicity equal to 1 the radial forces appear.

By looking at the requirements, and having considered the advantages and the disadvantages of each topology, for this designer was chosen the fractional for the following reasons:

- fractional winding have a very low cogging torque compared to the distributed one
- On the contrary this configuration lead an high radial force of the magnitude around 2100 Newton, but this problem can be solved by using an additional mechanical design for the bearings that should contain these forces or in different cases from that one it will be considered 2 use a winding layout with more than three phases in which one of them at least should work in order to cancel out this force, this is a solution is also called bearingless
- by looking to a stator with nine slot, is a convenient choice because first of all we obtain a low multiplicity of the machine in order to obtain the maximum qr as possible [1], in order to smooth the shape of the magneto motive force produce at the air gap. But at the same time, having a multiplicity of 1 introduce the radial forces
- for academic proposal it is also interesting to look at a different state or layout, as since the distributed layout with these input constrain it will lead to and number of slot of 62 with the distribution of winding in free slot, leading the air gap flux density to a more sinusoidal shape instead the one of the tooth wound layout that will present a strong effect of the slotting effect.

To better choose the Number of slot, it is important to have some consideration on the winding layout. The three phase winding are assigned to the slots by following an analysis based on the electrical position of each slot(A). This procedure is a repeated process that with the multiplicity of the machine equal to the greatest common divisor between

$$M = GCD\frac{N_s}{3}, 2p = 1 \tag{3.5}$$

The electrical position of the slot in a multiplicity is different, but each slot of each phase can be assumed q_r different electrical position

$$q_r = \frac{N_s}{3M} = 3 \tag{3.6}$$

This value is the equivalent number of slots per pole and per phase.

The coil pith $\tau_{coil} = \frac{\pi D}{N_s} = 0.0663(rad)$that emerge from this consideration must be as close as possible to the (magnet) pole pitch $\tau = \frac{\pi D}{2p} = 0.0746(rad)$, in order to maximize the EMF.In the fractional layout these two value can not be equal, and the shortening angle is determined by the numbers of slots

[1]lead to a more sinusoidal MMF (lower torque ripple and rotor AC losses). The distribution slightly reduces the fundamental harmonic while can significantly reduce higher order harmonics $E_{Rh} = w\frac{N}{2\sqrt{2}}K_d K_s \frac{2}{\pi} B_{MR} L\tau$

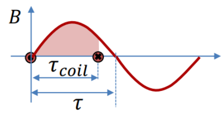

Figure 3.3: Tau

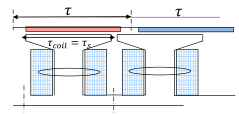

Figure 3.4: Shortening

The above statement refers to the torque producing harmonics only. Despite distributed windings, a fractional winding MMF also produces non-torque producing harmonics. The extra-harmonics

- increase the losses (eddy current in the magnet, so it is needed to segment them)
- interact with the rotor generating radial forces
- Magnitude comparable to the fundamental one, and also close to the fundamental

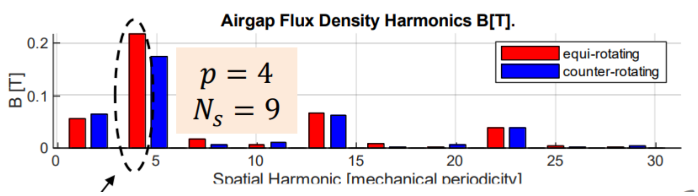

Figure 3.5: Airgap flux density fft (qualitative)

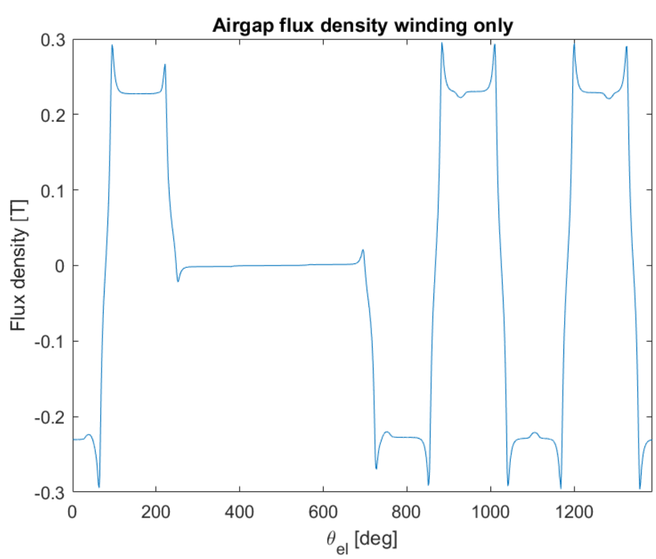

Figure 3.6: Airgap flux denisty, winding only

Radial forces act on the rotor as a rotating force with a frequency $f_{Force} = 2pf_m = 893.33(Hz)$

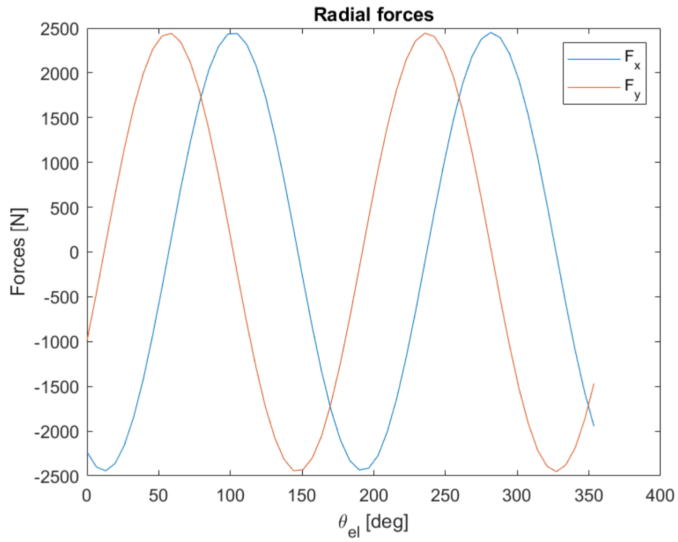

Figure 3.7: Radial forces

The number of slot should not be equal to the number of poles because they both produce flux at the fundamental harmonic (with a fundamental mechanical harmonic) and the interaction of these two lead to the production of an average toque. (A)

3.2.2 Dimension constrain

By continuing with the stator design, the requirement imposes a limit on the external diameter and on the active length. Having fixed also the number of poles $2p = 8$[2] it is fair to said that the diameter will be larger compared to one with a lower number of poles and this lead to have also thin yoke. To take into consideration the desired rated torque, by looking at the torque density it results that the value of the airgap diameter is crucial, so this design aim to obtain a larger diameter instead of having an high active length:

$$T \propto B_M \Delta L D^2 \propto B_M \Delta G D \qquad \frac{T}{G} \propto B_M \Delta D \tag{3.7}$$

where $G = weight \propto LD$ if $p \propto D$.

$$D = \frac{4sqrt_2 pT}{\pi^2 K_{skew} K_{wind} B_{MR} \Delta m} = 0.187(m) \tag{3.8}$$

and then the active length is related to the aspect ratio, that in this case is the degree of freedom

$$L = m\frac{\pi D}{2p} = 0.134(m) \qquad m = \frac{L}{\tau} = 0.134 \tag{3.9}$$

In these equation appear also the winding and skewing factor that contribute as factor that take care of how good is the winding of the stator and how it is arranged the skewing of the permanent magnet in the rotor. In order to introduce the effect of these quantities, it is convenient to increase a little the diameter to reach the desired torque and also to obtain a more feasible value for the manufacturing process $D = 0.190m$

3.2.3 Slot

The actual number of slot should be taken into consideration many aspects :

[2]also the speed is fixed $n = 3350$ rpm so this motor can be considered as a low speed motor

- the manufacture feasibility (slot geometry)
- a good winding manufacturing (winding layout)

As it was previously discussed, a 9 slot fractional winding is the chosen layout for that motor. The evaluation of the number of series turn in each phase can be evaluated by two different procedure, one more accurate than the other because the first one is to provide a rough estimation of that value in order to have a clue in terms of qualitative way:

$$N \simeq \frac{_{rms,ph}}{w\frac{1}{2\sqrt{2}}K_{skew}K_{wind}\frac{2}{\pi}B_{MR}L\tau} - 70.67 \tag{3.10}$$

than at the end of the design procedure this value can have a better estimation can be done

3.2.4 Winding layout and harmonics

This parameter introduces the effect of having the pitch of the coil that is equal to the pitch of the slot (that are near to the pole pitch and this difference is introduced by a shortening contribute $\beta = \pi(\frac{\tau-\tau_s}{\tau}))$. The flux produced by a magnet link the coil with a good winding factor a so lot of flux cross this coil by maximizing the flux linkage that is reflected on the maximization of BEMF (that have its maximum when the coil pitch is equal to the pole pitch, but for a fractional layout this is unfeasible).

This condition allow the magnet to be in front of the same portion of iron for the whole mechanical period being the pole pitch a multiple (in this case multiplicity $\simeq 1$) of the stator slot pitch, so the cogging torque is reduced to a low value (order of magnitude of $0.5Nm$) with a frequency $f_{cogg} = f_m lcm(N_s, 2p$

$$\alpha_m = (K_{integer} + 0.03 \div 0.07)\frac{2\pi}{N_s} = 0.733(rad) \tag{3.11}$$

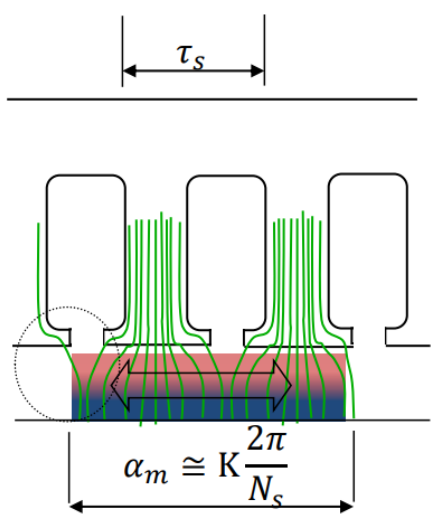

Figure 3.8: alpha m

$$K_{wind} = K_{distr}K_{short} = 0.9452 \tag{3.12}$$

Higher slot per pole per phase (q) $N_s = 6pq$ lead to a more sinusoidal MMF (lower torque ripple and rotor losses). The distribution slightly reduces the fundamental harmonic, while can significantly reduce higher order harmonics E_{Rh}.

$$E_{Rh} = w\frac{N}{2\sqrt{2}}K_d K_s \frac{2}{\pi} B_{MR} L\tau \tag{3.13}$$

The contribution of the stator winding only to the aigap flux density is:

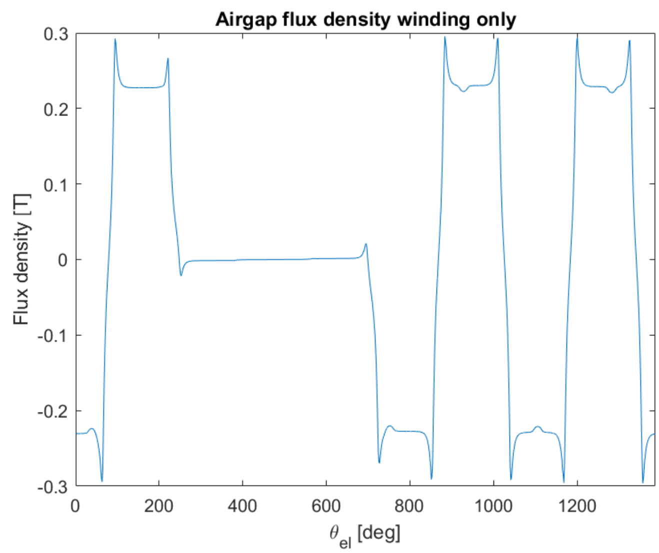

Figure 3.9: Radial forces

3.3 Rotor

The rotor under analysis can be seen as a system made by three main elements: a soft magnetic material for the crown (the yoke), the hard magnetic material (the permanent magnets) and the sleeve made of a non electrical material in order to not interfere with the fields in the airgap (usually carbon fibre for high level application). Since the level of flux density are lower compared with the whole motor, it is possible sometimes also to avoid the lamination of the iron. what are very crucial are the permanent magnet that can lead to many degrees of freedom in terms of the choice of the material, the dimension, the number of segments

3.3.1 Rotor flux distribution

The first step to evaluate the rotor flux design is to neglect:

- the slotting distortion, so the rotor flux contribution appear in the airgap circumference as a rectangular wave form (can be evaluated in a 2D model)
- the fringing effect, mainly caused by the presence of the slots, the flux density at the airgap can be assumed as constant in front of the magnets and null in the intra-magnet areas.

At the end of the design the actual flux density at the airgap can be seen in a no load analysis (zero current) and it appears not perfectly sinusoidal due to the presence of the previous effect that were neglected[3].

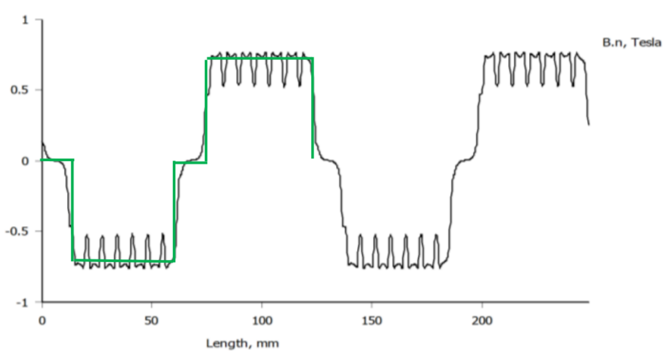

Figure 3.10: Flux density at airgap

Permanent magnet

The permanent magnet (or hard magnetic material) and their properties are deeply explained in the (A). For a preliminary evaluation the equation that describe them can be simplified as a straight line when they are working far prom the demagnetization region (tho have a clue of this condition is suggested to look at the intrinsic magnetization curve, usually the first 90% of the region before the intrinsic coercivity can be considered almost linear[4]).

[3]the contribution of the magnetic flux that is zero between the two peaks is due to the fact that the magnet pitch is different from the coil pitch, this introduces a more sinusoidal shape

[4]neglecting the recoil loop for a good permanent magnet because the working point is assumed in a linear region

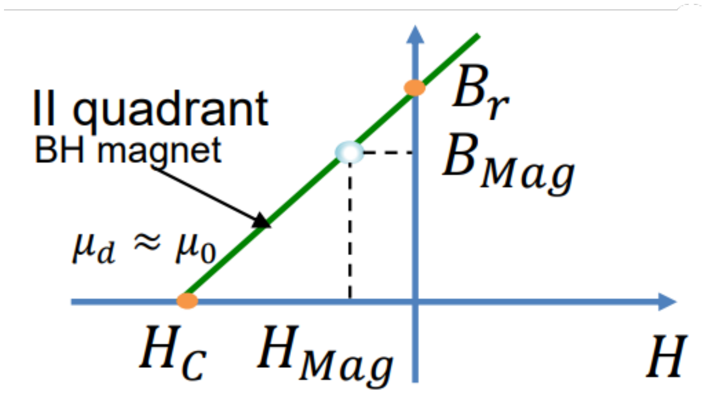

Figure 3.11: II quadrant operation

And the behaviour is described by this simplified equation:

$$B_{Mag} = B_r + \mu_d H_{mag} \tag{3.14}$$

Since the values of interest in this curve are strongly affected by the working temperature[5] of the magnet, it is better to choose the magnet[6] with a safety margin since there is not a direct way to estimate the working temperature of them.

No load

The airgap flux density can be evaluated from the solution of the magnetic circuit. The flux crosses the magnet and the airgap through a path at constant cross-section.

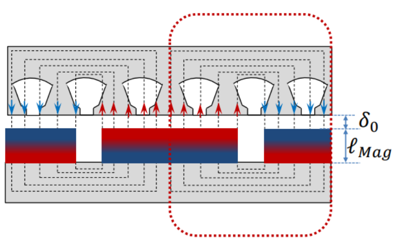

Figure 3.12: flux paths

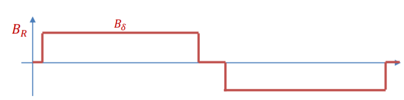

Figure 3.13: Flux density distribution(ideal)

Now by considering the intersection between the no load curves and the demagnetization curve of the material is possible to evaluate the maximum absolute value of the flux at airgap at no load condition, so due only to the contribution of the magnet $B_\delta = M_{mag,0} = -H_{mag}\frac{\mu_0 l_{mag}}{\delta_0}$

[5]the reduction of the remanence is proportional to the reduction of the BEFM so in order to be able to work at the constant torque required, is needed to increase the current and so increase also the joule losses

[6]Neodymium Iron Boron (NdFeB, rare earth)

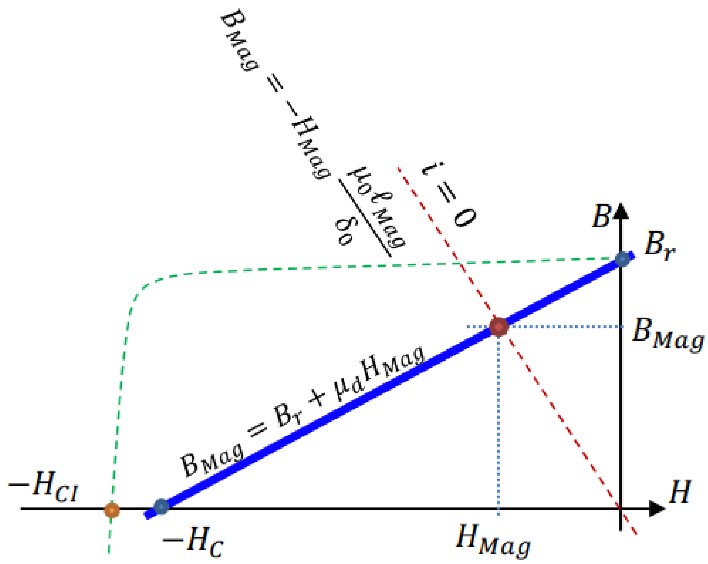

Figure 3.14: No load

To a better estimation of the B_δ is possible to introduce the distortion due to the presence of the non ideality of the geometry (so presence of slot) by the Carter's factor.

$$B_\delta = B_r \frac{l_{mag}}{l_{mag} + \delta_0 \frac{\mu_d}{\mu_0 K_c}} \simeq B_r \frac{l_{mag}}{\delta} = 0.71(T) \tag{3.15}$$

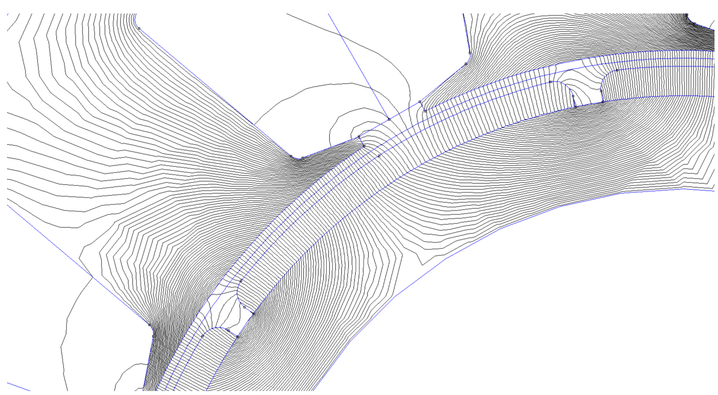

Figure 3.15: Slotting effect

From the rotor flux B_δ it is possible to evaluate the magnitude of the respective harmonics:

$$B_{Mh} = \frac{4}{\pi} B_\delta \frac{sin(hp\frac{\alpha_m}{2})}{h} = 0.90(T) \tag{3.16}$$

This is the resulting harmonic content at no load, is

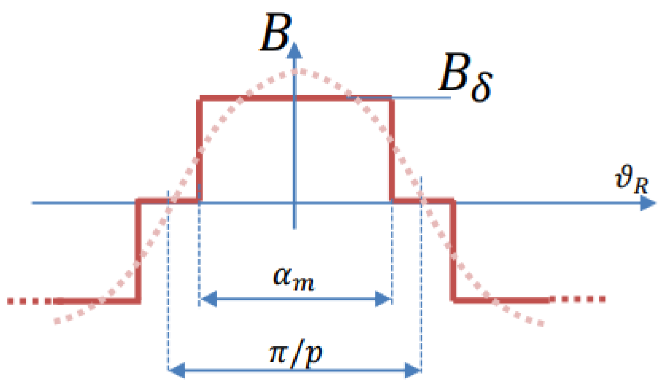

Figure 3.16: Flux distribution

An additional degree of freedom can be achieved by looking to the magnetic pitch, in this case in order to minimize the cogging torque (so have the pole pitch similar to the coil pitch) is no more a degree of freedom but in case it is possible to change α_m is possible to choose between different value in order to reduce the mechanical harmonic

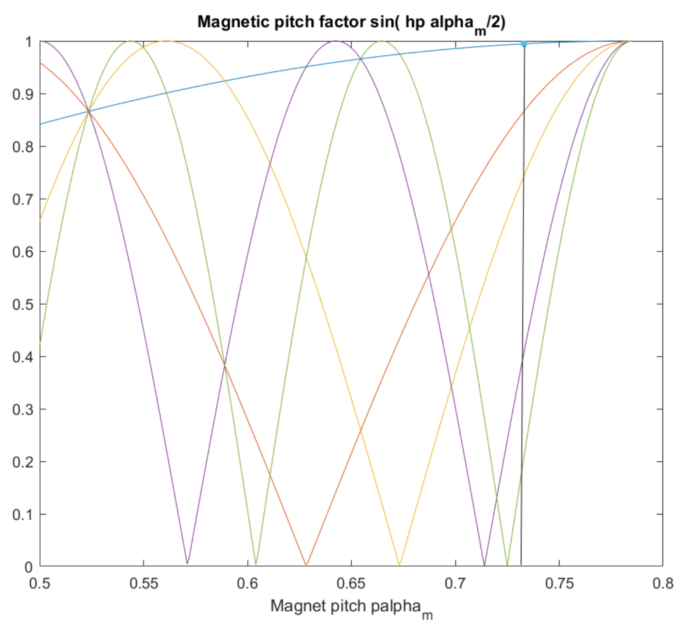

Figure 3.17: MAgnetic pitch factor

The contribution at airgap coming from only the magnet (NO LOAD) is :

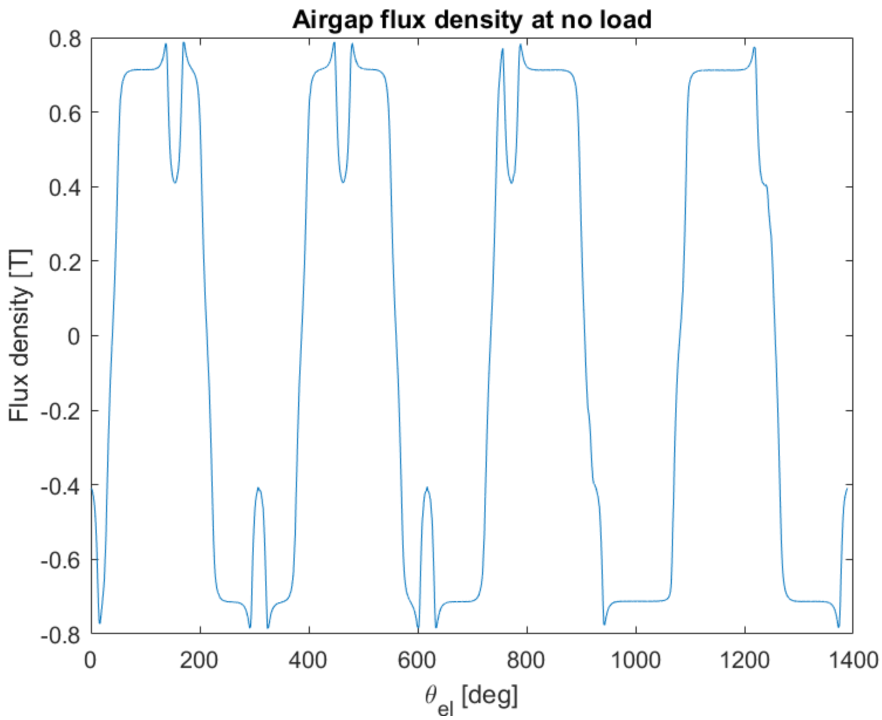

Figure 3.18: No load airgap flux density

3.3.2 Material

All the previous evaluation were done by using a magnet that was chosen from an industrial catalogue and all the details about the properties and how the characteristic curves of the material are made, is shown in the appendix A

3.4 Airgap

delta 0 = vacuum lmag The physical evaluation of the arigap thickness should take into consideration the height oh the magnet and the distance between the surface of the magneto from the stator(δ_0

$$airgap = l_{mag} + \delta_0 = 0.00485 + 0.0026 = 0.00745(m) \tag{3.17}$$

Where δ_0 has to take into consideration the minimum thickness due to mechanical tolerances $\delta_{min,tol} = (3.06 - (\frac{6560}{D(m)+2280}))/1000$ plus a rough estimation of the thickness of the sleeves that are needed to have a physical constrain on the magnet(about 2 mm more)

Then the height of the magnet depends on from the magnetic loading B_{MR} that depends on from the chosen material for the α_m angle.

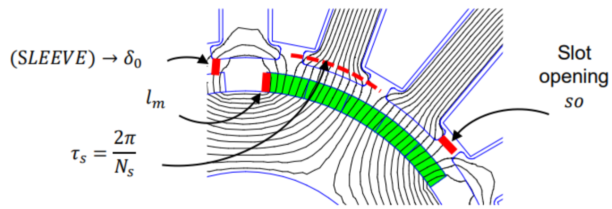

Figure 3.19: Airgap

3.4.1 Linked flux

For each phase, it is possible to represent the flux linked as the sum of two contribution. One come from the stator (leakage and inductive contribution) = $\phi ss = L_{sx} i_{sx}$, the second terms represent the harmonic components of the rotor magnet flux that link the stator winding of a phase x.

$$\phi sx = \phi_{ssx} + \sum_{h=1,3,5}^{\sim ..} R(\frac{N}{2} K_{wh} \phi_{MR,\tau,h} e^{jhp\omega_m t}) \tag{3.18}$$

where the fundamental harmonic are synchronized while the other, for the rotor one they rotate at W_m but the stator one rotate at $w_m hp$

The variation in time of the total linked flux determine the presence of the induced EMF in the phase x: [7]

$$v_x = R_s i_x + \frac{d\phi_{sx}}{dt} \tag{3.19}$$

$$v_x = R_s i_x + L_s \frac{di_{sx}}{dt} \sum_{h=1,3,5}^{\sim ..} (\frac{N}{2} p\omega_m K_{wh} \frac{2}{\pi} B_{MR,h} L\tau sin(w_h t) \tag{3.20}$$

The last component is the EMF induced. Take this value apart, it is possible to identify some parameter that are helpful in order to control this effect. The following equation is the rms value of the EMF:

$$E_{R.h} = p\omega_m \frac{N}{2\sqrt{2}} K_{wh} \frac{2}{\pi} B_{MR,h} L\tau \tag{3.21}$$

In order to reduce the no load distortion due to the harmonic of order grater than 1, it is possible to adjust the winding factor K_{wh} and the arc of the magnet in a coordinated way:

$$K_{wh} \frac{sin(h\frac{p\alpha_m}{2})}{h} \propto q, q_{sh}, \alpha_m \tag{3.22}$$

[7] so by considering the equivalent circuit of this machine this calculation can be seen as the circuital analysis of the circuit, pointing out the voltage component

Harmonic reduction

The magnet can be modelled in order to provide a reduction of the harmonic of the EMf induced in the stator. To do that, there are two possibilities:

- A continuos skewing con be an option, but the manufacturing process is expensive and difficult and the lack of segmentation provide no solution against the eddy currents that can be present inside the magnets, so it requires a skew along the cutting direction that lead to a delicate magnetization process; this solution can be equivalent achieved by having continuos magnet without be skewed, but the stator lamination must be skewed;

- A discrete segmentation is preferred even if the manufacturing process still difficult to benefit in therms of harmonic reduction and ac losses reduction are evident (segment that goes above 3 are considered an high number);

$$K_{skew,h} = \frac{sin(n_{seg}\frac{hp}{2})}{n_{seg}sin(\frac{hp\sigma}{2})} = 0.970 \tag{3.23}$$

If the argument of the sin function is equal to $n_{seg}\frac{p}{2} = \frac{\pi}{h}$[8] the h^{th} harmonic is cancelled out in this project, it is possible to reduced harmonic 7^{th}. Also, the choice of the magnet pitch (thought $B_{MR,h}$) can affect the harmonic reduction, as it was shown before in this project the skewing effect reduces the 11^{th} and 13^{th} of the 30% while the 5^{th} and 7^{th} of 80% and 70% [9] but there is not a complete reduction of an harmonic since it is more convenient to maintain the ratio between the pole pitch and the coil pitch near to one to reduce the cogging torque and since this stator is a fractional layout with 9 slots, this ration can not be far from 1.

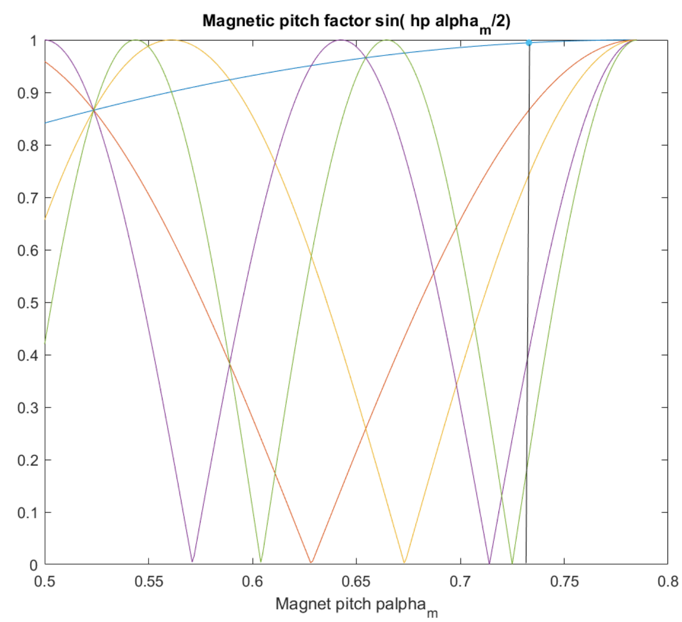

Figure 3.20: Magnetic pitch factor

At the end also the choice of factor q_r (q) and q_{sh} affect the harmonic content

Load

in MTPA operation

[8] $n_{seg} = 3$
[9] the reduction of those harmonic at the airgap reduce the induced EMF and the torque ripple

The current of the stator is shifted by 90 degree respect to the flux of the magnets, so the flux product by the stator is in phase with the rotor one

Demagnetization

Another interaction between stator and rotor can lead to a phenomena called demagnetization. Some area of the magnet can experience across them the MMF produced by the stator, in the opposite polarization compared to their stady state magnetization

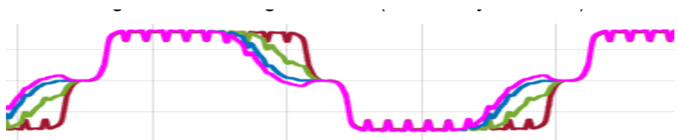

Figure 3.21: Demagnetization at different current

Since the machine is designed to avoid this event, it can happen under overload operation if they are not considered in the design.

The airgap flux density can be evaluated from the solution of the magnetic circuit:

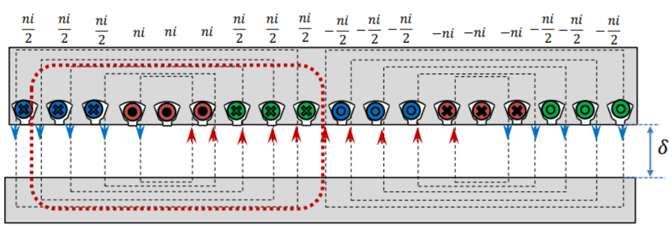

Figure 3.22: path

$$\oint H dl = MMF \tag{3.24}$$

$$H_s = \frac{MMF}{\delta} \qquad\qquad B_{MS} = \mu_0 \frac{MMF_{max}}{\delta} \tag{3.25}$$

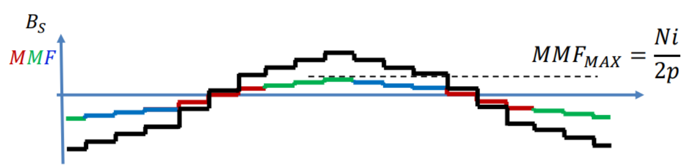

Figure 3.23: MMf

And now considering also the flux density from the magnet at no load condition[10]:

$$2H_0\delta_0 + 2H_{mag}l_{mag} = MMF_{max} \qquad\qquad B_{mag} = \frac{\mu_0 Ni}{2p\delta_0} - H_{mag}\frac{\mu_0 l_{mag}}{\delta_0} \tag{3.26}$$

[10]flux density in the magnet equal to the one in the air $H_0 = B_{mag}/\mu_0$

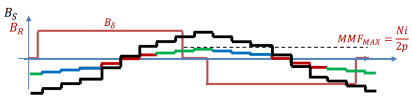

Figure 3.24: MMF

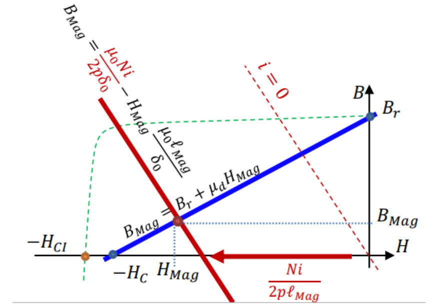

Figure 3.25: Limit condition

If the overload curve exceed the limit and the resultant magnetic field H is 90% of the intrinsic coercivity, the magnet start to demagnetize

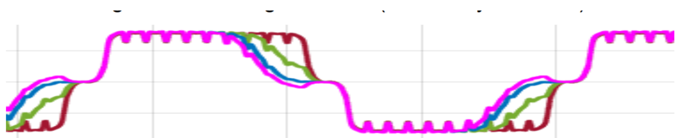

Figure 3.26: Demagnetization

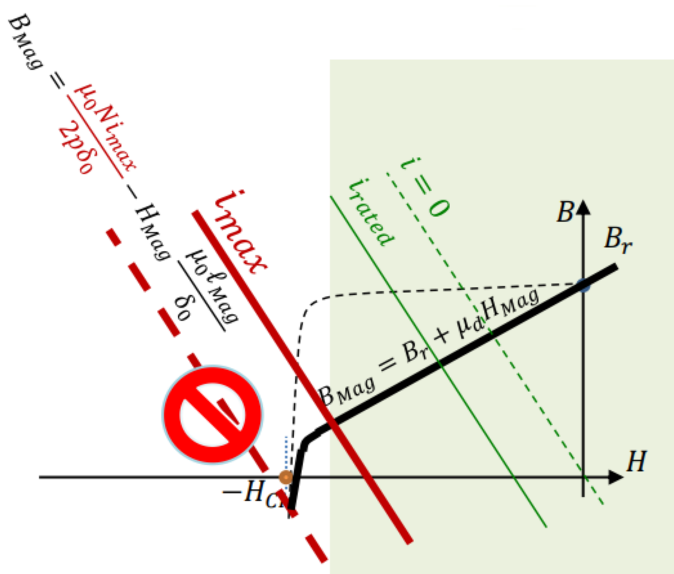

Figure 3.27: Demagnetization

To avoid magnetization, a parameter that take in consideration both the maximum current and the limit imposed by the intrinsic coercivity is the height of the magnet l_{mag} that should be greater than a minimum value:

$$l_{mag} > \frac{\frac{N|I_{max}|\sqrt{2}}{2p} + \frac{\delta_0 B_r}{\mu_0}}{0.9|H_{Ci}|} - \frac{\mu_d \delta_0}{\mu_0} = 0.00450(m) \tag{3.27}$$

and the value of the magnetic field at maximum overload admissible is:

$$H_{mag} = \frac{\frac{N|I_{max}|\sqrt{2}}{2p} + \frac{\delta_0 B_r}{\mu_0}}{l_{mag} + \delta_0 \frac{\mu_0}{\mu_d}} = 399456(\frac{A}{m}) < 0.9H_{ci} = 1074600(\frac{A}{m}) \tag{3.28}$$

At the end the overload current is no more sufficient for checking the demagnetization since the highest current is no the overload but the short circuit one($V = 0$):

$$|I| = |\frac{E_R}{R_S + jX_S}| = \frac{p\omega_m \Phi_R}{\sqrt{R_s^2 + (p\omega_m L_s)^2}} \qquad \Phi = \frac{N}{2\sqrt{2}} K_{Skew} K_{wind} \frac{2}{\pi} B_{MR} L\tau \tag{3.29}$$

$$I_{max} = \frac{\Phi_R}{L_S} = 468.714(A) \tag{3.30}$$

3.5 Sizing

By continuing with the unconstrained design, it is possible to fix at priori the expected flux density that is desired in the different region of the motor and from that chose the proper geometry dimension that allow the flux estimation. Since some parameters like the airgap diameter are already chosen, there are some constrain to take into consideration before starting the sizing of the geometry:

- The slot opening should be not too small to avoid the short circuit of the flux lines.To avoid this usually are done some cut, or it is possible to manage the wedge of the geometry by using tools once the lamination it is realised

- The height of the internal rotor yoke can be reduced by using a magnetic shaft that provide additional cross section to the flux that otherwise it wasted

- If the fractional winding (wounded tooth) layout is obtained by separate modules, is needed to take care of the airgap between the yoke, this region should be the lowest as possible in order to become an high reluctance path

Figure 3.28: Tooth wound

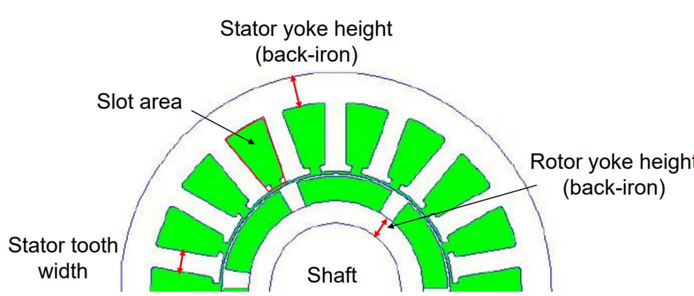

Figure 3.29: Dimension

3.5.1 Stator tooth width

$$1.3 \leq B_{Mt} \leq 1.6 \div 1.8 \qquad w_t = \frac{B_M \tau_s}{B_{Mt}} = 0.0362(m)(B_{Mt} = 1.65(T)) \tag{3.31}$$

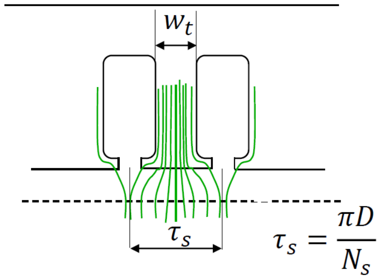

Figure 3.30: Geometry

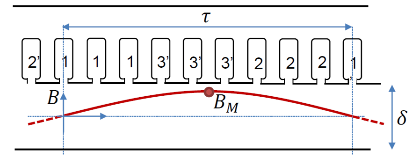

Figure 3.31: Tau

3.5.2 Slot Area

Assuming the constant distribution of current along all the conductive material, the slot area can be find by looking at the Electric leading Δ formula:

$$S_{slot} = \frac{\Delta \pi D}{N_s F_f J} = 1.69e + 03(mm^2) \tag{3.32}$$

where the current density can be assumed $J = 3.5 \frac{A_{rms}}{mm^2}$ in order to be able to exploit the maximum current density available for this type of motor cooling (natural convection). The Fill factor can be chosen by considering that this winding need a double layer and also there are present several bundles, so the best choice for this parameter that usually range between $0.35 \div 0.7$ is $F_f = 0.37$[11]

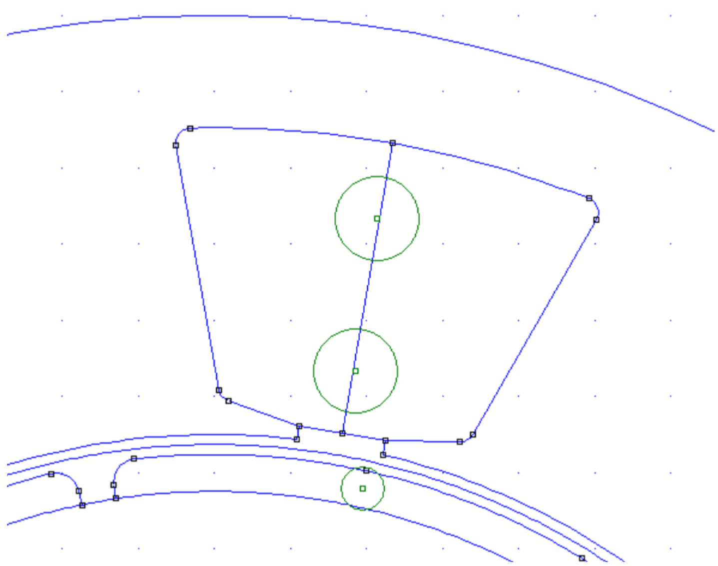

Figure 3.32: Slot

Now for the slot is possible to exploit also the geometrical parameters as the maximum and minimum slot's width and the height of the slots.

$$w_{s,min} \simeq \tau_s - w_t = \frac{\pi D}{N_s} - w_t \qquad w_{s,max} \simeq \frac{\pi(D + 2h_s)}{N_s} - w_t \tag{3.33}$$

$$S_{slot} = \frac{w_{s.min} + w_{s,max} h_s}{2} \qquad h_s^2 + (\tau_s - w_t)\frac{N_s h_s}{\pi} - S_{slot}\frac{N_s}{\pi} = 0(h_s = 0.0387(m)) \tag{3.34}$$

[11] By considering also the manufacturing effort, the insulation, and the slot shape

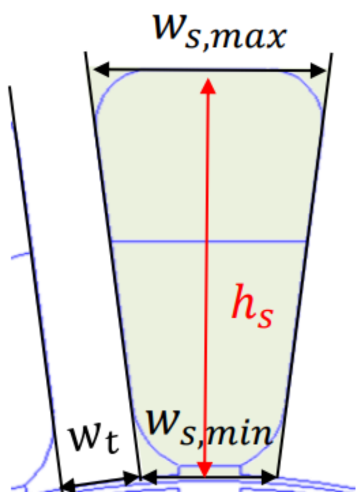

Figure 3.33: Slot design

3.5.3 Stator yoke hight

Here the high number of pole pair can help in order to reduce the height of the yoke since the vale of the flux that cross the yoke cross section depend on $\propto \frac{1}{p}$, so have high poles implies lower flux per pole and so h_y decrease

$$\Phi_{M\tau} = \frac{2}{\pi} B_M L \tau \frac{1}{p} \qquad B_{My} = \frac{\Phi_{My}}{S_y} = \frac{\frac{\Phi_{M\tau}}{2}}{L h_y} \tag{3.35}$$

$$1.1 \leq B_{My} \leq 1.5 \qquad h_y = \frac{B_M D}{B_{My} 2p} = 0.0147(m)(B_{My} = 1.45(T)) \tag{3.36}$$

These values are lower than the ones in the teeth because here the flux path is longer and there is more volume.

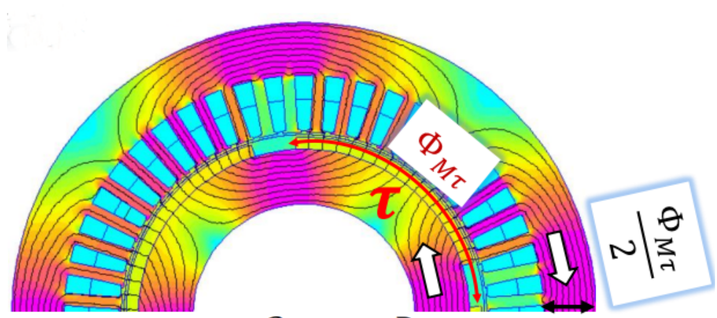

Figure 3.34: Yoke flux

3.5.4 Rotor yoke hight

$$1.2 \leq B_{MyR} \leq 1.6 \qquad h_{yR} = \frac{B_M D}{B_{MyR} 2p} = 0.0152(m)(B_{MyR} = 1.4(T)) \tag{3.37}$$

To reduce this value is possible to use a magnetic shaft, but in this project it is no needed

3.5.5 Aspect ratio check on dimension

By following the requirement of this project, there are limitation in terms of maximum external diameter and the active length. In order to be able to fit in the constraints, these values should be evaluated:

$$D_{ext} = D + 2(h_s + h_y) = 0.297 \simeq 0.300(m) \qquad D_{int} = D - 2(\delta + l_{mag} + h_{yR}) = 0.145(m) \tag{3.38}$$

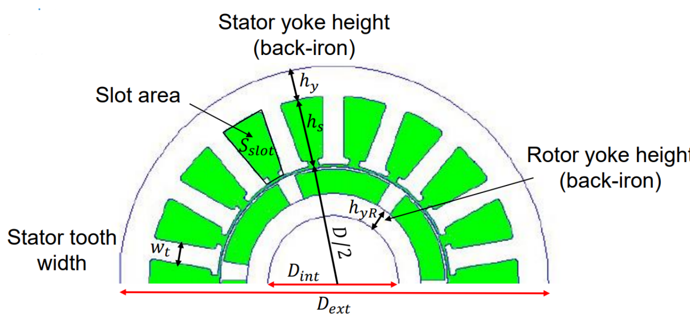

Figure 3.35: Design requirements

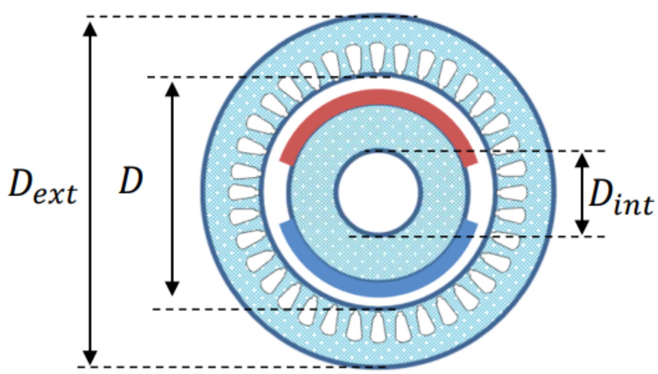

Figure 3.36: Design requirements

End winding

$$L_{ew} = k_{ew}\tau_{ew} = k_{ew}\frac{2\pi}{N_s}\frac{D+h_s}{2}y_q = 0.1277(m) \tag{3.39}$$

Figure 3.37: End winding

3.6 Volume and weight

To have a rough idea of the raw material cost, is inserting to look at the total weight of the materials inside the motor

iron

Stotor teeth

$$V_t = N_s w_t h_s L \qquad\qquad G_t = \gamma_{lam} V_t \tag{3.40}$$

Stotor yoke

$$V_y = \frac{}{4}(D_{ext}^2 - (D_{ext} - sh_y)^2)L \qquad\qquad G_y = \gamma_{lam} V_y \tag{3.41}$$

Rotor yoke

$$V_{yR} = \frac{}{4}(D_{int} + 2h_{yR})^2 - D_{int}^2)L \qquad\qquad G_y = \gamma_{lam} V_y \tag{3.42}$$

copper

$$V_{cu} = S_{cu} N_s (L + L_{ew}) \qquad\qquad G_{cu} = \gamma_{cu} V_{cu} \tag{3.43}$$

mag

$$V_{mag} = 2p \frac{\alpha_m}{2}(D - 2\delta_0 - l_{mag}) l_{mag} L \qquad\qquad G_{mag} = \gamma_{mag} V_{mag} \tag{3.44}$$

3.6.1 Cost

Material	Weight	Eur/kg	Eur	Total
Iron	34.17	1.6	54.67	
Copper	13.11	8	104,8	
Magnet	2.57	x	x	
Total				159.55

3.7 Performaces

The performances of this machine are evaluated by following the MTPA strategy. This control aim to maximize the torque with the minimum current for the stator. In fact, the contribution of the magnetic loading of the rotor is grater than the one that come from the stator:

$$B_M = \sqrt{(B_{MR}^2 + B_{MS}^2)} \tag{3.45}$$

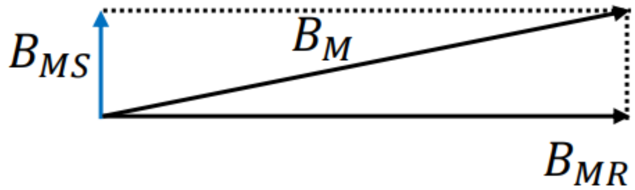

Figure 3.38: MTPA control

where the analytical contribution are:

$$B_{MR} = \mu_0 \frac{MMF_{MR}}{\delta_{prime}} \qquad B_{MS} = \mu_0 \frac{MMF_{MS}}{\delta_{prime}} = 0.1629(T) \tag{3.46}$$

$$MMF_{MS} = \frac{\sqrt{2} D K_w \Delta}{2p} \tag{3.47}$$

3.7.1 Losses

The following evaluation take into consideration the general losses coming from copper, iron and losses due to friction and ventilation (if present), so the efficiency it is based on these type of losses. It is important to underline that some other effect are neglected in the evaluation of the efficiency like the current ripple that come from the control and PWM but also the harmonic distortion due to the MMF produced by magnet and winding (and also the slotting effect) are additional contribution that should be taken into consideration for a more accurate result

Iron losses

As it was done for the induction motor the evaluation of the iron losses is mainly due to the hysteretic behaviour and eddy currents

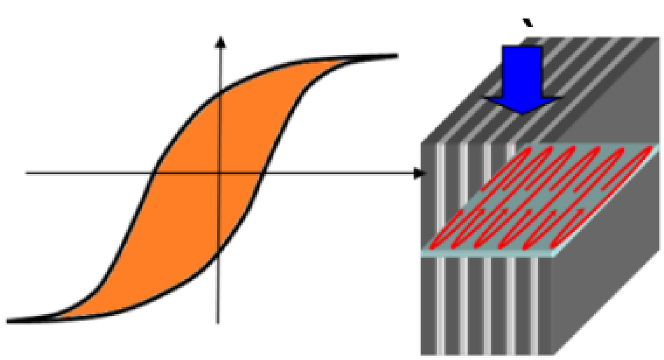

Figure 3.39: Iron losses

$$\frac{P_{loss}}{G_{fe}} = K_i f B^2 \alpha + K_c f^2 B^2 (\frac{W}{kg}) \tag{3.48}$$

$K_c = \frac{s^2}{\rho}$ is the contribution that take care of the iron loses due to the eddy current, and it depends on the lamination thickness that since the working frequency is a medium/high frequency is possible to use lamination with lower thickness (= 0.35mm usually) and on the ρ resistivity.

$$P_{fe,total} = P_{fe,t} + P_{fe,y} + P_{fe,yr} = 374 + 299 + 163 = 1211.8(W) \tag{3.49}$$

$$P_{fe,x} = k_l G_x P_{loss} \tag{3.50}$$

Here the lamination factor $1 < k_l < 2$ take into consideration the manufacturing process needed to realize the desired lamination geometries and also the post process like the post aneling that is needed to restore a part of the magnetic properties of the material

Additional iron Losses

A non laminated rotor yoke and a non segmented magnet can lead to eddy currents and iron losses that can produce an over temperature higher than the expected one, even at no load condition the slotting effect can induce eddy current in the magnet.

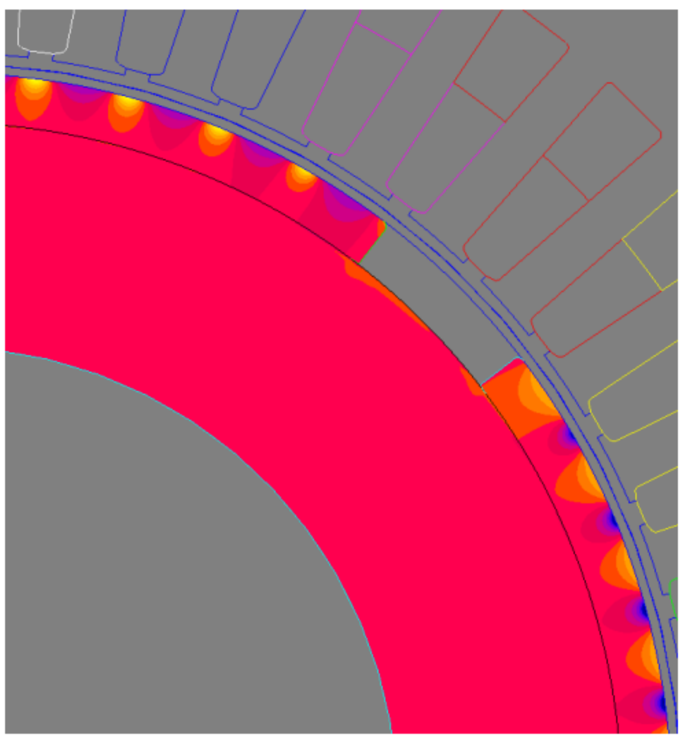

Figure 3.40: Eddy current

The fractional winding layout generate filed harmonic of order and magnitude close to the fundamental counter rotating one, this interaction induces eddy current in the magnet (EDDY current) so it can be needed to laminate both the magnet and the rotor yoke.

For the design these effects are taken into consideration but not for the efficiency calculation.

Copper losses

The Joule losses in the stator of induction motors can be calculated from the copper volume, the resistivity of the conductors at the operating temperature, and the current density as:

$$P_{jS} = P_{Cu} = \rho_{cu} V_{Cu} J^2 = 375.27(W) \tag{3.51}$$

Note: in case of uneven current distribution, additional losses must be considered. This can be due to high frequency currents (e.g., above 400 Hz for high-speed applications) or, more often, current distortion (harmonics and/or inverter supply). For this project, the assumption is to consider the current equally distributed in the conductor

Friction losses

Ventilation, windage, and friction losses depend on the speed, machine geometry, and mechanical design (ventilation system, aerodynamic, and bearings).

Figure 3.41: Friction losses

This contribution can be evaluated by considering that these mechanical losses are typically correlated by an exponential relation between these losses and the mechanical speed, in a qualitative way the following plot represent this relation[12]:

[12]TEFC induction motor

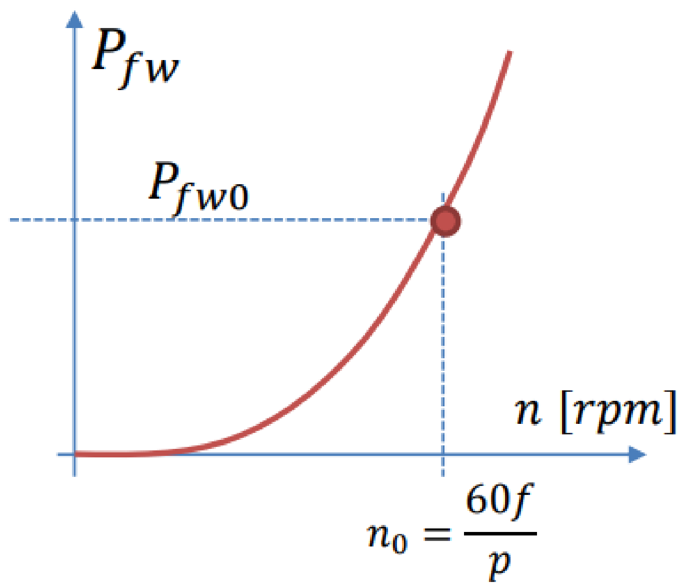

Figure 3.42: Friction losses

The equation that provide a good estimation of the total mechanical power

$$P_{fw} = P_{fw0}(\frac{n}{n_0})^3 = 113.17(W) \tag{3.52}$$

$$P_{fw0} = k_w D(L + 0.6\tau)(\frac{\omega_m D}{2})^2 = 565.88(W) \tag{3.53}$$

If the motor is not self-ventilated, ventilation losses are null. The windage and friction contributions can be calculated separately but require the use of complex models or semi empirical equations. Overall, the expected losses are significantly lower, (15% $\div$ 20%) compared to a TEFC self-ventilated motor)

where $k_w = 15(\frac{Ws^2}{m^4})$ this is a small and medium size TEFC motor so this value it is considered 20% lower

3.7.2 Efficiency

The efficiency of the motor is defined as

$$\eta = \frac{P}{P + P_{fe} + P_j + P_{jR} + P_{fw} + P_{add}} = 0.9665 \tag{3.54}$$

The efficiency is important to reduce costs. Even in applications where high efficiency has not strict requirements, the losses $P_f e$, $P_C u$, $P_f w$) must be kept low to limit the temperatures of the components and avoid damaging the motor materials:

- Insulating system then accelerated ageing then machine electrical failure
- Magnets can demagnetise and reduce the performances leading to a mandatory derating

3.8 Equivalent circuit

The equivalent circuit of the SPM is the following:

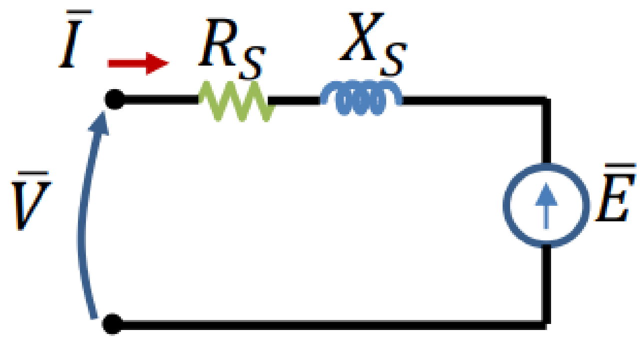

Figure 3.43: Equivalent circuit

The solution of that circuit can be useful to evaluate the equivalent parameter that take part in further calculation needed to better evaluate some parameters.

3.8.1 Resistance

Stator resistance

The stator resistance represent the winding resistance in fact it can be evaluated as it follow or reversing the power formulas.

$$R_s = \frac{2^2(L + L_{ew})}{S_{cu}N_s} = 0.0126\Omega \tag{3.55}$$

3.8.2 Inductance

Stator inductance

The stator inductance is the sum of two contribution, the stator leakage inductance and the contribution that came from the stator current.

$$L_s = L_l + L_{ss} = 2.615e - 04(H) \tag{3.56}$$

To better evaluate these factors it is fair to introduce the steady state phase or equation in which appear the contribution of the total flux. This flux is composed by the air gap flux produced by the rotor, the air gap flux produced by the stator currents and then the leakage flux produced by the stator currents that are not crossing the air gap. Their inductances are evaluated through these flux contribution

$$V = R_s I + \frac{d\Phi_{tot}}{dt} \qquad \Phi_{tot} = \Phi_r + \Phi_{ss} + \Phi_l = \Phi_r + L_{ss}I + L_l I \tag{3.57}$$

where:

$$L_{ss} = \frac{\Phi_{ss}}{I} = \mu_0 \frac{3(K_w N)^2 L\tau}{2p\pi^2\delta_{prime}} \qquad \delta_{prime} = \delta_0 K_{carter} + l_{mag}\mu_r \simeq \delta \tag{3.58}$$

This result can be obtained by simulating the motor without the magnet (or having a remanence $B_r = 0$, The leakage inductance estimation comes from analytical calculation done under some specific hypothesis that follow the experience of the literature and the industrial world that produced some analytical models and empiric formulas to use in a preliminary design.

$$L_l = L_{l,slot} + L_{l,ew} + L_{l,\delta} = 3.1683e - 05(H) \tag{3.59}$$

- Slot leakage $L_{l,slot} = \frac{3N^2 L\lambda_{slot}}{N_s} = 1.732e - 05(H)$
- $L_{l,ew} = \frac{N^2 \tau_{ew} \lambda_{ew}}{2p} = 1.263e - 05(H)$
- $L_{l,\delta} = \frac{3N^2 L\lambda_\delta}{N_s} = 1.724e - 06(H)$

All the previous equation presents the contribution that is also called permeance, and it is represented by the values $L\lambda$. Each lambda is a permeance per unit length, and it is fair to distinguish them for the different contribution that they carry .

Slot leakage permeance per unit length λ_{slot} con be evaluated by assuming the slot rectangular (instead of the real geometry that is trapezoidal in order to maintain the teeth width constant)

$$\lambda_{slot} = \frac{\mu_0}{q}((\frac{h_1}{3a} + \frac{h_2}{a} + \frac{h_3}{a - s_o} ln(\frac{a}{s_o}) + \frac{h_4}{s_o})q - \frac{1}{4}(\frac{h_1}{4a} + \frac{h_2}{a} + \frac{h_3}{a - s_o} ln(\frac{a}{s_o}) + \frac{h_4}{s_o})q_{sh}) \tag{3.60}$$

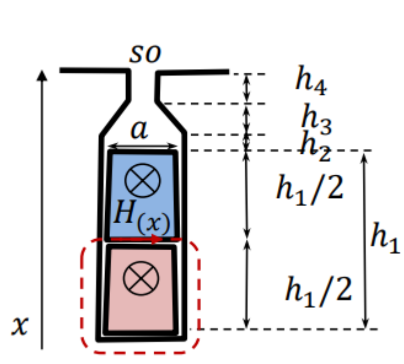

Figure 3.44: Slot geometry (qualitative)

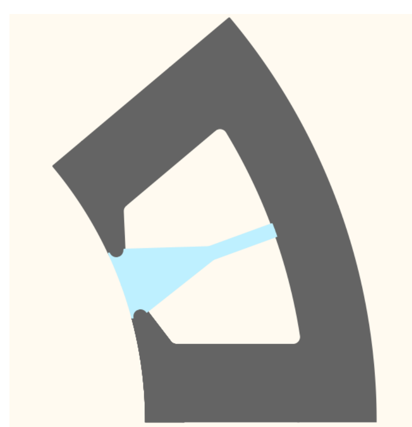
Figure 3.45: Slot geometry (quantitative)

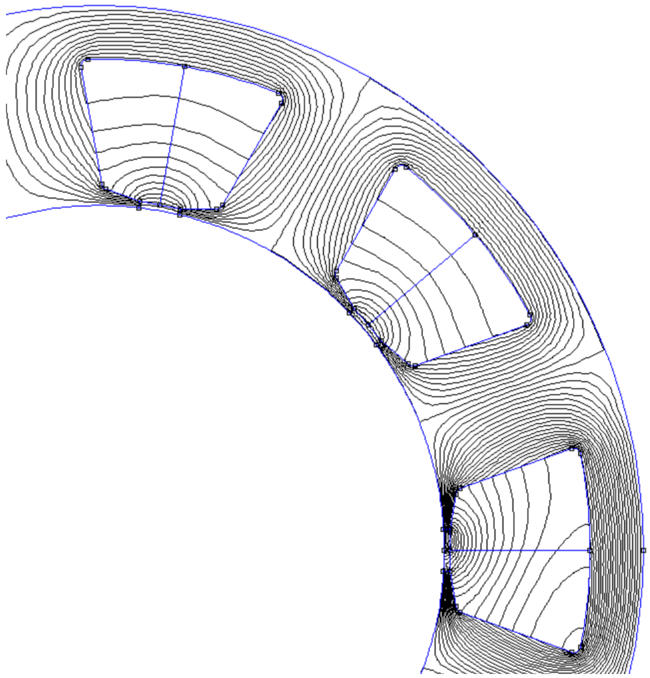

Figure 3.46: Slot geometry (quantative)

The end winding leakage permeance per unit length (λ_{ew}) is a complex contribution to take into consideration, and it strongly depends on the end winding layout (how are manufactured) so for a three phase windings it can be approximated with the following equations:

$$\lambda_{ew} = mu_0(0.18 \div 0.30) = mu_0 0.26 \tag{3.61}$$

The tooth top permeance is used to consider for the leakage fluxes that appear in case of high magnetic airgaps ($\delta = \delta_0 + l_{mag}$) in synchronous machines. In case of SPM machines with a constant airgap:

$$\lambda_{\delta} = mu_0 \frac{\frac{5(\delta_0 + l_{mag}}{so}}{\frac{4(\delta_0 + l_{mag}}{so}} \tag{3.62}$$

it is possible to see some lines that close between teeth similar to the leakage inductance because they do not cross the airgap so they do not contribute to the torque production.

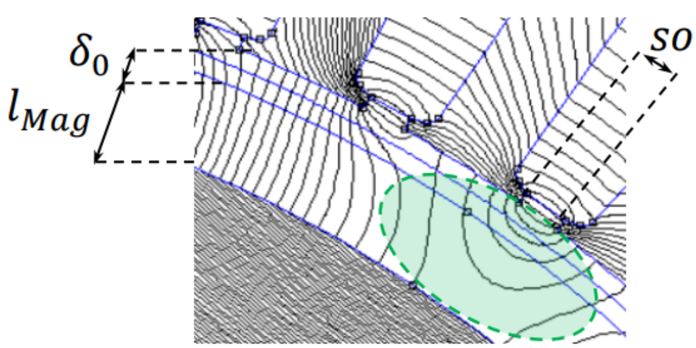

Figure 3.47: Leakage

3.8.3 Power factor

The power factor of the motor is defined as:

$$\phi = \angle\overline{V} - \angle\overline{I} = \arctan\left(\frac{X_S I}{R_S I + E_R}\right) = \tag{3.63}$$

$$PF = \cos\phi = 98\% \tag{3.64}$$

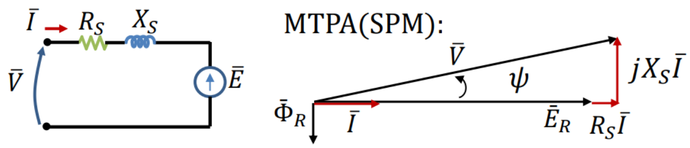

Figure 3.48: MTPA

This contribution came from the resolution of the equivalent circuit that is now presented. This parameter is important because to provide an estimation of the absorbed apparent power $A = 3VI$ in order to determine the size of the converter since at given active power a machine with a larger power factor can operate with a converter with reduced current or voltage rating.

To evaluate this factor, it is essential to find the phase voltage of this motor:

$$V = R_s I + jX_s I + E_r \tag{3.65}$$

3.8.4 Number of conductors in series per phase

This machine should be drive in order to control phase voltage in relation to the DC link. To do that, a control margin is taken from the total DC link in order to let some irregularity in the maximum amplitude due to the harmonic distortion or overload condition if considered. At the conclusion of the design, the machine must be adapted to the converter and control requirements. These determine the DC link voltage V_{dc} the voltage control margin (e.g., 0.95), and the maximum peak current $I_{pk,max}$. These voltage limits identify the actual number of series conductors per phase (N), which indirectly determines the inverter current rating and its peak value (check demagnetization risk).

In order to evaluate the number of conductors in series per phase, it is possible to have a different analytic strategy from the one seen previously[13]

By considering the MTPA operation, where the current is in phase with the $BEMF = j\omega\Phi_R$ and the control aim to keep the stator MMF (I) in quadrature with the rotor flux

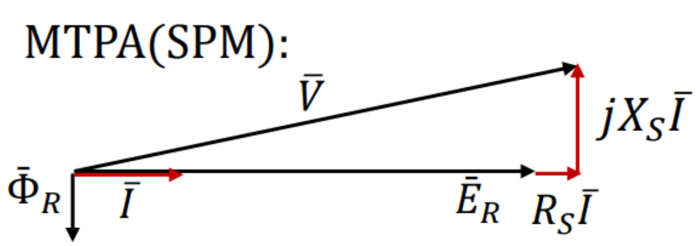

Figure 3.49: MTPA

[13]the previous evaluation was a rough estimation based on parameter that now is udpted

Now is possible to create a system of equation that depend on many design parameters:

$$I = \frac{\Delta \pi D}{3\boldsymbol{N}}$$

$$\begin{cases} E_R = \omega \dfrac{\boldsymbol{N}}{2\sqrt{2}} K_s K_w \dfrac{2}{\pi} B_{MR} L \tau = a_1 \boldsymbol{N} \\ R_S = \dfrac{3\rho \boldsymbol{N}^2 (L + L_{ew})}{S_{Cu} N_s} \longrightarrow R_S I = a_2 \boldsymbol{N} \\ X_S = \omega \left(\left[\dfrac{3\boldsymbol{N}^2}{N_S} L\lambda_{slot} + \dfrac{\boldsymbol{N}^2}{2p} \tau_{ew} \lambda_{ew} + \dfrac{3\boldsymbol{N}^2}{N_S} L\lambda_\delta \right] + \mu_0 \dfrac{3K_w^2 \boldsymbol{N}^2}{2p\pi^2 \delta'} L\tau \right) \longrightarrow X_S I = a_3 \boldsymbol{N} \end{cases}$$

$$V = \sqrt{(a_1 \boldsymbol{N} + a_2 \boldsymbol{N})^2 + (a_3 \boldsymbol{N})^2} = a_V \boldsymbol{N} \propto \boldsymbol{N}$$

Figure 3.50: N claculation

Where the parameter a_v is the voltage per conductor. For the fractional winding the equivalent number of conductor for each slot

$$n = \frac{N}{\frac{N_s}{3}} = 22 \tag{3.66}$$

This configuration is a fractional layout do not allow parallel because there are no the condition to have the parallel path in slots with the same electrical position (A). In order to have an integer number of n it was better to approximate in defect in order to avoid an extra increase of the BEMF that can be critical with the control limit

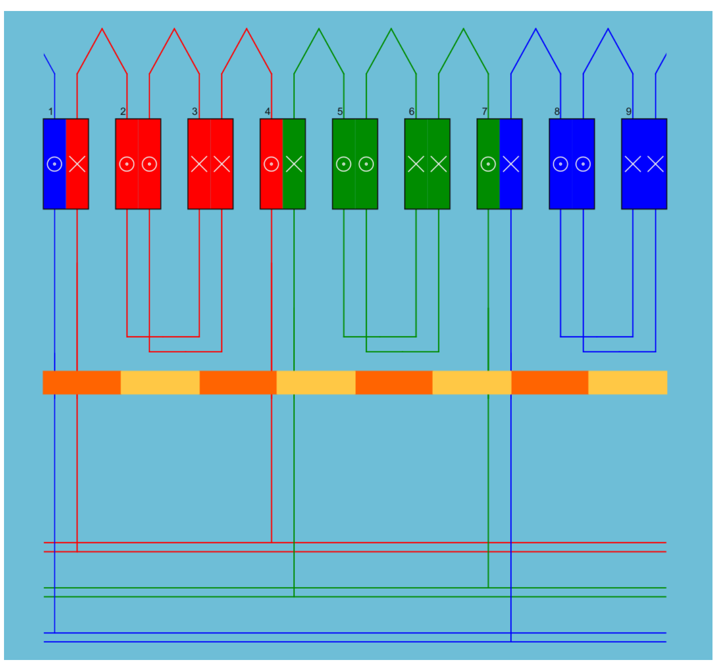

Figure 3.51: Winding layout

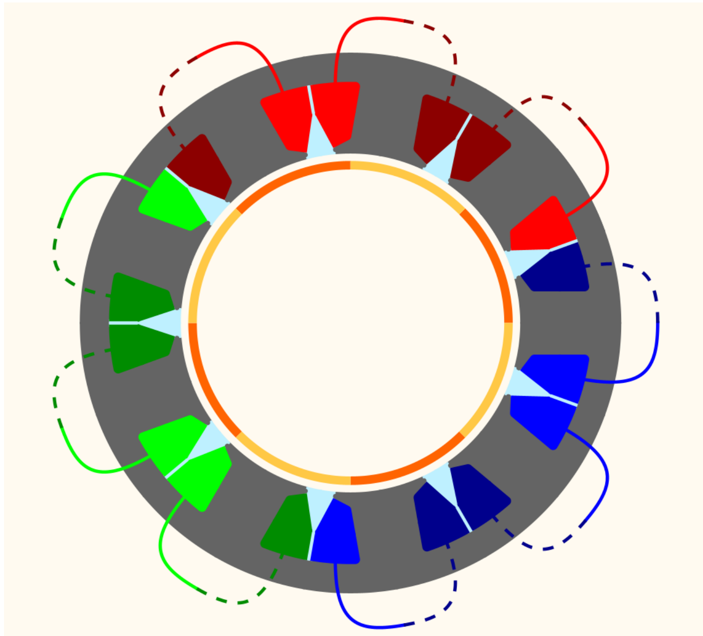

Figure 3.52: Winding layout

So, the other things that is possible to do is to make a bundle of parallels wire for each conductor in order to facilitate the manufacturing and at the same time increasing the field factor. This solution reduce the diameter of each wire in order to limit the skin effect, but also it is helpful two have a constant current density along the wire since the working condition of this machine are not at very low frequencies (this problem can be avoided also by using litz wires, but in this design they are not used)

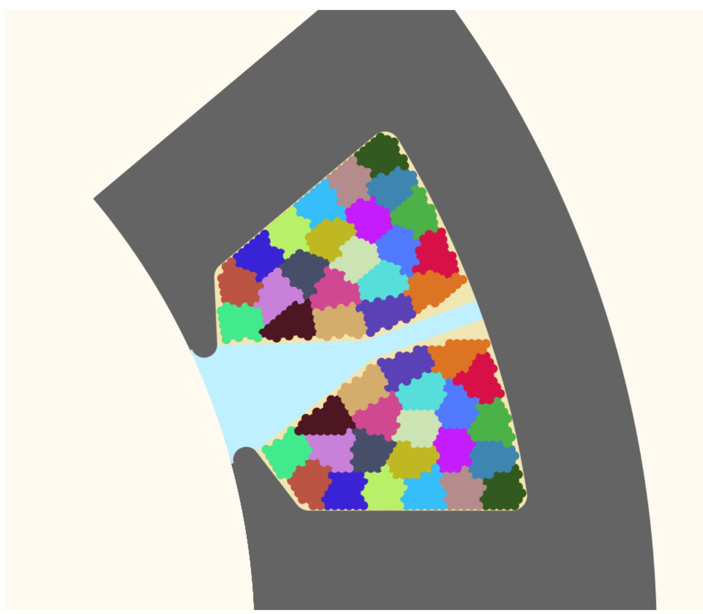

Figure 3.53: Slot and wire

$$S_{cu} = F_f S_{slot} \qquad\qquad S_w = S_{\frac{S_{cu}}{n n_b}} \tag{3.67}$$

$$d_w = 2\sqrt{\frac{S_w}{\pi}} = 1mm \tag{3.68}$$

New values

Var	Simplified	1^{st}	2^{nd}
N	70	68	66
n	23.3	22.6	22
E		184.22	172.04
I			99.48

3.8.5 Voltages

For a given DC link voltage, the maximum instantaneous face to face voltage is . Now to completely exploit the DC link capability and at the same time maximize the current through the switching device it will be enough to size the number of conductor in series per face in order to operate at voltage rated condition

$$\sqrt{2}V = \frac{v_{ll,max}}{\sqrt{3}} = \frac{V_{dc}}{\sqrt{3}} \tag{3.69}$$

however, a voltage margin is essential to ensure controllability, including the voltage distortion to maintain a sinusoidal current and the changing of the DC link voltage. This margin should not be too much large in order to not reduce too much the modulation index that it can introduce I current that can be a problem for there is reaching devices. At the end the maximum inverter current is also used to check the non demagnetization as one of the possible Wrose cakes approach

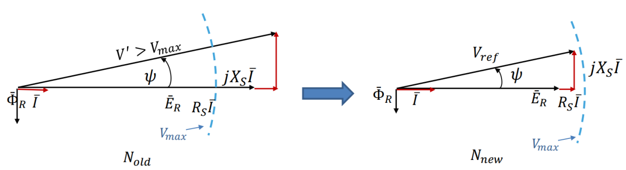

Figure 3.54: Control margin

If this condition is not respected, in order to avoid damage in the circuit it is better to evaluate again the number of conductor in series per phase by using a voltage reference $V_{ref} = 0.95\frac{V_{dc}}{\sqrt{3}\sqrt{2}}$ so $N_{new} = V_{ref}\frac{N_{old}}{V_{old}}$

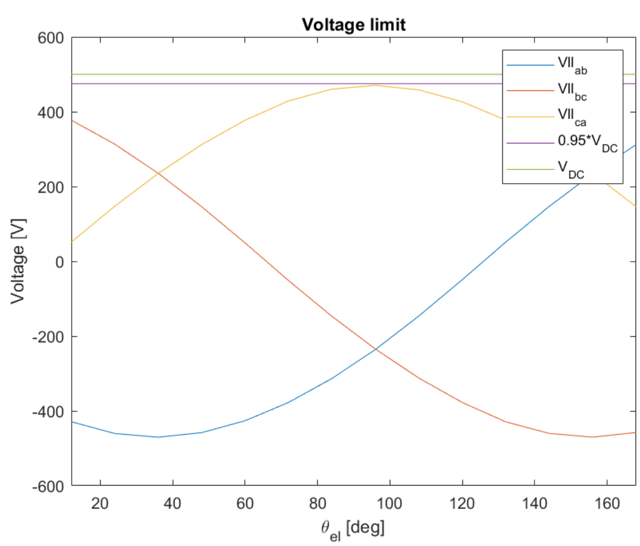

Figure 3.55: Voltage line to line

3.9 Motor characteristic and FEA

The motor characteristic are evaluated thanks to the support of the finite element analysis performed with FEMM

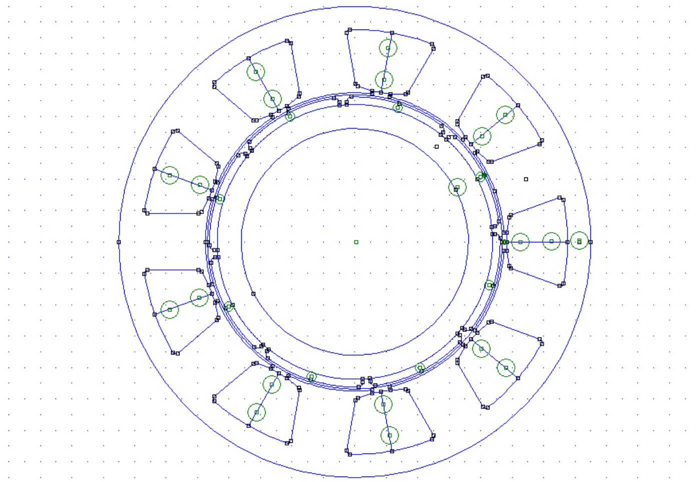

Figure 3.56: FEA

Cogging torque

The shape of the cogging torque should be periodic and centred around the x axle. In this case, it was not possible to obtain a good shaped plot for this parameter because the mash was not exploited at its best for this type of simulation. By the way, the expected value has a low magnitude and for further deeper analysis it can be convenient to work on the mesh in order to achieve a more precise result.

$$T_{cogg} = \frac{1}{2} MMF_R^2 \frac{dP_m}{d\theta_m} \tag{3.70}$$

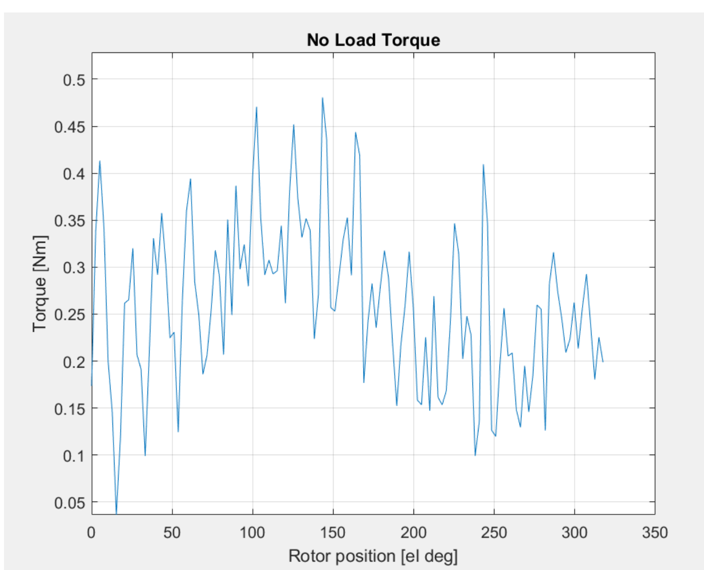

Figure 3.57: Cogging torque attempt

$$f_{cogg} = k\frac{f}{p}lcm(N_s, 2p) \tag{3.71}$$

From the harmonic spectrum of the cogging torque is possible to evaluate the coefficient k

$$\frac{f_{cogg,k}}{f} = \frac{klcmN_s, 20}{p} = \frac{kN_s}{p} = \frac{k72}{4} = k18 \tag{3.72}$$

MTPA

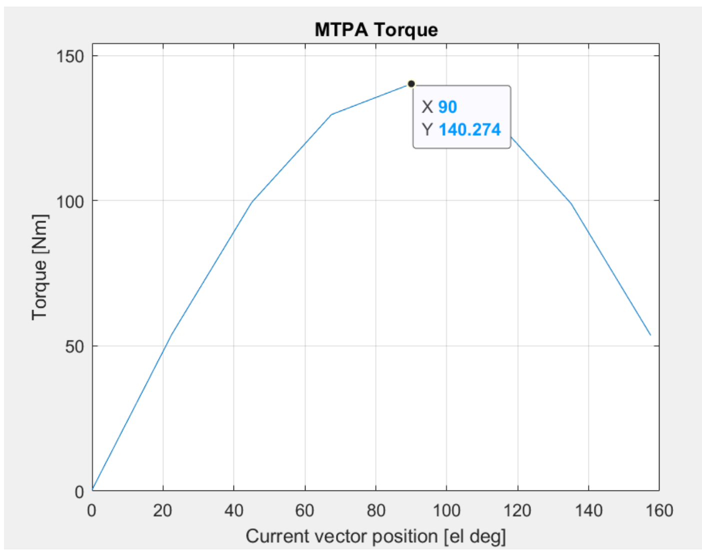

Figure 3.58: MTPA

$$T_{PM} = \frac{3}{2}p\phi_{PM}I_M sin(\gamma) \tag{3.73}$$

$$T_{PM,MTPA(\gamma=90^\circ C)} = \frac{3}{2}p\phi_{PM}I_q \tag{3.74}$$

Note: for a better prediction the average of the torque in 360 electrical degrees of rotor position should be considered due to cogging and torque ripple distortion.

Airgap Flux Analytical

ONLY WIND
The winding produce also non electrical harmonic, the harmonic of order lower than the fundamental and the non electrical do not contribute to the production of the torque since the rotor does not proceed them so at rated condition there is not the batch between these harmonic with their equivalent produced by the stator. These mechanical harmonic induces eddy currents in the magnet and produce radial forces.

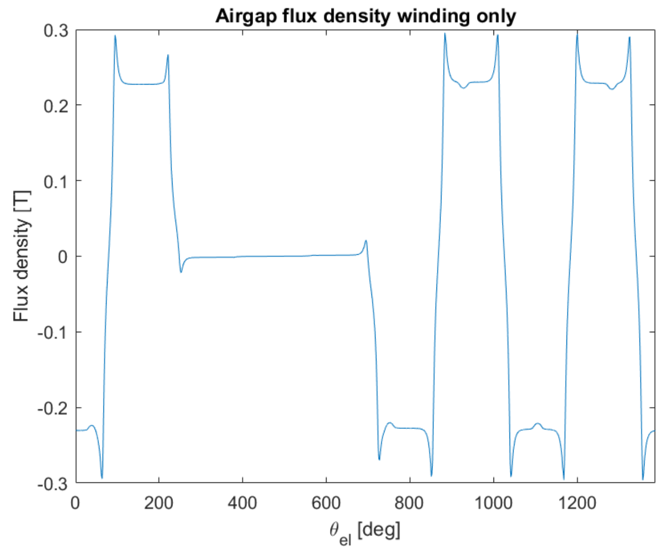

Figure 3.59: Airgap flux density winding only

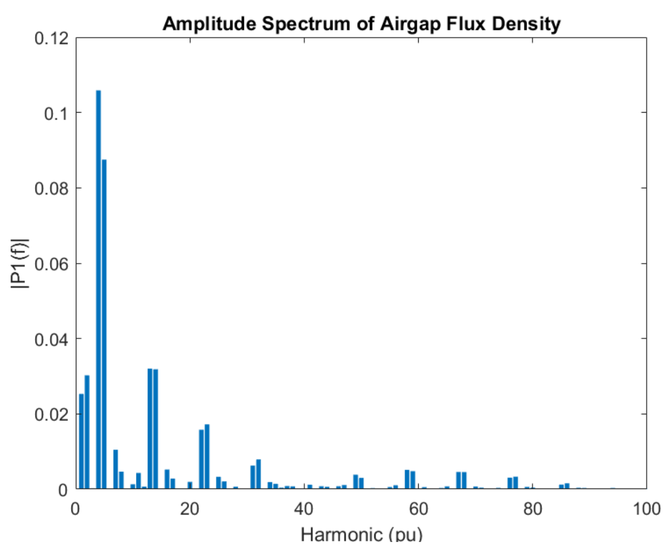

Figure 3.60: FFT only winding

ONLY PM

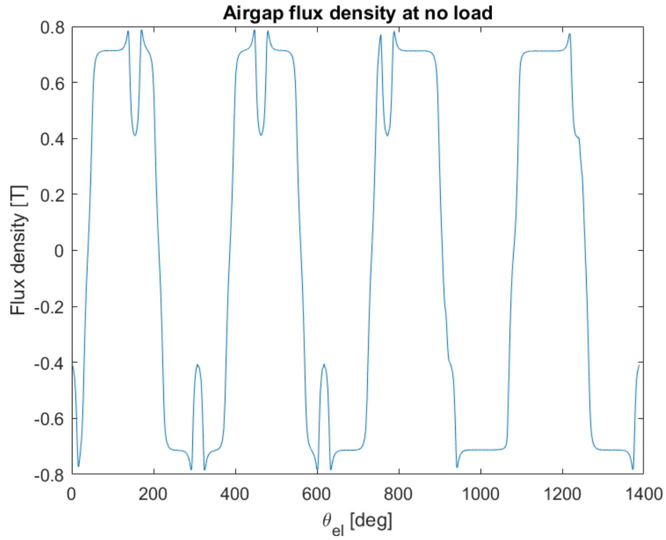

Figure 3.61: Airgap flux density magnet only

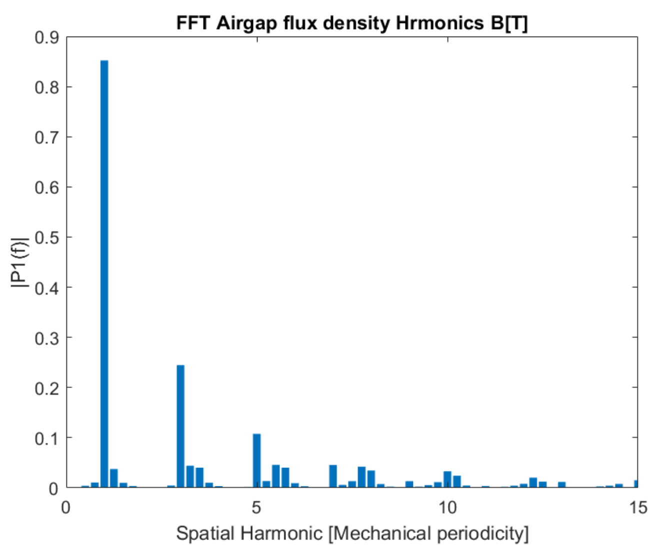

Figure 3.62: FFT no load

BOTH

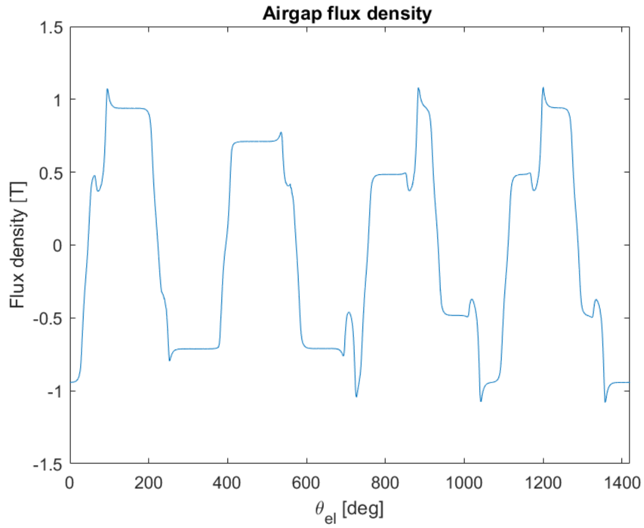

Figure 3.63: Airgap flux density total

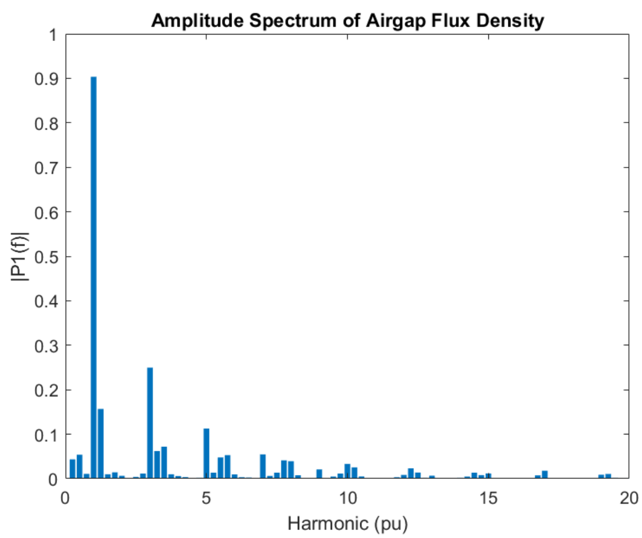

Figure 3.64: FFT Airgap flux density total

Torque

The following plot shows the total toque contribution and the contribution of each of the three segment in the same time instant. It is interesting to underline that the central magnet give the maximum contribute because its axle is in phase with the winding contribution obtained at MTPA condition, while the two side magnet are shifted ± to the centred position

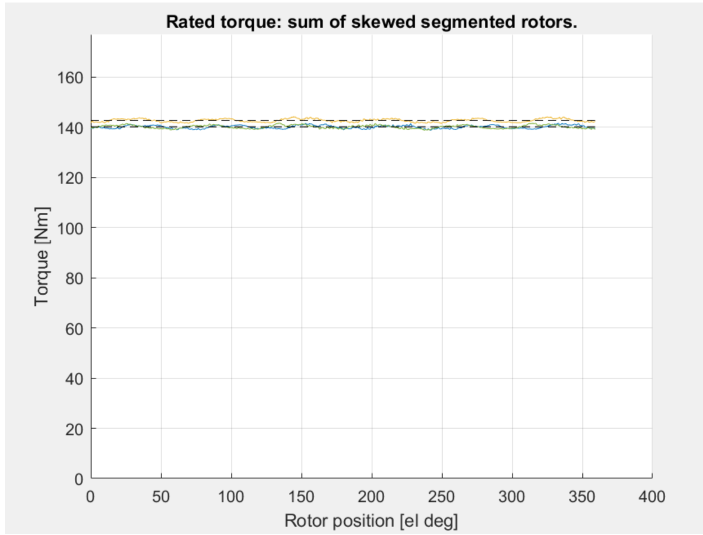

Figure 3.65: Rated torque for each segment

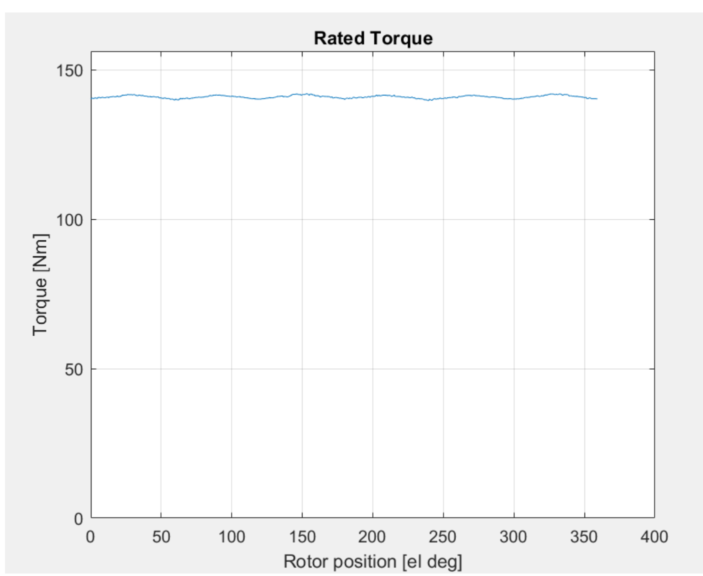

Figure 3.66: Rated torque

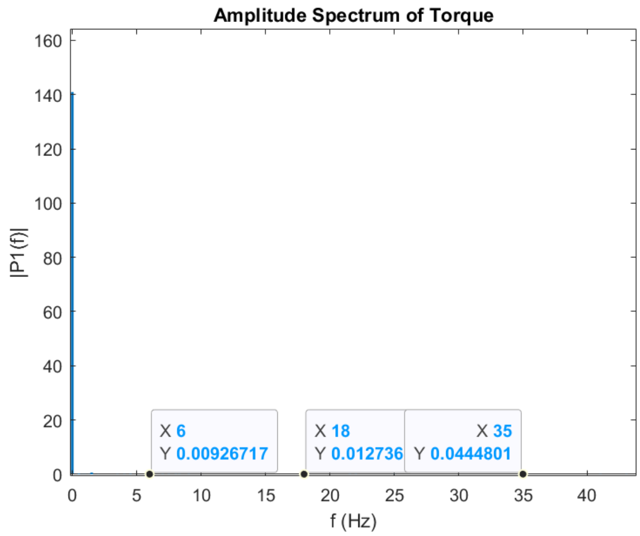

Figure 3.67: FFT rated torque

It is possible to see the effect of the toque ripple thanks the harmonic distribution. Since the 7th and 5th affect the 6 (as the 17th and 19th affect the 18 th)

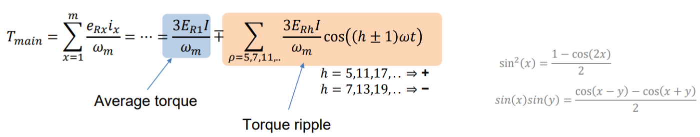

Figure 3.68: FFT rated torque

Radial Forces

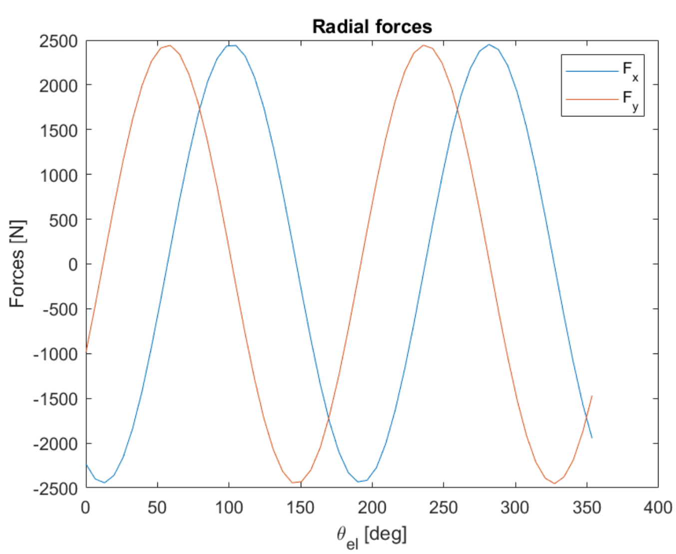

Figure 3.69: Radial Forces

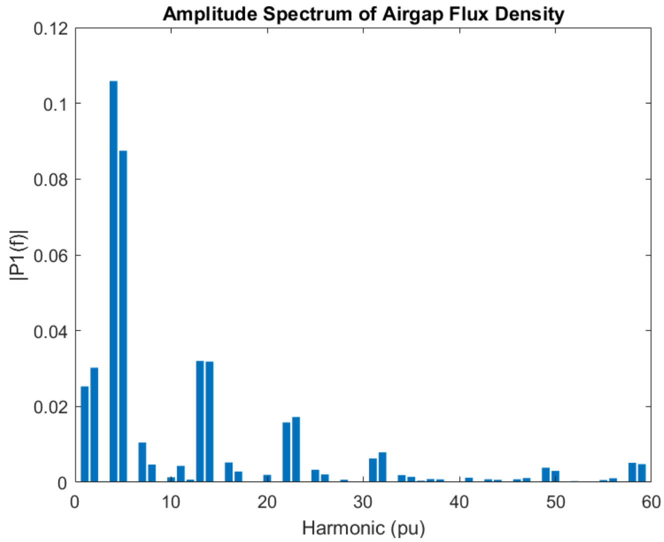

Figure 3.70: FFT radial forces

Voltages

Phase voltage

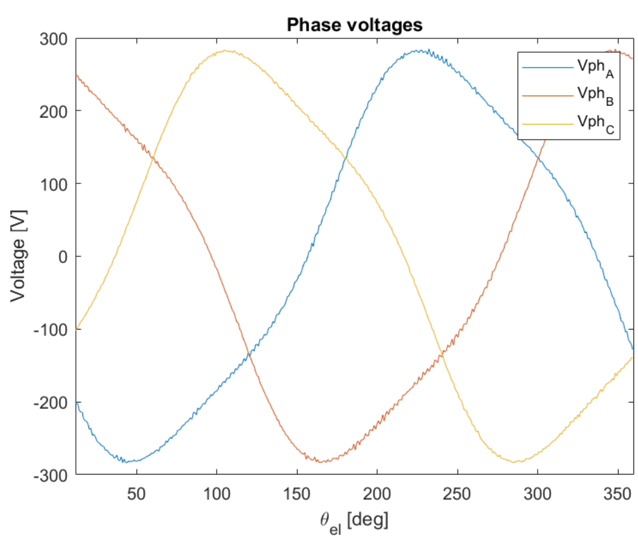

Figure 3.71: Phase voltage

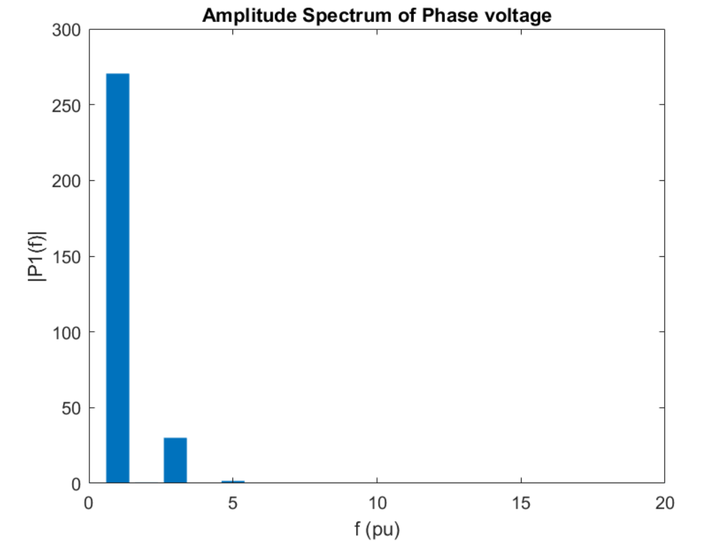

Figure 3.72: FFT Phase voltage

Line to line voltage with control limit on

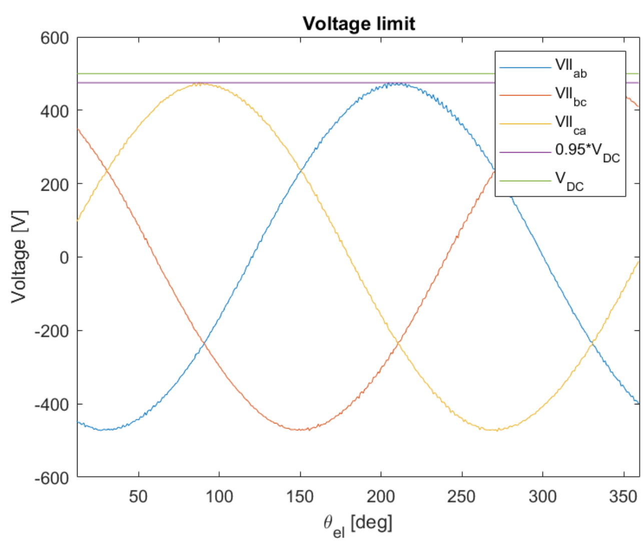

Figure 3.73: Voltage line to line

Overload torque

Overload capability: if B_{MMR} the overload is mainly limited by the voltage and the demagnetization limits. Above a current value, the torque is not increasing proportionally to the current (due to saturation)

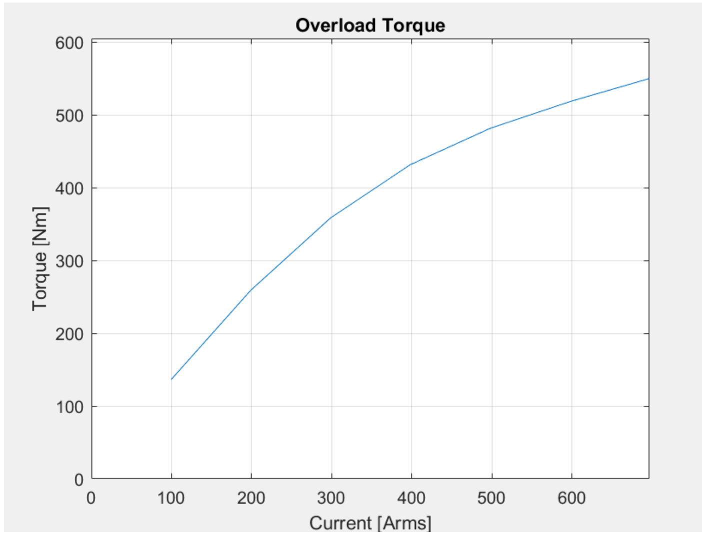

Figure 3.74: Overload torque

Slot leakage

From this simulation is possible to obtain the value of the stator slot leakage inductance 0.000181658(H), that is 1 order of magnitude greater than the one evaluated analytically $1.585192200792561e-05$ (H). This difference can be attributed to the way of evaluation of the slot area, since it was follow the same workflow of a distributed winding that for example have a different final slot and winding layout, so it can be acceptable to take the FE result as the best one

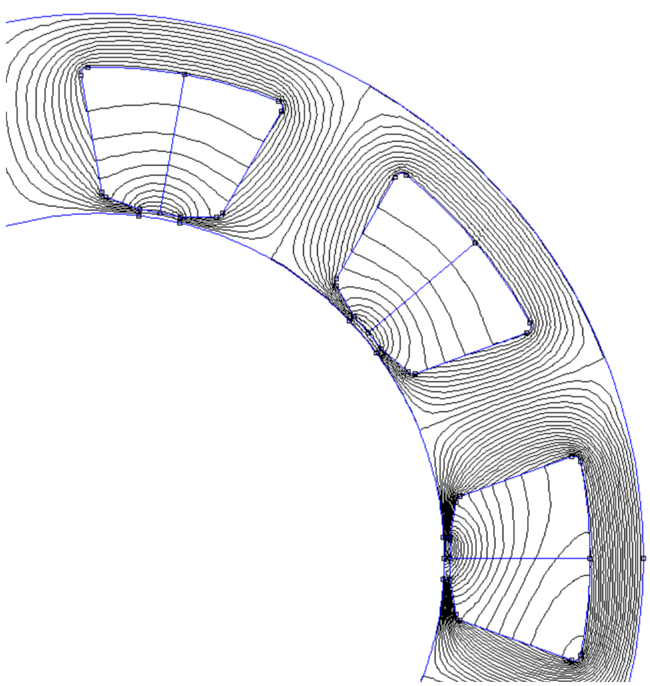

Figure 3.75: Slot leakage

Appendix A

Appendix and Catalogues

A.1 Wire

ANCHE toto eoh e isolamento

Choice of Conductor

Copper wire is the most common choice as conductor used throughout the Electrical Industry. Electrical conductivity is the most important characteristic of any conductor. Choices are usually restricted to unalloyed pure metals rather than to alloys.

For equal diameters, aluminium, the second choice of conductor, has about 61% greater resistance than copper. Furthermore, aluminium has a lower thermal conductivity, which reduces the efficiency of cooling by thermal conduction to heat sinks or by convection of moving air.

When considering volume, particularly in small sealed motors, copper is a more efficient material.

A comparison between copper and aluminium

POSITIVE

Copper	Aluminum
High electrical conductivity	Lower density
High thermal conductivity	Lower costs
Low cost	Higher temperature
Volume Efficient	Enamelled rating
Easy to solder	Weight efficient
Easy to work	
Good corrosion resistance	
Easy to coat	

NEGATIVE

Copper	Aluminum
Low strength	Lower strength
Low oxidation resistance	Lower conductivity
Difficult to machine	Lower corrosion resistance
Some brazing problems	Poor stress relaxation
Gas diffusion	Poor solderability
High temperature creep	

A comparison between copper and aluminium

Characteristics	Copper	Aluminum
Specific Weight (g/cm^3)	8.89	2.70
Melting Point (°C)	1,083	658
Specific Heat (cal/g °C)	0.093	0.0220
Coefficient of linear expansion (1/°C)	0.000017	0.000023
Tensile Strength (MPa)	262	82.7
Elongation at break (%)	15–35	10–30
Conductivity IACS at 20°C (%)	101	61.5
Resistivity at 20°C (Ω mm^2/m)	0.01707	0.02803
Temperature coefficient of resistivity at 20°C (1/°K)	0.00397	0.00406

For the Same Voltage Drop

Diameters ratio	1	1.27
Cross section ratio	1	1.63
Weight ratio	1	0.50

For the Same Intensity of Current (thermal exchange)

Diameters ratio	1	1.19
Cross section ratio	1	1.42
Weight ratio	1	0.40

Figure A.1: Wire charatteristic

The diameter $d_w$of each parallel wire that compose a single series conductor in each slot, is evaluated by looking at the following and by considering the nuomber of boundel n_b a degree of freedom in order to obtaina proper industrial diameter

Conductor Diameter			Cross-Section Area	Maximum Resistance at 20°C		Current Rating
Nominal (mm)	Maximum (mm)	Minimum (mm)	(mm)	CU ΩΩ/1,000mm²	AL Ω/1,000m	2.565A/mm² A
0.050	0.052	0.048	0.00196	9,528	15,492	0.0050
0.063	0.065	0.061	0.00312	5,899	9,593	0.0080
0.071	0.074	0.068	0.00396	4,747	7,719	0.0102
0.080	0.083	0.077	0.00503	3,702	6,020	0.0129
0.090	0.093	0.087	0.00636	2,900	4,716	0.0163
0.100	0.103	0.097	0.00785	2,333	3,794	0.0201
0.112	0.115	0.109	0.00985	1,848	3,004	0.0253
0.125	0.128	0.122	0.01227	1,475	2,398	0.0315
0.140	0.143	0.137	0.01539	1,170	1,902	0.0395
0.160	0.163	0.157	0.02011	890.6	1,448	0.0516
0.180	0.183	0.177	0.02545	700.7	1,139	0.0653
0.200	0.203	0.197	0.03142	565.6	919.7	0.0806
0.224	0.227	0.221	0.03941	449.5	730.8	0.1011
0.250	0.254	0.246	0.04909	362.7	589.8	0.1259
0.280	0.284	0.276	0.06158	288.2	468.6	0.1579
0.315	0.319	0.311	0.07793	227.0	369.0	0.1999
0.355	0.359	0.351	0.09898	178.2	289.7	0.2539
0.400	0.405	0.395	0.12566	140.7	228.8	0.3223
0.450	0.455	0.445	0.15904	110.9	180.3	0.4079
0.500	0.505	0.495	0.19635	89.59	145.7	0.5036
0.560	0.566	0.554	0.24630	71.52	116.3	0.6318
0.630	0.636	0.624	0.31172	56.38	91.67	0.7996
0.710	0.717	0.703	0.39592	44.42	72.22	1.0155
0.750	0.758	0.742	0.44179	39.87	64.83	1.1332
0.800	0.808	0.792	0.50265	35.00	56.90	1.2893
0.850	0.859	0.841	0.56745	31.04	50.47	1.4555
0.900	0.909	0.891	0.63617	27.65	44.96	1.6318
0.950	0.960	0.940	0.70882	24.84	40.40	1.8181
1.000	1.010	0.990	0.78540	22.40	36.42	2.0145

Figure A.2: Wire diameter

The value of resistivity and the maximum current density are respected, since in this simulation the used values are the equivalent ones that represent also this level of detail.

	Grade 1 Enamel		Grade 2 Enamel		Grade 2 Enamel	
Nominal Conductor Diameter (mm)	Maximum Overall Diameter (mm)	Minimum Enamel Increase (mm)	Maximum Overall Diameter (mm)	Minimum Enamel Increase (mm)	Maximum Overall Diameter (mm)	Minimum Enamel Increase (mm)
0.050	0.060	-	0.066	-	-	-
0.063	0.076	-	0.083	-	-	-
0.071	0.084	0.007	0.091	0.012	0.097	0.018
0.080	0.094	0.007	0.101	0.014	0.108	0.020
0.090	0.105	0.008	0.113	0.015	0.120	0.022
0.100	0.117	0.008	0.125	0.016	0.132	0.023
0.112	0.130	0.009	0.139	0.017	0.147	0.026
0.125	0.144	0.010	0.154	0.019	0.163	0.028
0.140	0.160	0.011	0.171	0.021	0.181	0.030
0.160	0.182	0.012	0.194	0.023	0.205	0.033
0.180	0.204	0.013	0.217	0.025	0.229	0.036
0.200	0.226	0.014	0.239	0.027	0.252	0.039
0.224	0.252	0.015	0.266	0.029	0.280	0.043
0.250	0.281	0.017	0.297	0.032	0.312	0.048
0.280	0.312	0.018	0.329	0.033	0.345	0.050
0.315	0.349	0.019	0.367	0.035	0.384	0.053
0.355	0.392	0.020	0.411	0.038	0.428	0.057
0.400	0.439	0.021	0.459	0.040	0.478	0.060
0.450	0.491	0.022	0.513	0.042	0.533	0.064
0.500	0.544	0.024	0.566	0.045	0.587	0.067
0.560	0.606	0.025	0.630	0.047	0.653	0.071
0.630	0.679	0.027	0.704	0.050	0.728	0.075
0.710	0.762	0.028	0.789	0.053	0.814	0.080
0.750	0.805	0.030	0.834	0.056	0.861	0.085
0.800	0.855	0.030	0.884	0.056	0.911	0.085
0.850	0.909	0.032	0.939	0.060	0.968	0.090
0.900	0.959	0.032	0.989	0.060	1.018	0.090
0.950	1.012	0.034	1.044	0.063	1.074	0.095
1.000	1.062	0.034	1.094	0.063	1.124	0.095
1.060	1.124	0.034	1.157	0.065	1.188	0.098
1.120	1.184	0.034	1.217	0.065	1.248	0.098
1.180	1.246	0.035	1.279	0.067	1.311	0.100
1.250	1.316	0.035	1.349	0.067	1.381	0.100
1.320	1.388	0.036	1.422	0.069	1.455	0.103
1.400	1.468	0.036	1.502	0.069	1.535	0.103
1.500	1.570	0.038	1.606	0.071	1.640	0.107
1.600	1.670	0.038	1.706	0.071	1.740	0.113
1.700	1.772	0.039	1.809	0.073	1.844	0.116
1.800	1.872	0.039	1.909	0.073	1.944	0.116
1.900	1.974	0.040	2.012	0.075	2.048	0.119
2.000	2.074	0.040	2.112	0.075	2.148	0.119
2.120	2.196	0.041	2.235	0.077	2.272	0.123
2.240	2.316	0.041	2.355	0.077	2.392	0.123
2.360	2.438	0.042	2.478	0.079	2.516	0.113
2.500	2.587	0.042	2.618	0.079	2.656	0.127
2.650	2.730	0.043	2.772	0.081	2.811	0.130
2.800	2.880	0.043	2.922	0.081	2.961	0.130
3.000	3.083	0.045	3.126	0.084	3.166	0.134
3.150	3.233	0.045	3.276	0.084	3.316	0.134
3.350	3.435	0.046	3.479	0.086	3.521	0.138
3.550	3.635	0.046	3.679	0.086	3.721	0.138
3.750	3.838	0.047	3.833	0.089	3.926	0.142
4.000	4.088	0.047	4.133	0.089	4.176	0.142
4.250	4.341	0.049	4.387	0.092	4.431	36.3877
4.500	4.591	0.049	4.637	0.092	4.681	40.7946
4.750	4.843	0.050	4.891	0.094	4.936	45.4532
5.000	5.093	0.050	5.141	0.094	5.186	50.3637

Figure A.3: Grade of insulation

A.2 Lamination catalogue

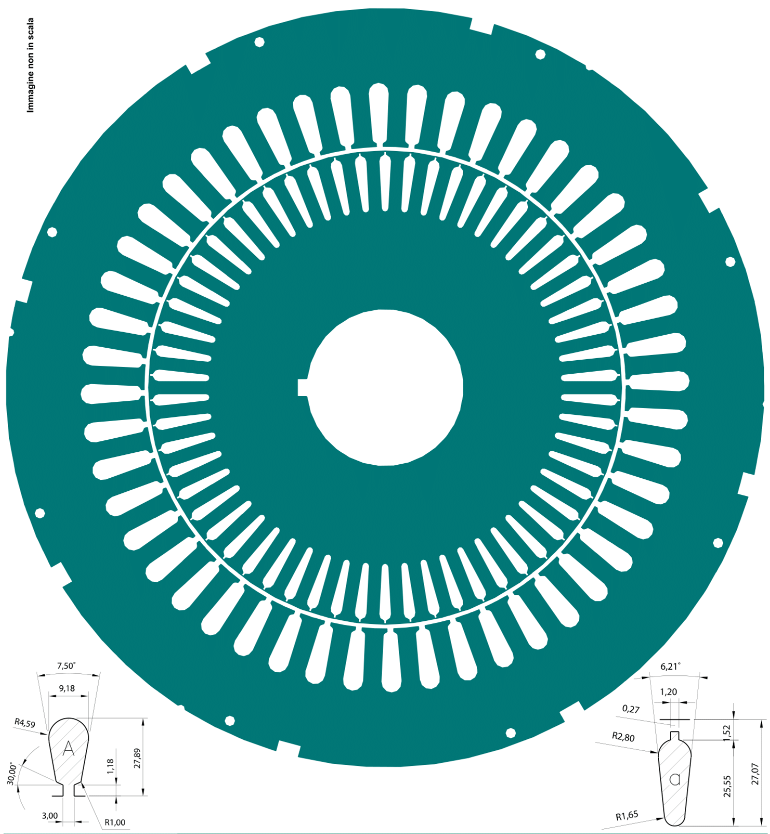

EU 5700A Lamierini tranciati - Macchine asincrone

SA330M

DE mm	DI mm	N	A mmq	LD mm	LC mm	LS mm	AC mm
330,00	210,00	48	202,70	7,60	32,11	0,00	3,00

#	RI	GR	SA	MT	PT	RF	V	$P_{1\,mm}$ g
1	✓				✓	✓		315,14

Ricottura	Tipo lamiera
SI	Altro (contattare ufficio commerciale)

Altezza pacco	Impaccaggio
174 (mm)	SI

RA210M

de mm	n	a mmq	ld mm	ac mm
210,00	58	112,25	5,32	1,20

#	di mm	pz	c	l	fv	ri	$P_{1\,mm}$ g
1	70		✓				189,11

Ricottura	Altezza pacco	Inclinazione
SI	174 (mm)	1 (passi cava)

Pressofusione	Lega di pressofusione
SI	Alluminio

EURO TRANCIATURA Euro Group Company
Eurotranciatura S.p.A.
Via Stella Rosa, 48/50
20021 Baranzate (MI) Italia

Pagina Configurato

UTE 31/01/2007
Rev. C

EURO GROUP LAMINATIONS

PDF generato il 09-12-2019

Figure A.4: Lamination catalogue

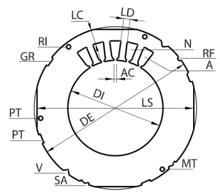

LEGENDA STATORE - sezione A	
DE	Diametro esterno
DI	Diametro interno
N	Numero cave
A	Area cava
LD	Larghezza dente
LC	Larghezza corona
LS	Larghezza sfaccettatura
AC	Apertura cava
RI	Fori per rivetti
GR	Cave per graffe
SA	Cava per saldatura
MT	Foro per messa a terra
PT	Fori per passaggio tiranti
RF	Riferimento
V	Tacche a V
$P_{1\,mm}$	Peso indicativo g per 1 mm/sp.

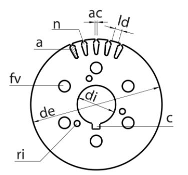

LEGENDA ROTORE - sezione A	
de	Diametro esterno
di	Diametro interno
n	Numero cave
a	Area cava
ld	Larghezza dente
ac	Apertura cava
pz	Pozzetto
c	Scanalatura per chiavetta
l	Foro lobato
fv	Fori di ventilazione
ri	Fori per rivetti
$P_{1\,mm}$	Peso indicativo g per 1 mm/sp.

NOTE

EURO TRANCIATURA Euro Group Company

Eurotranciatura S.p.A.
Via Stella Rosa, 48/50
20021 Baranzate (MI) Italia

EURO GROUP In motion around you.

PDF generato il 04-08-2012

Figure A.5: Lamination catalogue

A.3 tab

A.4 Winding table

Ns	Phislot	pPhislot	Orientation
1	7,5	15	+1
2	15	30	+1
3	22,5	45	'+1
4	30	60	-1
5	37,5	75	-1
6	45	90	-1
7	52,5	105	-1
8	60	120	+1
9	67,5	135	+1
10	75	150	'+1
11	82,5	165	'+1
12	90	180	-1
13	97,5	195	-1
14	105	210	-1
15	112,5	225	-1
16	120	240	+1
17	127,5	255	+1
18	135	270	'+1
19	142,5	285	'+1
20	150	300	-1
21	157,5	315	-1
22	165	330	-1
23	172,5	345	-1
24	180	360	+1
25	187,5	375	+1
26	195	390	'+1
27	202,5	405	'+1
28	210	420	-1
29	217,5	435	-1
30	225	450	-1
31	232,5	465	-1
32	240	480	+1
33	247,5	495	+1
34	255	510	'+1
35	262,5	525	'+1
36	270	540	-1
37	277,5	555	-1
38	285	570	-1
39	292,5	585	-1
40	300	600	+1
41	307,5	615	+1
42	315	630	'+1
43	322,5	645	'+1
44	330	660	-1
45	337,5	675	-1
46	345	690	-1
47	352,5	705	-1
48	360	720	1

A.5 Materials properties

A.5.1 Copper

Copper is used in conducting parts, as in the winding of the rotor

Mass density	$\psi =$	$8\ 900\ \dfrac{K_g}{m^3}$
Critical Temperature	$\eta_c =$	$234.5°C$
Resistivity at $0°C$	$\rho_0 =$	$1.6 * 10^{-8}\Omega m$

Now is possible to evaluate the value of the resistivity at every temperature by using the following formula:

$$\rho_{(\theta)} = \rho_{(0)}(1 + \alpha_0\theta) \tag{A.1}$$

$$\rho_{(\theta)} = 0.016\frac{234.5 + \theta}{234.5} = 0.016(1 + 0.00426 * \theta) = 2.0797 * 10^8 \tag{A.2}$$

So the resistivity at some interesting temperature are :

Temperature	Resistivity $\dfrac{\Omega mm^2}{m}$
$0°C$	0.016
$20°C$	0.0173
$75°C$	0.021
$100°C$	0.00228
$130°C$	0.00248

A.5.2 Alluminum

This conductor is used in the rotor bar and in the rotor end winding. Die cast and post aneling processes increase, the resistivity of this material up to $+8 \div 10\%$

Mass density	$\psi =$	$2\ 700\ \dfrac{K_g}{m^3}$
Critical Temperature	$\eta_c =$	$230°C$
Resistivity at $20°C$	$\rho_0 =$	$2.6 * 10^8\Omega m$

Now is possible to evaluate the value of the resistivity at every temperature by using the following formula:

$$\rho_{(\theta)} = \rho_{(0)}(1 + \alpha_0\theta) \tag{A.3}$$

$$\rho_{(\theta)} = 0.026(1 + 0.00434 * \theta) = 3.5943 * 10^8 \tag{A.4}$$

So the resistivity at some interesting temperature are :

Temperature	Resistivity $\dfrac{\Omega mm^2}{m}$
$0°C$	0.026)
$20°C$	0.0282)
$75°C$	0.0359)
$100°C$	39)

A.5.3 Insulating materials

The insulating material are used in order to bear the following stresses

- Dielectric
- Mechanical
- Thermal

The main properties are the following:

- • high dielectric strength (to allow thin insulating layers)
- size stability (do not change their shape/thickness with time)
- high sheet resistivity
- low hygroscopicity (not attract and not hold water molecules via absorption)
- low dielectric losses
- high thermal conductivity and good mechanical properties

The dielectric material that is present in the motor should pass some permittivity test in order to prove that the dielectric can stand at the imposed electric field.

It is important that all the region where it is present an insulation (solid layer or semi liquid) there are not other external materials (like air or dust) because the electric field that cross a series of material, is greater in the region in which the relative permeability is lower. SO in the case of an insulating layer made of air and insulation material, the electric field of the air can be more critical than the same situation but with just the air as insulation material.

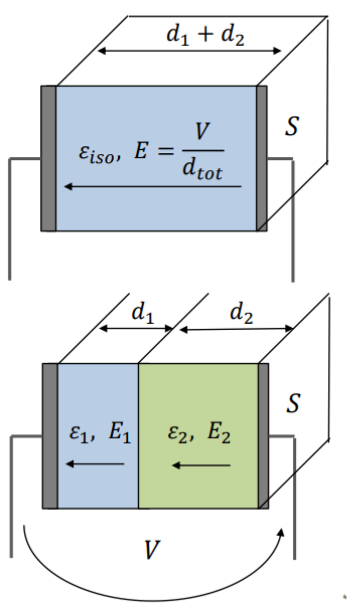

Figure A.6: Insulating materials

The best design solution is (if needed) to couple two material with the product of the dielectric strength times the relative permittivity, constant $Kx\epsilon_r = const$. From the Paschen's curve is possible to see that decreasing the thickness of insulation, some material can stand to higher electric field

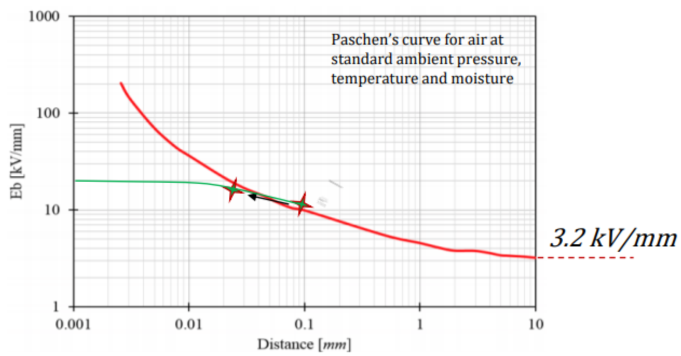

Figure A.7: Paschen's curve

In addition, is important o consider thermal class of insulation by following CEI EN60034 1

Thermal class **IEC 60085**	Y	A	E	B	F	H	C(N)	C(R)	C(S)
Maximum hotspot temperature	***90°***	***105°***	***120°***	***130°***	***155°***	***180°***	***200°***	***220°***	***240°***
Maximum overtemperature	***50°***	***65°***	***80°***	***90°***	***115°***	***140°***	***160°***	***180°***	***200°***

Figure A.8: Thermal classes

The adopted insulation are:

- Epoxy resin to fill the slot vacuum, increase the dielectric strength, increase the mechanical performances, improve thermal conductivity, extend insulation life time
- Enamel for wire insulation, phase insulation and ground wall (high thermal properties), strongly depend on the winding layout because it should be stood to the voltage between the coils, the thickness increase by the increasing of the thermal class

A.6 IEC

The following table put in evidence the difference behaviour of motors with different efficiency grade

Table 1 – Motor technologies and their energy efficiency potential

Motor type		IE1	IE2	IE3	IE4	IE5
Three-phase cage-rotor induction motors (ASM)	Random wound windings (all enclosures, all ratings)	Yes	Yes	Yes	Difficult	No
	Form wound windings; IP2x (open motors)	Yes	Yes	Difficult	No	No
	Form wound windings; IP4x and above	Yes	Yes	Yes	Difficult	No
Three-phase wound-rotor induction motors		Yes	Yes	Yes	Difficult	No
Single-phase induction motors	Start capacitor	Difficult	No	No	No	No
	Run capacitor	Yes	Difficult	No	No	No
	Start/run capacitor	Yes	Difficult	No	No	No
	Split-phase	Difficult	No	No	No	No
Synchronous motors	Line-start permanent-magnet (LSPM [a])	Yes	Yes	Yes	Difficult	No

[a] Line-start permanent-magnet motors have limitations on their line-start capabilities with respect to torque and external inertia and may not be suitable for all types of applications.

NOTE 1 With regard to the IE levels, "Yes" means the efficiency class is achievable with present technology (although in some cases it may not be economical); "No" means the efficiency class is not generally achievable with present technology; "Difficult" means that the energy-efficiency level may be achieved with present technology for some but not all power ratings and the standardized frame-size may be exceeded. "Line-start" means the capability of the motor to start direct on-line (Design N of IEC 60034-12 for single-speed, three-phase cage induction motors) without the need for a frequency converter.

Figure A.9: Efficiency standards

A.6.1 nodi e anti nodi

mettere foto che spiega la pulsazioned del campo di una fasse e poi la combinazione delle tre fasi che genera un campo rotante.

A.7 Magnetic materials

The best characteristic that a magnetic material can have are the following :

- High magnetic permeability μ
- Low AC losses
- Good mechanical properties like (mechanical stress should sustain high speed of the rotor; good manufacturability; high thermal and chemical compatibility)
- Low cost (for some application high tec material are not affordable)

The magnetic flux density B represents the overall reaction of a material that is subject to the effect of magnetic field strength sources H. For Vacuum:

$$B = \mu_0 H \tag{A.5}$$

where μ_0 is the vacuum permeability. For all the other material:

$$B = \mu H = \mu_0 H + \mu_0 M = \mu_0 (1 + X_m) H + \mu_0 \mu_r H \tag{A.6}$$

where μ_r is the relative permeability and the X_m is the magnetic susceptibility that thought M that is the magnetization vector, express the response of a material under the effect of an external magnetic field.

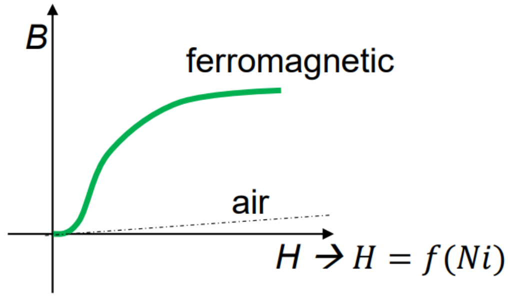

Figure A.10: B-H curve (qualitative)

This behaviour underline the effect of a magnetic field on the Weiss. These magnetic domain present in the ferromagnetic materials have the tendency to orient themselves in the direction of the applied magnetic field H. The result is a significant increase of B (this is evident in the previous picture when the behaviour of the ferromagnetic material start to be different from the one of the air).

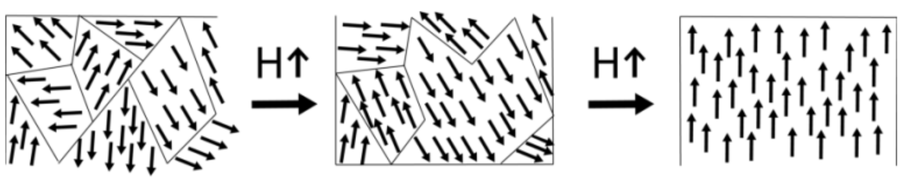

Figure A.11: MAgnetic domain

This material con be divided in three main categories that are differentiated by the value of the permeability to the magnetic flux:

- Diamagnetic : $\mu_r < 1 \simeq 1$ (Copper, silver, water, superconductors)
- Paramagnetic : $\mu_r > 1 \simeq 1$ (Aluminium and tungsten)
- Ferromagnetic : $\mu_r >> 1$ (Iron, cobalt, rare earths)

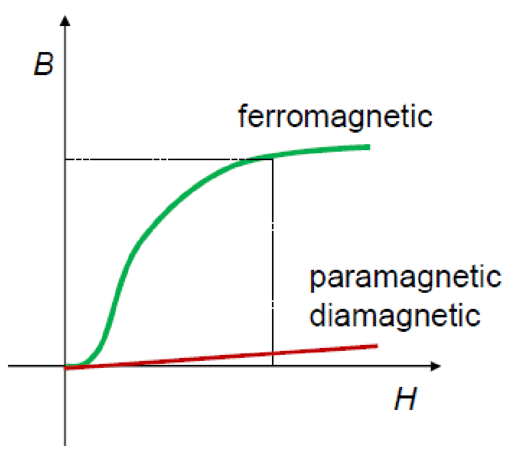

Figure A.12: B-H curve (qualitative)

A.7.1 Soft and Hard magnetic material

Initial magnetization curve: The Weiss domain orient until magnetic saturation (they are all oriented).

Hysteresis loop: Decreasing the external magnetic field H, the flux density remains at the remanence value Br (the Weiss domains partially keep their orientation). To bring B to zero, an inverse magnetic field Hc (coercivity) is required. Beyond this, value B becomes negative.

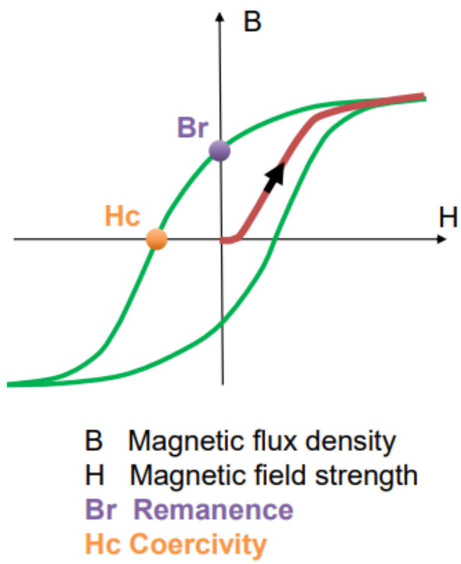

Figure A.13: B-H curve (qualitative)

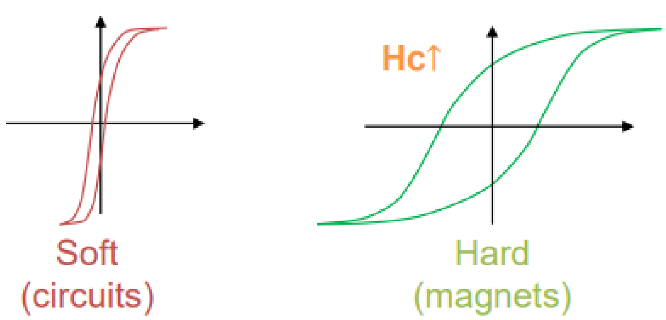

Figure A.14: B-H curve (qualitative)

The behaviour of ferromagnetic materials is non-linear (hysteretic), and non-bijective (one-to-one). The energy required to perform a hysteresis loop is proportional to the area of the loop.

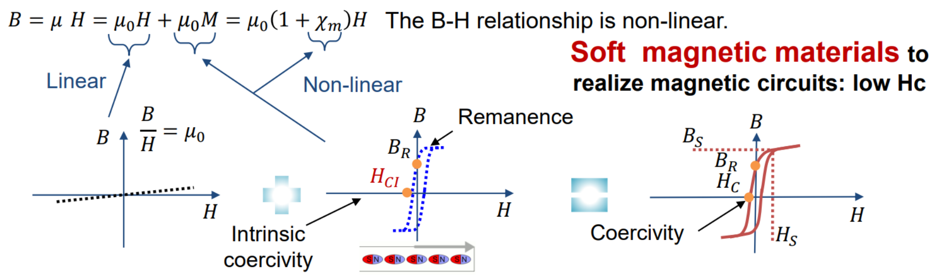

Figure A.15: B-H curve (qualitative)

Saturation Polarization (Js) The value of M $= M_s$ corresponds to the saturation magnetization point of the material. The saturation flux density is $B_s = \mu_0 M_s + \mu_0 H_s$. In datasheets, the saturation polarization $J_s = \mu_0 M_s$ [T], instead of M_s, can be found. Intrinsic Coercivity (Hci) To obtain a neutral material (without privileged orientation of the Weiss domains), it is necessary to apply an external field Hci (intrinsic coercivity). Consequently, the material is demagnetized.

Curie temperature

Curie's temperature is the temperature in which the materials completely lose their magnetic properties becoming paramagnetic (Iron can generally reach $770°C$ while the NdFeB at least 400°

Hysteresis loop

Soft magnetic materials with a tight hysteresis loop are commonly used to realize magnetic circuits in electrical machines. Hard magnets with significant hysteresis loops and high intrinsic coercivity are used as permanent magnets. (IEC 60404-1:2000: "The classification of magnetic materials is based upon the generally recognized existence of two main groups of products:

- soft magnetic materials (coercivity less than or equal to 1000 A/m)
- hard magnetic materials (coercivity greater than 1000 A/m)"

For the purpose of a preliminary motor design, in case of soft magnetic materials the "normal magnetization curve" is considered. This curve is the BH function obtained by the trajectory of the tips of the possible hysteresis loop of the material:

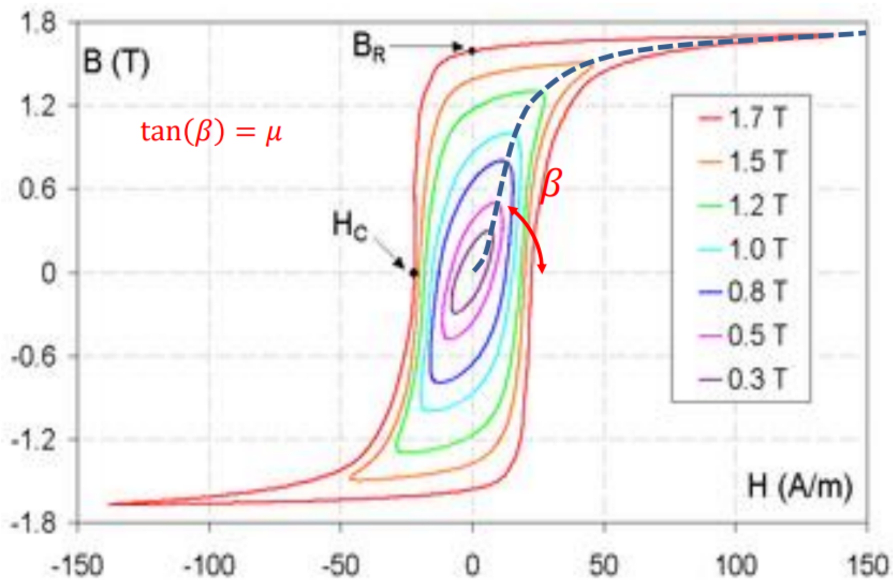

Figure A.16: B-H curve (qualitative)

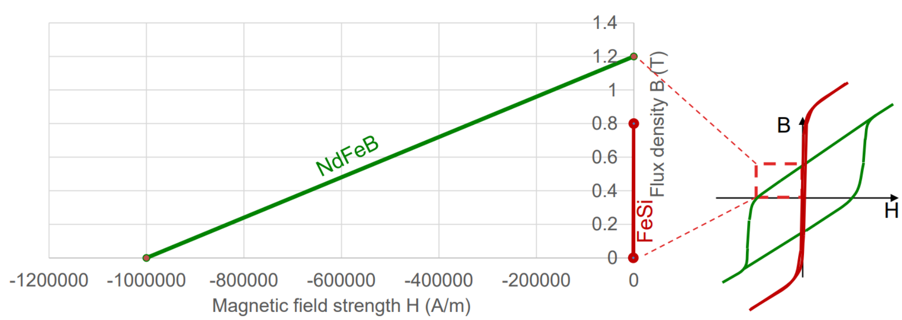

Figure A.17: B-H curve (qualitative)

Iron losses: Eddy currents

Eddy current are the results of the Faraday Lenz equation.

To reduce the eddy currents, ferromagnetic circuits working with AC fluxes are laminated in a direction parallel to the flux. This helps significantly reducing the linked flux, and the resulting currents and losses.

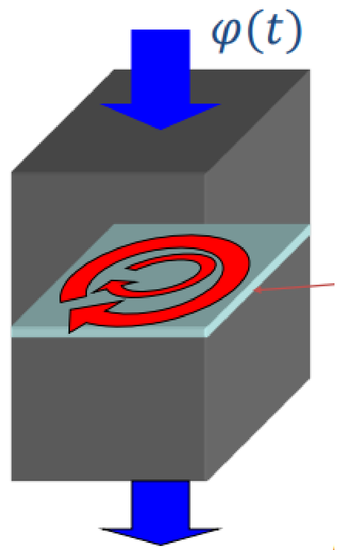

Figure A.18: Eddy current

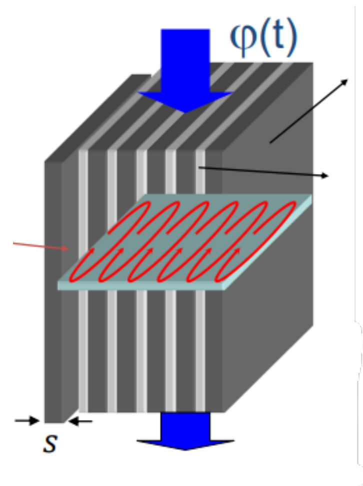

Figure A.19: Lamination for eddy current

Between lamination sheets, there is a thin insulating layer (varnish). Increasing the percentage of silicon (Si) in the alloy (FeSi) helps to reduce the conductivity (J decrease).

The losses due to eddy current:

$$P_c = K_c B_M^2 f^2 \tag{A.7}$$

Iron losses: Hysteresis

Hysteresis losses are associated with the energy dissipated while performing a hysteresis loop, which increases with the area of the loop itself.

The losses due to hysteresis:

$$P_i = K_i B_\alpha^2 f \tag{A.8}$$

where $1.5 < \alpha < 2.2$ this value is usually between this range, and it strongly depends on the shape of the hysteresis loop.

Increasing the percentage of silicon (Si% increase) results in a lower coercivity Hc, helping to reduce the hysteresis losses. However, this implies a lower saturation knee (Bmax decrease), and above 4.5% the mechanical properties significantly deteriorates (it loses ductility becoming brittle) with conventional manufacturing processes.

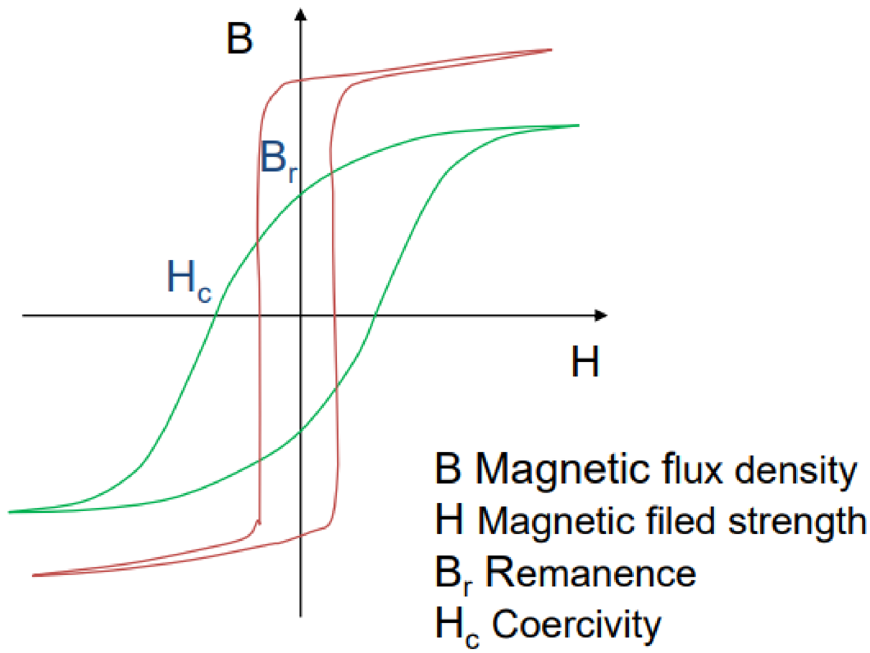

Figure A.20: B-H curve (qualitative)

So the main contribution of iron losses are due to eddy current induced into the lamination (that at high frequency became dominant) and to the hysteretic behaviour.

Total evaluation (VEDI PERFROMANCES)

The manufacturing process can affect the magnetic properties is some direction (like in the direction of the cut) and to recover this lack of performance, some after treatment process (reheated, post aneling and so on) can improve the magnetic behaviour of the lamination, correction are taken into consideration by the lamination factor k_l

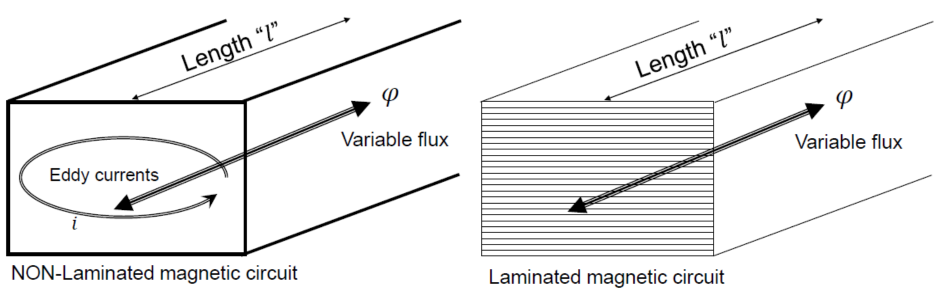

Figure A.21: Lamination for eddy current

A.7.2 Electrical steel

Effect of Silicon on performance (losses, and BH curve). By increasing the Si% :

- $\rho \uparrow$ significantly increases (up to 10%Si) so less eddy currents (P_c)
- H_c decreases $\rightarrow$ thinner hysteresis loops (P_i)

- Magnetostriction (shape change) is reduced so less noise
- B_{max} decrease so torque density could decrease
- Mechanical properties significantly deteriorate above 6 % Si

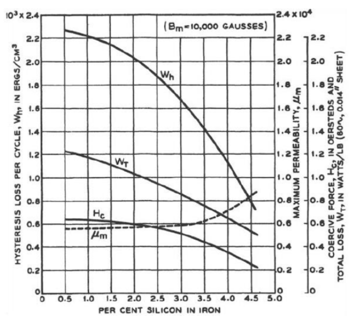

Figure A.22: Material

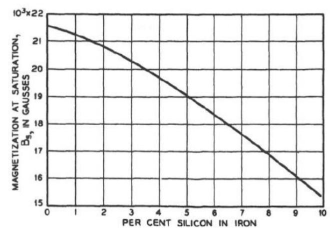

Figure A.23: Material

Increasing the maximum flux density using conventional FeSi laminations, for example with materials with lower Si content, results in higher losses.

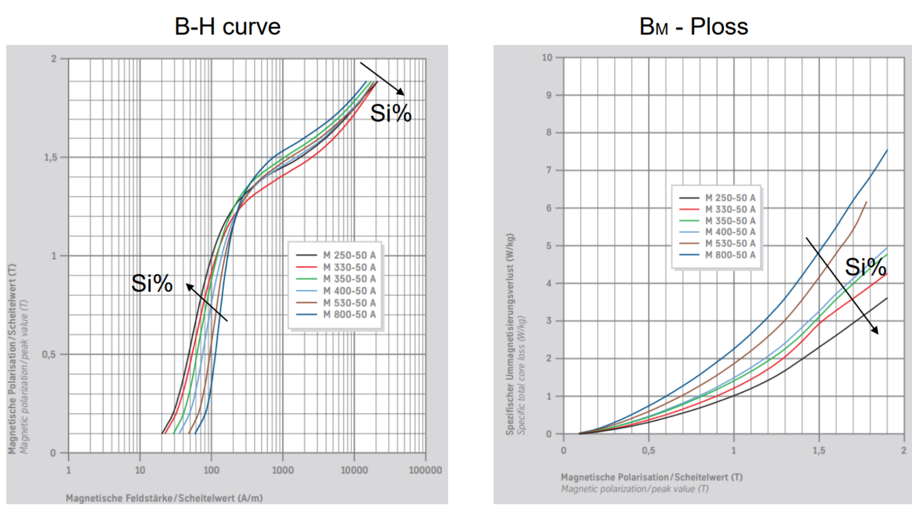

Figure A.24: B-H curve (qualitative)

A.7.3 Permanent magnet

This kind of magnetic material is characterized by a high value of intrinsic coercivity(that is the value of magnetic filed needed to fully demagnetize the material , no more privileged orientation of the Weiss domains). This value is also strongly affected by the working temperature (at high Temperature the intrinsic coercivity decrease, leading the material easier to demagnetize with lower current)

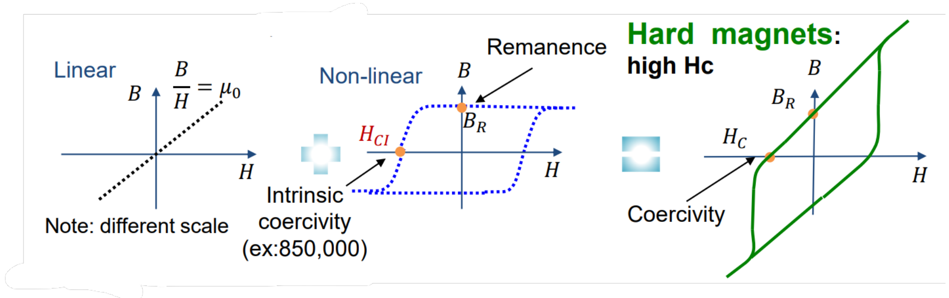

Figure A.25: B-H curve (qualitative)

Despite relatively high resistivity, magnets are conductive materials. Therefore, they are affected by eddy current losses when they are crossed by AC flux components (asynchronous fields and/or PWM). Sintered magnets feature higher performance compared to the bonded alternative, but significantly increased electrical conductivity. Because magnets' performance are significantly affected by temperature, these losses must be limited when significant.

A bulk magnet crossed by AC flux can be affected by significant eddy currents. To limit the magnet losses, it is possible to:

- enhance the motor design and increase the PWM frequency
- employ magnets with higher resistivity
- laminate the magnets (magnet segmentation

A.7.4 Iron losses

IM

The evaluation of iron losses, starts from the choice of the material for the lamination. Since this motor has no application in high frequency feeding, it is possible to have a larger degree of freedom in the thickness of the lamination. A good value is the M330-50A (or M27). The value represent Soft magnetic material

Lamination grade M300-35A5 so M = electrical steel; 3.00 = maximum total specific loss W/kg at 1.5 T; 0.35 mm nominal lamination thickness; A= cold-rolled non-oriented sheet; 5 = one tenth of the frequency at which the maximum specific loss is specified (50 Hz).

3,30	M330-50A	CK-33	M330-50A5	M-27	47F190	1,90	3,30

Figure A.26: Mat

3,30	M330-50A	CK-33	M330-50A5	M-27	47F190	1,90	3,30

Figure A.27: Mat

Grade EN 10106	Thickness mm	Specific total loss, W/kg at 50 Hz and peak magnetic polarization $\hat{J}$ (T) of									
		0,10	0,20	0,30	0,40	0,50	0,60	0,70	0,80	0,90	1,00

Figure A.28: Mat

M330-50A	0,50	0,03	0,09	0,18	0,28	0,41	0,55	0,71	0,89	1,08	1,29

Figure A.29: Mat

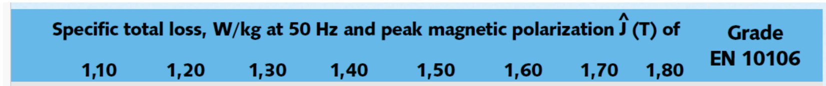

Specific total loss, W/kg at 50 Hz and peak magnetic polarization $\hat{J}$ (T) of								Grade EN 10106
1,10	1,20	1,30	1,40	1,50	1,60	1,70	1,80	

Figure A.30: Mat

Now is possible to evaluate the 3D and 2D curve that describe the specific losses (density of losses) compared to many point of flux density (at a chosen frequency 50 Hz)

```
M-27
clear; clc; close all;
materialname='Test';
B=[ 0 0.10 0.20 0.30 0.40 0.50 0.60 0.70 0.80 0.90 1.00 1.10 1.20 1.30
     1.40 1.50 1.60 1.70 1.80]';
f=[0 50 50 50 50 50 50 50 50 50 50 50 50 50 50 50 50 50 50]';
PFe=[0 0.03 0.09 0.18 0.28 0.41 0.55 0.71 0.89 1.08 1.29 1.53 1.81
    2.12 2.56 3.03 3.49 3.84 4.15]';
ftest=50;Btest=1;
figure(13);plot3(B,f,PFe,'ro') % plot points for comparison
% first iteration (try a first set of values)
x0 = [1e-2; 2; 1e-4];
options=optimset('Display','iter');
fprintf('Convergence history:\n')
ff = @(c)norm(-PFe+(c(1)*f(:,1).*(B(:,1)).^c(2))+(c(3)*(f(:,1).^2).*B
    (:,1).^2));
%find solution
c1 = fminsearch(ff,x0);
% plot results
x=min(B)/1.5:0.1:max(B)*1.5;
y=min(f)/1.5:1:max(f)*1.5;
z1=zeros(size(x,2),size(y,2));x1=z1;y1=z1;
for cx=1:size(x,2)
for cy=1:size(y,2)
z1(cx,cy) = c1(1)*y(cy).*(x(cx).^c1(2))+(c1(3)*y(cy).^2).*x(cx).^2;
x1(cx,cy)=x(1,cx);
y1(cx,cy)=y(1,cy);
end
end
hold on
surf(x1,y1,z1,'FaceColor','none')
xlabel('B [T]');ylabel('f [Hz]');zlabel('Losses [W(kg]')
title(['Ki = ' num2str(c1(1)) '[W/kg]; a = ' num2str(c1(2)) '; Kc = '
    num2str(c1(3)) '[W/kg]; Material = ' materialname '.'])
fprintf('\n\nEvaluated Parameters:\n')
fprintf('Ki = %1.3d\n',c1(1));
fprintf('a = %1.3d\n',c1(2));
fprintf('Kc = %1.3d\n',c1(3));
pi=c1(1)*ftest*Btest^c1(2);
pc=c1(3)*ftest^2*Btest^2;
fprintf('Pc/(Pc+Pi) = %1.3d\n',pc/(pc+pi));
hold on
PFetest=pc+pi;
plot3(Btest,ftest,PFetest,'bo')

Ki=0.016914;
Kc=0.00014104;
alpha=2.3662;
```

pp

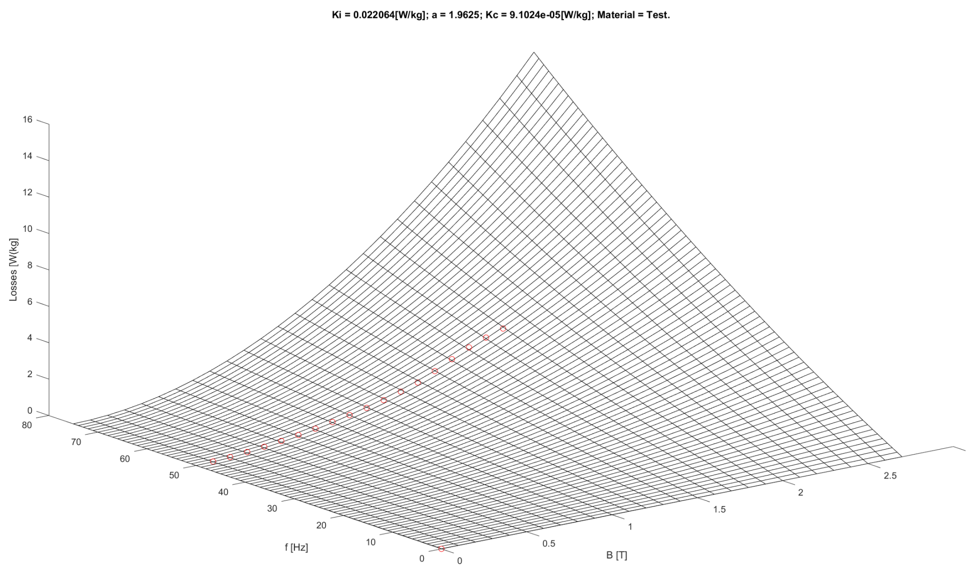

.

Figure A.31: 3D

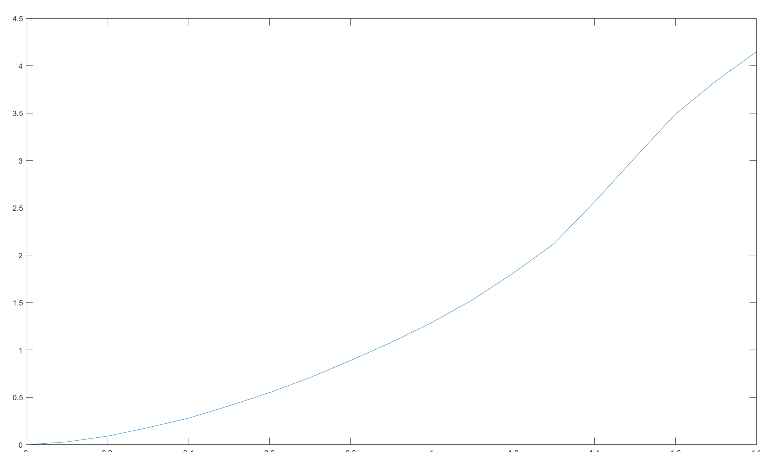

Figure A.32: 2D

SPM

As it was done before for the electrical steel of the IM, now can be evaluated by looking at the $M250-35A$

200 Hz

Grade EN 10106	Specific total loss, W/kg at 200 Hz and a peak magnetic polarization $\hat{J}$ (T) of														
	0,10	0,20	0,30	0,40	0,50	0,60	0,70	0,80	0,90	1,00	1,10	1,20	1,30	1,40	1,50
M235-35A	0,08	0,32	0,73	1,21	1,78	2,44	3,19	4,03	4,97	6,01	7,19	8,54	10,1	12,2	14,4
M250-35A	0,08	0,33	0,73	1,23	1,82	2,49	3,26	4,12	5,07	6,14	7,33	8,69	10,3	12,4	14,7

Figure A.33: Medium frequency electric steel

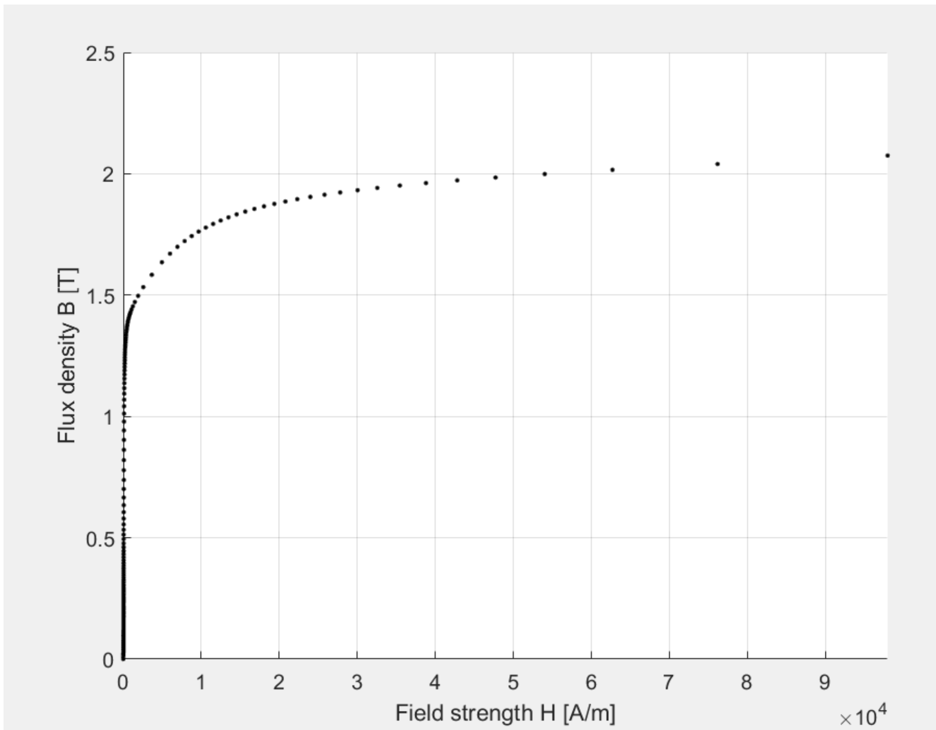

Figure A.34: BH curve

A.8 Alpha and K sat evaluation

This two values are related by the following relation:

$$\alpha_{sat} \simeq 0.0108k_{sat}^3 - 0.01147k_{sat}^2 - 0.4234k_{sat} - 0.3175 \tag{A.9}$$

And to better evaluate them is suggested from the literature to start with $k_{sat} = 1$ and $B_{Msat} = B_M$ and then iterate until the stability of the system.

```
k_sat(1)=1;
alpha_sat(1)=2/pi;
Bm_sat(1)=Bm;
phi_m_tau=2*Bm*L1*Tau/pi;

for i=1:100

    MMF_delta(i) =(Bm_sat(i)*airgap*K_C)/mu0;

    Bm_MT_sat_s(i) =(Taus * Bm_sat(i) )/wt_s;%%% bm sat
    H_MT_s_sat(i) =(x1* Bm_MT_sat_s(i))+x2*( Bm_MT_sat_s(i)^x3);
    MMF_t(i) = H_MT_s_sat(i) *hs;
```

```
    Bm_MT_sat_r (i)= (Taur * Bm_sat(i)) / wt_r ;
    H_MT_r_sat (i)=(x1* Bm_MT_sat_r(i))+x2*( Bm_MT_sat_r(i)^x3);
    MMF_tr(i)= H_MT_r_sat(i)* hr ;

    k_sat(i+1) =( MMF_delta(i) + MMF_t(i) + MMF_tr(i))/ MMF_delta(i) ;
    alpha_sat(i+1) =0.0108*(k_sat(i+1) ^3)-0.1147*(k_sat(i+1) ^2)
        +(0.4234* k_sat(i+1)) +0.3175;
    % phi_m_tau(i+1)=2*Bm_sat(i)*L1*Tau/pi;
    Bm_sat(i+1)= phi_m_tau/( alpha_sat(i+1) *L1*Tau );

    Bm_v (i)= Bm_sat(i+1) ;
    k_vect (i)= k_sat(i+1) ;
    a_vect (i)= alpha_sat(i+1) ;
    if Bm_MT_sat_s(i)>1.8
        Bm_MT_sat_s_new(i)=Bm_MT_sat_s(i)-(mu0*H_MT_s_sat(i)*(Taus-
            wt_s)/wt_s);
    else
        Bm_MT_sat_s_new(i)=Bm_MT_sat_s(i);
    end
    if Bm_MT_sat_r(i)>1.6
        Bm_MT_sat_r_new(i)=Bm_MT_sat_r(i)-(mu0*H_MT_r_sat(i)*(Taur-
            wt_r)/wt_r);
    else
        Bm_MT_sat_r_new(i)=Bm_MT_sat_r(i);

    end

end
```

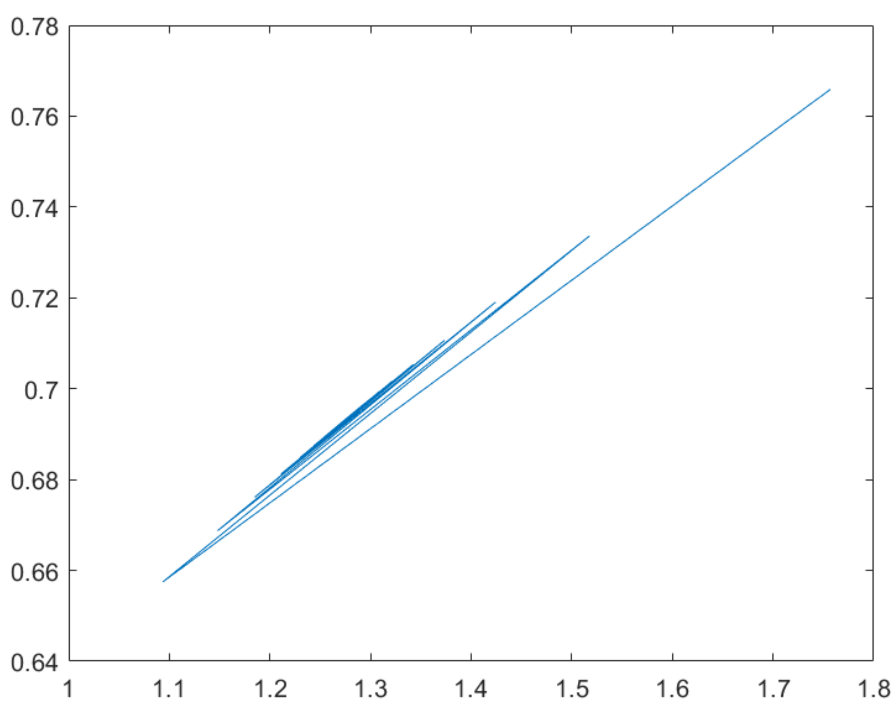

Figure A.35: alpha and k

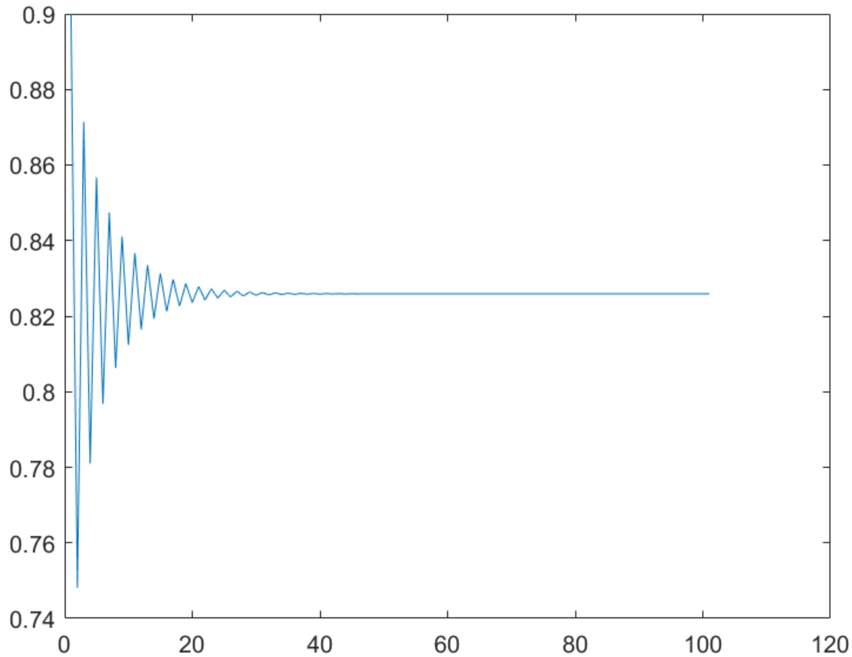

Figure A.36: B sat and number of interation

A.8.1 BH curve charatteristic

```
materialname='M300-50A';
Hin=[0.000000 17.059828 25.634971 31.338354
35.778997 39.602124 43.123143 46.520439
49.908177 53.368284 56.966318 60.760271
64.806105 69.161803 73.890922 79.066315
84.774676 91.122722 98.246299 106.324591
115.603417 126.435124 139.349759 155.187082
175.350538 202.312017 240.640455 299.118027
394.993386 561.726177 859.328763 1375.466888
2191.246914 3328.145908 4760.506172 6535.339449
8788.970657 11670.804347 15385.186211 20246.553031
26995.131141 38724.496369 64917.284463 101489.309338
137202.828961 176835.706764 216374.283609 ];

Bin=[0.000000 0.050000 0.100000 0.150000
0.200000 0.250000 0.300000 0.350000
0.400000 0.450000 0.500000 0.550000
0.600000 0.650000 0.700000 0.750000
0.800000 0.850000 0.900000 0.950000
1.000000 1.050000 1.100000 1.150000
1.200000 1.250000 1.300000 1.350000
1.400000 1.450000 1.500000 1.550000
1.600000 1.650000 1.700000 1.750000
1.800000 1.850000 1.900000 1.950000
2.000000 2.050000 2.100000 2.150000
2.200000 2.250000 2.300000 ];
HBin=[Hin Bin]
BHin=[HBin(:,2) HBin(:,1)];
Bcut=0.1; % do not consider the B values below Bcut
```

```
Hcut=20000; % do not consider the H values above Hcut

B=BHin(:,1);H=BHin(:,2);
Bcut=max(Bcut,B(2));
cBoffset=find(min(abs(B-Bcut))==abs(B-Bcut));
cHoffset=find(min(abs(H-Hcut))==abs(H-Hcut));
B=B(cBoffset:cHoffset);H=H(cBoffset:cHoffset);
B=[0;B];H=[0;H];H(1)=1e-6;
x0 = [100;10;10];
options=optimset('Display','iter');
fprintf('Convergence history:\n')
ff = @(x)norm(((- H+ x(1)*B+ x(2)*B.^x(3)).*(B./H)));% @(x)norm(-H+(x
    (1)*B+x(2).*B.^x(3)));
x = fminsearch(ff,x0); % find solution
fprintf('\n\nEval:\n');fprintf('x1 = %1.3d\n',x(1));fprintf('x2 = %1.3
    d\n',x(2));fprintf('x3 = %1.3d\n\n',x(3));
B_=0:0.001:B(size(B,1));%B;
H_x= x(1).*B + x(2).*B.^x(3);
H_= x(1).*B_ + x(2).*B_.^x(3);
figure (1)
subplot (2,1,1)
plot(BHin(:,2),BHin(:,1),'*b');hold on
plot(H_x,B,'xr');plot(H_,B_,'r'); grid on; xlabel('H [A/m]'); ylabel('
    B [T]');
%xlim([H(1) H(cHoffset-cBoffset+2)])% xlim([0 10000])
xlim([0 20000])
title('B-H curve',['Material = ' materialname '; x1 = ' num2str(round
    (100*x(1))/100) '; x2 = ' num2str(round(100*x(2))/100) '; x3 = '
    num2str(round(100*x(3))/100) '.'])
subplot (2,1,2)
mu0=4*pi*1e-7;
plot(BHin(:,2),BHin(:,1)./BHin(:,2)/mu0,'*b');hold on
plot(H_x,B./H_x/mu0,'xr');plot(H_,B_./H_/mu0,'r'); grid on; xlabel('H
    [A/m]'); ylabel('\mu_r [pu]');
%xlim([H(1) H(cHoffset-cBoffset+2)])% xlim([0 10000])
xlim([0 20000])
title('Relative permeability \mu_r.')
%
x1=1.08*10^2;
x2=3.753;
x3=1.305*10^1;
```

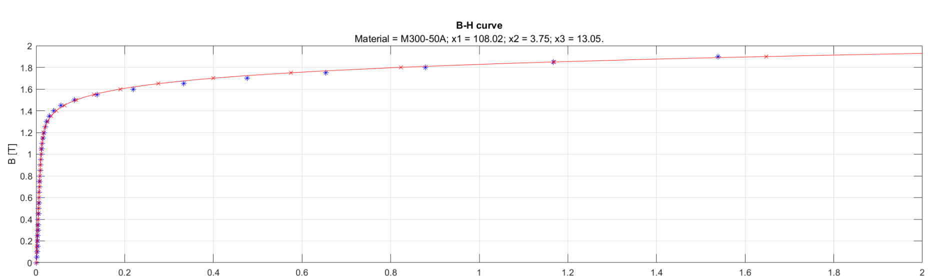

Figure A.37: BH curve

A.9 Winding table SPM

Ns	Phislot	pPhislot	Layer1.or,phase	Layer2.or,phase
1	0	0	+1	-2
2	40	160	+1	+2
3	80	320	+1	-2
4	120	120	+1	-3
5	160	280	+1	+3
6	200	80	+1	-3
7	240	240	+1	-1
8	280	40	+1	+1
9	320	200	+1	-1

Assign a phase to a slot can windings with $2p/M$ multiple of three are not considered in order to avoid asymmetrical or unfeasible winding.

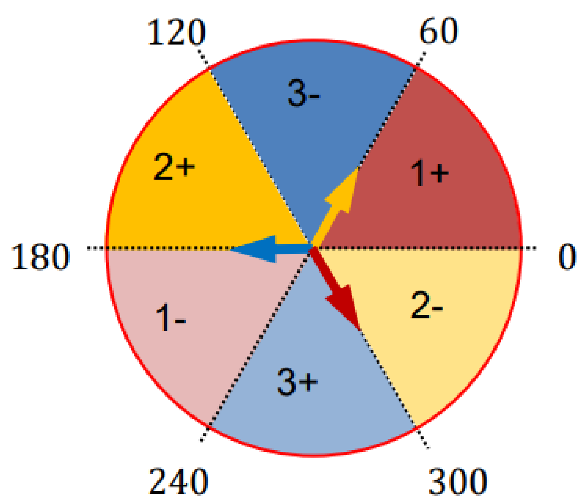

Figure A.38: Electrical angle

A.9.1 Permanent magnet

Magnetic properties

Raw material		Remanent magnetization		Coercivity				Energy product		Operation temperature	Temperature coefficient	
		B_r		H_{cJ}		H_{cB}		$(BH)_{max}$		T_{max}*	$TK(B_r)$	$TK(H_{cJ})$
		mT	kG	kA/m	kOe	kA/m	kOe	kJ/m³	MGOe	°C	%/K	%/K
NdFeB 410/88	min	1470	14.7	880	11	836	10.5	414	52	70	-0.110	-0.75
NdFeB 370/110	min	1400	14.0	1100	14	1040	13.1	374	47	80	-0.100	-0.65
NdFeB 330/140	min	1300	13.0	1350	17	970	12.2	330	41	120	-0.110	-0.55
NdFeB 340/160	min	1330	13.3	1590	20	995	12.5	340	43	150	-0.100	-0.50
NdFeB 300/200	min	1260	12.6	1990	25	940	11.8	300	38	180	-0.100	-0.50
NdFeB 300/240	min	1260	12.6	2400	30	940	11.8	300	38	200	-0.095	-0.50
NdFeB 225/280	min	1140	11.4	2800	35	850	10.7	225	31	225	-0.090	-0.45
NdFeB 200/320	min	1050	10.5	3200	40	770	9.7	200	26	250	-0.090	-0.45

The relative permeability (μ_p) is between 1.04–1.12.

* The actual maximum application temperature depends on the magnet's shear. This can only be precisely determined through a field-numeric calculation.

Selected material qualities (according EN 60404-8-1:2015). Further qualities on request.

Figure A.39: PM

Physical properties										
									Coefficient of linear thermal expansion	
Raw material	Density	Young's modulus	Flexural strength	Com-pressive strength	Vickers hardness	Electrical resistivity	Heat capacity	Thermal conductivity	in mag. direction	normal to mag. direction
	ρ g/cm³	E kN/mm²	F_B N/mm²	F_P N/mm²	H_v	ρ Ω mm²/m	C J/kg K	λ W/m K	Δdl_0 10^{-6}/K	Δdl_0 10^{-6}/K
NdFeB	~7.5	140	250	750	570	1.5	440	9	5	-1

Curie temperature
Tc = 310-370°C

Figure A.40: Pm

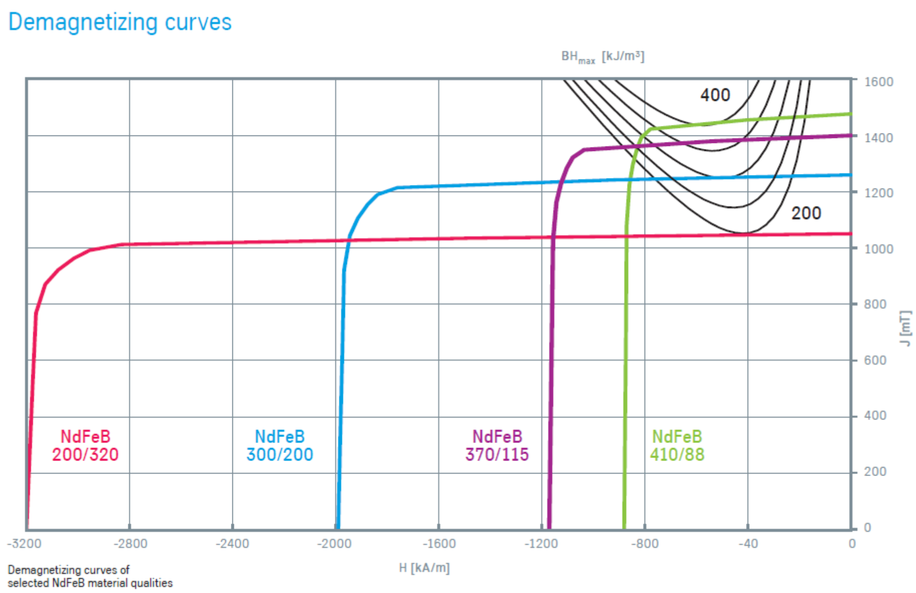

Figure A.41: Pm

$$B_r = B_{r0}(1 + \alpha_{Br}(T - T_0) \qquad H_{ci} = H_{ci0}(1 + \alpha_{Hci}(T - T_0) \tag{A.10}$$

Magneto motive force and Demagnetization

A permanent magnet in a magnetic circuit has two effects:

- Adds a magneto motive force (MMF)
- Increases the reluctance of the magnetic circuit ($\frac{l_{mag}}{S\mu_d} \simeq \frac{l_m ag}{S\mu_0}$)

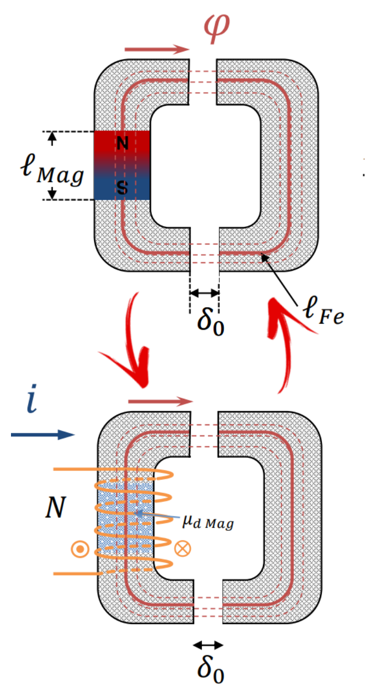

Figure A.42: MMF

$$R\phi = MMF \tag{A.11}$$

By considering the flux constant in all the cross section and $\mu_{fe}H_{fe} = \mu_0 H_0 = B_r + \mu_d H_{mag} = \frac{\phi}{S}$:

$$((\frac{2l_{fe}}{S\mu_{fe}}) + (\frac{2\delta_0}{S\mu_0}) + (\frac{2l_{mag}}{S\mu_d}))\phi = Relactance * flux = \frac{B_r l_{mag}}{\mu_d} = MMF_{Magnet} \tag{A.12}$$

The distribution of the magnetic field depends on the magnetic circuit and the distribution of magneto motive forces (currents and magnets). So the total MMF is :

$$\frac{B_r l_{mag}}{\mu_d} + Ni = MMF \tag{A.13}$$

And the operating point is the intersection between the demagnetization curve $B_{mag} = B_r + \mu_d H_{mag}$ and the load curve $B_{mag} = \frac{\mu_0 l_m ag}{2\delta_0}(\frac{Ni}{l_m ag} - H_{mag})$:

$$H_{mag} = \frac{Ni - \frac{2\delta_0 B_r}{\mu_0}}{l_{mag} + 2\delta_0 \frac{\mu_d}{\mu_0}} \tag{A.14}$$

And this value of H_{mag} should be checked $< HCi$ both in absolute value in order to avoid demagnetization

Appendix B

Bibliography

- Material and lesson of Professor Giacomo Sala